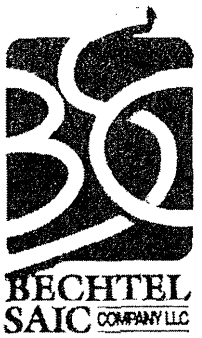

QA: QA

000-30R-WIS0-00100-000-~~003~~ 004

September 2007 12/18/07
na

Waste Package Component Design Methodology Report

Edited By:
Nakachew A. Alemu

Prepared for:
U.S. Department of Energy
Office of Civilian Radioactive Waste Management
Office of Repository Development
1551 Hillshire Drive
Las Vegas, Nevada 89134-6321

Prepared by:
Bechtel SAIC Company, LLC
1180 Town Center Drive
Las Vegas, Nevada 89144
Under Contract Number
DE-AC28-01RW12101

DISCLAIMER

004 na 12/18/07

This document was developed by Bechtel SAIC Company, LLC (BSC) and is solely intended for the use of BSC in its work ~~in~~ for the Yucca Mountain Project.

na 12/18/07

This report was prepared as an account of work sponsored by an agency of the United States Government. Neither the United States Government nor any agency thereof, nor any of their employees, nor any of their contractors, subcontractors or their employees, makes any warranty, express or implied, or assumes any legal liability or responsibility for the accuracy, completeness, or any third party's use or the results of such use of any information, apparatus, product, or process disclosed, or represents that its use would not infringe privately owned rights. Reference herein to any specific commercial product, process, or service by trade name, trademark, manufacturer, or otherwise, does not necessarily constitute or imply its endorsement, recommendation, or favoring by the United States Government or any agency thereof or its contractors or subcontractors. The views and opinions of authors expressed herein do not necessarily state or reflect those of the United States Government or any agency thereof.

BSC	**Technical Report Signature Page/ Change History** *Complete only applicable items.*	1. QA:QA 2. Total Pages: 166

3. Technical Report Title
Waste Package Component Design Methodology Report

4. DI (including Rev. No.)
000-30R-WIS0-00100-000-~~003~~ 004 na 12/18/07

	Printed Name	Signature	Date
5. Originator	Nakachew A. Alemu Lead Author		09/26/07
	Kenneth R. Jaquay Structural Analysis		09/26/07
	Delwin C. Mecham Thermal Analysis		9/26/07
	Charlotta E. Sanders Source Term and Shielding		9/26/07
6. Checker	Mohan Durani Structural Analysis		9/26/07
	Daniel J. Wang Thermal Analysis		9/26/07
	Jason C. Viggato Source Term and Shielding		9/26/07
7. QER	Daniel J. Tunney		9/26/07
8. Lead or Supervisor	Jason C. Viggato		9/26/07
9. Responsible Manager or Project Engineer	Michael J. Anderson		9/26/07 12/19/07

10. Remarks

Revision change history of the document continue on page 4.

Pages 1, 2, 3, 4, 13, 72, 113 are impacted by this editorial revision. See Change History on page 4.

004 na 12/18/07

Change History

11. Revision No.	12. Description of Change
00	Initial issue of ANL-EBS-MD-000053 REV 00, *Waste Package Design Methodology Report*, ACC: MOL.20000526.0335. Change effective date, 5/16/2000.
01	Initial issue. Supersedes ANL-EBS-MD-000053 REV 00, *Waste Package Design Methodology Report*, ACC: MOL.20000526.0335. Modified to reflect changes in waste package design and updates to the design methodology used in the development and verification of design processes. Change effective date, 9/28/2001.
02	Modified to reflect changes in waste package design and updates to the design methodology used in the development and verification of design processes. Change effective date, 3/19/2002.

History of TDR-MGR-MD-000006 is provided above.

CHANGE HISTORY (CONTINUED)	
11. Revision No.	12. Description of Change
000	Extensive revision to reflect design changes and updates to design methodology during transition from Site Recommendation to License Application effort. Revised DI number from TDR-MGR-MD-000006 to 000-30R-WIS0-00100-000-000. Changed name of report from Waste Package Design Methodology Report to Waste Package Component Design Methodology Report. ACC: ENG.20040113.0001. Change effective date, 01/06/2004.
001	Minor revisions marked by change bars: updated references, deleted use of ACUSOLVE, clarified use of B&W fuel as representative of other PWR fuels in response to Condition Report 2261, improved description of criticality analysis, converted DIRS to new format, added structural failure criteria. Several editorial changes. ACC: ENG.20040617.0012. Change effective date, 06/16/2004.
002	Updated reference in 4.1.1 Added event sequence in 6.2.2.5. Typographical errors corrected in tiered failure criteria, section 6.2.4. ACC: ENG.20040713.0003. Change effective date, 07/12/2004.
003	Extensive revision to reflect design changes and updates to design methodology of the waste packages and ancillary components for the License Application (LA). The Transportation, Aging, and Disposal (TAD) canister based waste package design concept is incorporated. Some event sequences considered in the previous design are replaced by new event sequences. Sections are regrouped in the following order: structural, thermal, source term and shielding throughout the document. All Sections and Paragraphs related to Criticality are removed. Risk Informed Analysis to the waste package is added in the structural analysis section. Two appendices are included at the end of the document for the waste package capacity determination and NRC Key Technical Issue resolution results. No change bars are used since the changes are significant and throughout the document.

004
na
12/18/07

Changed disclaimer of the document as per management directive.

Incorporated changes issued by ACN-001

Replace cited reference (BSC 2003, [DIRS 165497]) in section 7.1.4, page 72 by BSC 2007. [DIRS 184420]

Added reference, BSC 2007 [DIRS 184420] in Section 9.1, page 113

na
12/18/07

CONTENTS

Page

CONTENTS (Continued)

Page

CONTENTS (Continued)

Page

INTENTIONALLY LEFT BLANK

CONTENTS

Page

FIGURES

Page

TABLES

Page

INTENTIONALLY LEFT BLANK

ACRONYMS

ACNW	Advisory Committee on Nuclear Waste
ADJ	Adjustment Needed
ANS	American Nuclear Society
ANSI	American National Standards Institute
ASM	American Society for Metals
ASME	The American Society of Mechanical Engineers
ASME B&PV	ASME Boiler & Pressure Vessel Code
B&W	Babcock & Wilcox
BCJ	Bammann-Chiesa-Johnson
BOD	Basis of Design for the TAD Canister-Based Repository Design Concept
BSC	Bechtel SAIC Company, LLC
BWR	Boiling Water Reactor
CDR	Yucca Mountain Project Conceptual Design Report
CFR	Code of Federal Regulation
CRWMS	Civilian Radioactive Waste Management System
CRWMS M&O	CRWMS Management & Operating Contractor
CS	Carbon Steel
CSNF	Commercial Spent Nuclear Fuel
DEM	Discipline Engineering Manager
DHLW	Defense High-Level Radioactive Waste
DIRS	Document Input Reference System
DOE	U.S. Department of Energy
DTN	Data Tracking Number
EMMI	Evolving Microstructure Model of Inelasticity
EP	Emplacement Pallet
ETF	Expended ~~Extended~~ Toughness Fraction
EWA	Element Wall Average
FEA	Finite Element Analysis
FER	Finite Element Representation
FLD	Forming Limit Diagram
GE	General Electric
GNT	Gurson-Needleman-Tvergaard
GWd/MTU	Gigawatt Days per Metric Ton Uranium
HLW	High-Level Radioactive Waste
IED	Information Exchange Document
ISG	Interim Staff Guidance
INEEL	Idaho National Engineering and Environmental Laboratory

004 na 12/18/07

12/18/07

INL	Idaho National Laboratory (formerly INEEL)
ITS	Important to Safety
ITWI	Important to Waste Isolation
IV	Inner Vessel
KTI	Key Technical Issue
LA	License Application
MCNP	Monte Carlo N-Particle
MCO	Multi-Canister Overpack
MSS	Maximum Shear Stress
MWd/MTU	Megawatt days per Metric Ton Uranium
NNPP	Naval Nuclear Propulsion Program
NRC	U.S. Nuclear Regulatory Commission
NUREG	NRC Technical Report Designation
NUREG/CR	NUREG Contractor Report
OCB	Outer Corrosion Barrier
OS	Operating System
PDC	Project Design Criteria (Document)
PWR	Pressurized Water Reactor
QMD	Quality Management Directive
RT	Room Temperature
SCL	Stress Classification Line
SCM	Software Configuration Management
SI	Stress Intensity
SNF	Spent Nuclear Fuel
SRS	Savannah River Site Defense Waste Processing Facility
SS	Stainless Steel
SSC	Structures, Systems, and Components
STN	Software Tracking Number
TAD	Transportation, Aging and Disposal
TEV	Transport and Emplacement Vehicle
TMI	Three Mile Island (Nuclear Reactor Power Station)
TR	Triaxiality Ratio
TRIGA	Training, Research Isotopes General Atomics
TSA	Thermal/Structural Analysis Discipline
TSPA	Total System Performance Assessment

UNS	Unified Numbering System
USW	Underground Southern Nevada Waste
UTS	Ultimate Tensile Stress
WCT	Worst-Case Triaxiality
WP	Waste Package
WQR	Waste Form Qualification Report
WTP	Waste Treatment and Immobilization Plant
WVNS	West Valley Nuclear Service Company
WVDP	West Valley Demonstration Project
YMP	Yucca Mountain Project

INTENTIONALLY LEFT BLANK

EXECUTIVE SUMMARY

This Executive Summary provides an overview of the methodology being used by the Yucca Mountain Project (YMP) to design waste packages (WP) and ancillary components, viz. emplacement pallets (EP) and drip shields. This summary information is intended for readers with general interest, and also provides technical readers a general framework surrounding a variety of technical details provided in the main body of the report.

The purpose of this report is to document and ensure appropriate design methods are used in the design of waste packages and ancillary components. This is a part of an overall design strategy for work scope relevant to the waste packages and ancillary components, and is documented in a discipline-specific execution plan, *Execution Plan for the Thermal-Structural Discipline Workflow for Design, Design Revision, and Prototyping Waste Packages and Related Components* (BSC 2007 [DIRS 183164], Section 2.3.1.2). The methodology includes identification of necessary design inputs, justification of design assumptions, and use of appropriate analytical methods and computational tools. This design work is subject to the *Quality Management Directive* (*QMD*) (BSC 2007 [DIRS 180474]). This document is primarily intended for internal use and technical guidance for a variety of design activities. It is recognized that a wide audience including project management, the United States Department of Energy (DOE), the United States Nuclear Regulatory Commission (NRC), and that others are interested to various levels of detail in the design methods and, therefore, the document covers a wide range of topics at varying levels of detail. Due to the preliminary nature of the design, readers can expect to encounter varied levels of detail in the body of the report. It is expected that project technical information used as input to design documents will be verified and taken from the latest versions of reference sources given herein.

The methodology report has evolved with changes in the waste package, emplacement pallet and drip shield designs over many years and will be further revised as the design is finalized. Different components and analyses are at different stages of development. Some parts of the report are detailed, while other, less detailed parts are likely to undergo further refinement. The design methodology is intended to provide designs that satisfy the safety and operational requirements of the YMP.

Three waste package configurations have been selected to illustrate the application of the methodology during the License Application (LA) process. These three configurations are the Transportation, Aging, and Disposal (TAD) canister bearing waste package, the 5–Defense High-Level Radioactive Waste (DHLW)/United States Department of Energy spent nuclear fuel (DOE SNF) short (5–DHLW/DOE SNF Short) co-disposal waste package, and the naval canistered SNF long (Naval SNF Long) waste package. Design work for the other four waste packages will be completed at a later date using the same design methodology. These include the TAD canister bearing long waste package, the 5–DHLW/DOE SNF Long co-disposal waste package, the DOE 2–Multi-Canister Overpack/2–Defense High-Level Radioactive Waste (2–MCO/2–DHLW) co-disposal waste package, and the naval canistered SNF short (Naval SNF Short) waste package.

This report is only part of the complete design description. Other reports related to the design include the Basis of Design document, the Project Design Criteria document, design reports,

drawings, manufacturing specifications, and numerous documents for the many detailed calculations. The relationships between this report and other project documents are shown in Figure A.

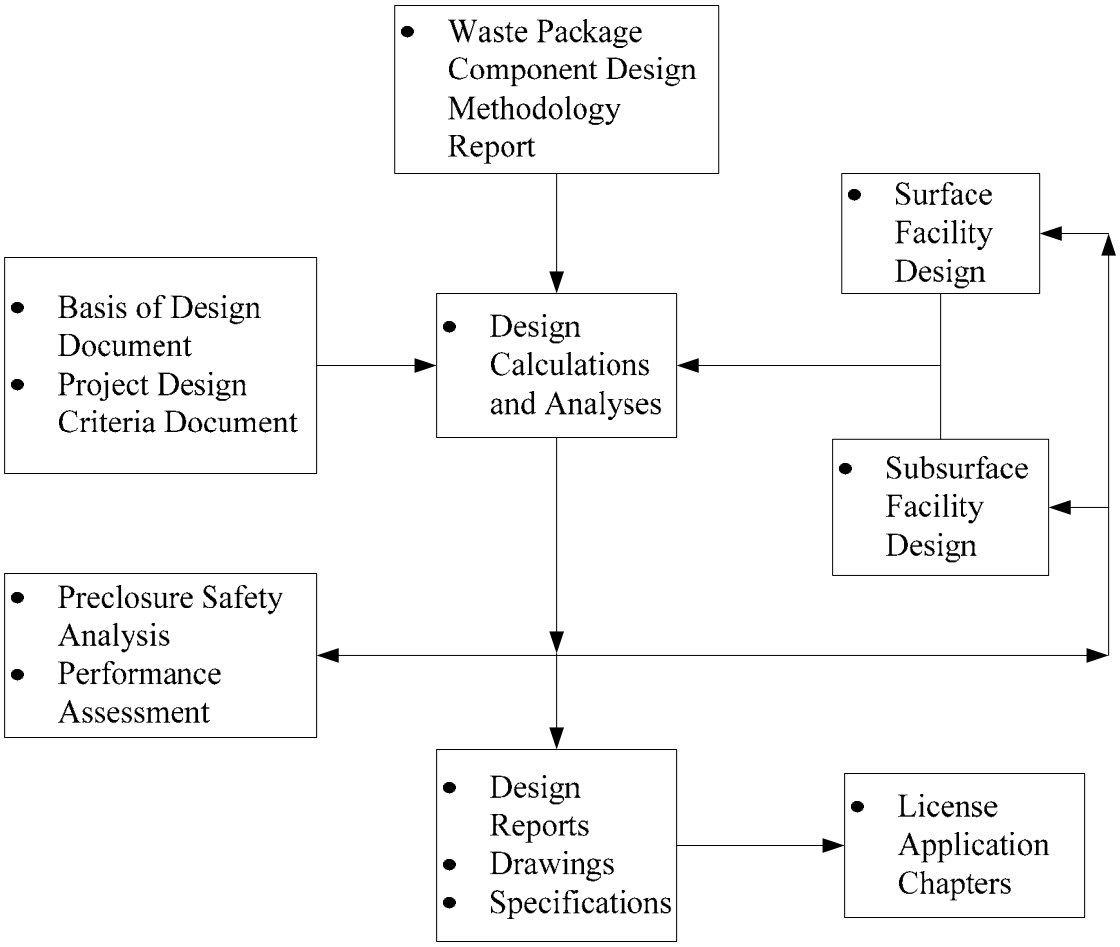

Figure A. Relationship between Methodology Report and other Design Documents

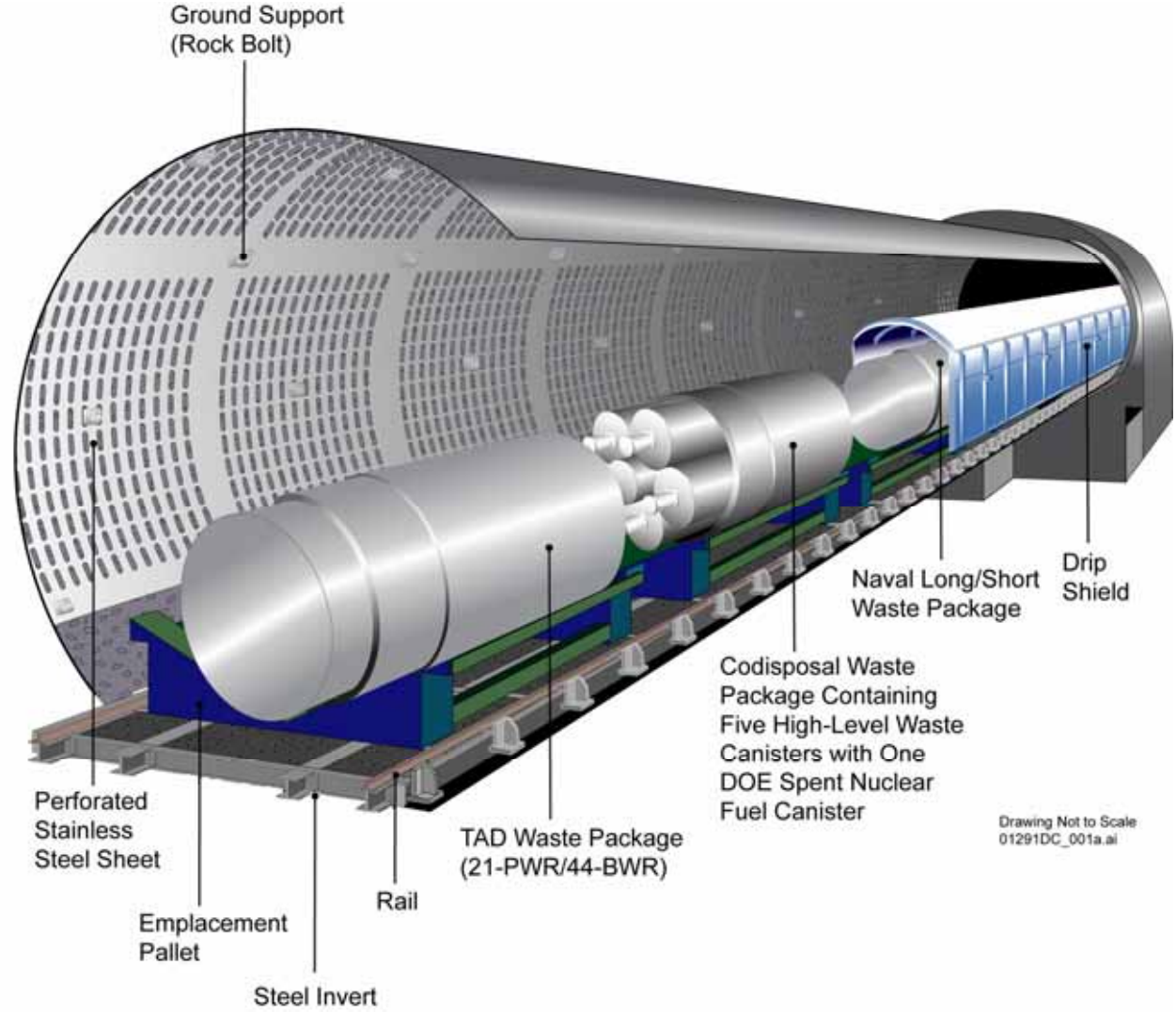

Figure B. Cutaway View of Different Waste Packages in a Repository Drift

Figure B shows a typical emplacement drift in the repository with waste packages beneath drip shields sitting on emplacement pallets, which rest on the steel invert structure. The invert structure will be packed with crushed tuff ballast (not shown in Figure B).

Overview of the Preliminary Waste Package Component Designs

This report applies to six specific waste package configurations and three ancillary components (viz. long and short emplacement pallets and drip shields). Different waste package configurations are designed for different waste forms and have different diameters, lengths, and in some cases internal structural arrangements. The internal structures, if present, separate waste canisters and provide structural support. The waste packages are supported by emplacement pallets and protected from dripping water and rock fall in the post-closure period by drip shields.

The fundamental design of waste packages applies to canistered SNF or HLW or both inside a dual cylinder comprised of an inner vessel (IV) and an outer corrosion barrier (OCB). Each end of the waste package has two lids, one for the inner vessel and one for the outer corrosion barrier. The sleeves at the ends of the waste package provide structural rigidity and serve as possible contact points for handling operations.

Design Methodology

The design methodology implemented can be viewed as: (1) understanding the requirements imposed on the design, (2) formulating a design concept, (3) gathering all the design input information, (4) making defensible assumptions, (5) selecting analytical methods and computational tools, and (6) demonstrating how design requirements are satisfied. Some iteration in this process occurs if compliance to the requirements cannot be comprehensively demonstrated, or if inputs to the design process, particularly those involving constraints imposed by other systems, structures, and components (SSCs) change. Each of these parts of the design methodology is quite extensive and discussed in subsequent detail in this report. The results of specific calculations and analyses performed using the design methodologies are contained in the design reports.

Design Requirements

A description of the requirements/processes hierarchy is included in Attachment I of procedure EG-PRO-3DP-G04B-00005, *Configuration Management*. Design requirements and regulations such as 10 CFR Part 63 [DIRS 176544], for the waste packages and ancillary components are included in the *Basis of Design for the TAD Canister-Based Repository Design Concept* (BOD) (Bechtel SAIC Company (BSC) 2006 [DIRS 177636]) and *Project Design Criteria Document* (PDC) (BSC 2006 [DIRS 178308]).

Design Evolution

The current design has progressed over many years as the Yucca Mountain Project (YMP) has evolved and will be further refined as the project matures.

The waste package has been designed using materials that perform well under the anticipated conditions at Yucca Mountain. The design analyses performed on the waste package include evaluation of the structural integrity, thermal performance, and shielding capability (*Yucca Mountain Project Conceptual Design Report* (CDR) (DOE 2006 [DIRS 176937], Section 2.4.4.2.3).

Design Inputs

In order to develop the necessary design output, detailed technical information and parameters are required, including radionuclide parameters, and structural and thermal properties of materials. Inputs are also developed by accounting for interfaces with other equipment and processes, the design responsibility for which belongs to other responsible organizations. Reference sources for design inputs are documented in the body of this report. These assure integration of the waste package into total engineering concept of operation.

Technical Information—Technical information includes, but is not limited to physical loadings, dimensions, masses, material properties, and radionuclide content. The physical forms, irradiation histories, and measured radionuclide content, among the commercial SNF, DOE SNF, and DHLW are used to generate source terms for pressurized water reactor (PWR) and boiling water reactor (BWR) commercial SNF, DOE SNF, and DHLW. Necessary technical information about the naval canister is obtained through an interface with the Naval Nuclear Propulsion Program (NNPP). Structural and thermal calculations use accepted mechanical and thermal properties from consensus national codes and standards, augmented by other appropriate sources where necessary.

Interfaces—Waste package component designs interface with other parts of the YMP, which include ties to fabrication and handling facilities. Some parts of the facilities design are in an early stage of development at the present time and will not be complete at the time of the License Application (LA) submittal. Additional design analyses will be performed as the total design matures and risks are evaluated. For example, in the passive component reliability methodology, average rather than minimum toughness properties are sought and "typical" properties from material vendors are utilized.

Assumptions

Design Assumptions—There are two categories of assumptions. The first category consists of generic assumptions that are part of a calculation process or computational tool. The second category is specific assumptions related to a particular analysis or calculation. The generic assumptions are detailed in the body of this report as well as some specific assumptions where more detail is needed for technical clarification of particular design issues. The assumptions documented in this report do not require verification.

Structural Analysis Assumptions—For a few materials, structural properties are not available but properties for materials with similar compositions are available and are used in their place. Structural calculations are based on nominal static properties, uniform strains and neglect strain rate effects. Generally bounding assumptions are made for temperature, coefficients of friction, boundary conditions, geometries, and orientations. Loading assumptions are required for external object impacts, drop events, transport events, rock falls, drift collapses, and natural events such as earthquakes (seismic motion). Risk-based demand considerations are included in these loading assumptions.

Thermal Analysis Assumptions—Thermal analysis of the waste package and ancillary components is performed on varying geometric scales, each with its own set of assumptions. For example, at the largest scale, a three-dimensional pillar representing a vertical segment of the mountain is used and assumes an average drift segment waste package distribution and thermal loading. Water movement through surrounding rock is not modeled explicitly, but is accounted for with a specific heat adjustment representing the latent heat of water as rock temperatures pass through the boiling point. At the smallest scale (waste package scale), a two-dimensional cross-section of the waste package taken at the mid-plane is analyzed and typically utilizes the highest heat load peaking factor and ignores axial conduction.

Source Term Assumptions—Commercial SNF source terms are approximated by calculating source terms for generic PWR and BWR assemblies at incremental enrichments and burnups and a generic burnup history (without the modeling of outages, intermittent down times, etc.) for fuel depletion calculations. The Babcock & Wilcox (B&W) Mark B 15 × 15 PWR fuel assembly is selected as the generic PWR lattice for analysis. This lattice has a high initial heavy metal loading and large amounts of stainless steel (SS) and Inconel assembly hardware, maximizing fission product generation and activation of structural hardware. For BWR commercial SNF, a General Electric (GE) 8 × 8 BWR fuel assembly is used. This design has a high initial heavy metal loading and an adequate amount of fuel assembly hardware. For PWR and BWR fuel, conservatively high fuel mass is added as increased length rather than increased density. An average uniform specific power over the entire length of the assembly is assumed, and the total irradiation interval is determined as the ratio of the assembly burnup to the specific power. It is assumed that the source terms can be generated for an array of various enrichments, burnups, and decay times and that interpolation can then be used to obtain the source terms of any specific assemblies in the waste stream without requiring explicit modeling of the assemblies. DOE SNF source terms are based on radionuclide inventories for several representative fuel types in the DOE SNF waste stream. For the DHLW, historical information regarding the inventory at the various sites is used in decay calculations to generate initial radionuclide inventories.

Shielding Assumptions—The composition of fresh fuel is used to represent the attenuation properties of spent fuel in shielding calculations. Because the radiation source terms assume burnup is uniformly distributed within a SNF assembly, an axial peaking factor or axial burnup profile is used for shielding analysis near the active fuel region. For three-dimensional shielding calculations, the contents and radiation sources of each waste type are uniformly homogenized with the internal structural components.

Analysis Methods and Computational Tools

Several calculations are performed to assure the chosen design(s) perform as expected. These calculations are made using several computer software packages specifically suited to each computational need.

Structural Calculations—Structural calculations demonstrate that the waste package, emplacement pallet, and drip shield meet the requirements for normal operations, and Category 1 and Category 2 event sequences. Structural calculations fall into the following broad groups:

- Normal Operations
- External Object Impacts
- Drops
- Transport Events
- Rock fall
- Seismic Motion

Waste packages, emplacement pallets, and drip shields can be represented with two-dimensional or three-dimensional finite element representations (FER's), depending on the symmetry of the design and the loading.

Thermal Calculations—Thermal calculations are performed to assure that waste form canister, waste package, and rock temperatures do not exceed maximum limits. Thermal analyses include calculations of all three modes of heat transfer: conduction, convection, and radiation. Thermal calculations are performed in one, two, or three dimensions; and at geometric scales ranging from waste package cross sections to pillar representations of a drift segment. Fire scenarios are analyzed to ensure WP survivability. In addition, loading calculations are performed to assure that the expected waste streams can be placed in waste packages, and then into emplacement drifts without violating thermal limits.

Source Term Calculations—Source term calculations provide heat generation rates, photon and neutron spectra and intensities, and radionuclide inventories of commercial SNF assemblies, DOE SNF, and DOE HLW. The thermal power values are used in thermal evaluations of the waste packages and the host rock of the repository. The photon and neutron sources are used to determine the ionizing radiation level surrounding a waste package. The radionuclide inventories are used to determine dose rates due to the release of radionuclides from the waste packages.

Shielding Calculations—For all waste package designs, radiation dose rates in the axial and radial directions are determined using segments of the waste package surfaces. The results of the shielding calculations allow an estimation of the average operation time of welding equipment, radiolysis-induced corrosion, and the radiation environment outside the waste packages for personnel access.

The details of the design methodology in the body of this report are organized around Design Requirements (Section 4), Design Inputs Parameters (Section 5), Design Assumptions (Section 6), and Analysis Methods and Computational Tools (Section 7). Within each of these sections, subsections are included for structural, thermal, source term, and shielding. The methodology should be considered together with information contained in other design reports, calculation reports, drawings, and specifications for specific design issues.

INTENTIONALLY LEFT BLANK

1. OBJECTIVE AND SCOPE

This report describes the design requirements, design inputs, assumptions, analytical methods, and computational tools used to establish the appropriateness of the design of waste package components. This methodology has progressed over many years as the Yucca Mountain Project (YMP) has evolved and will be refined as the project matures.

The purpose of this report is to document and ensure that appropriate design methods are used in the design of waste packages and ancillary components, viz., emplacement pallets and drip shields. The methodology includes identification of design requirements, selection of necessary design inputs, justification of design assumptions, and use of appropriate analysis methods and computational tools. The document is primarily intended for internal use as technical guidance for a variety of design activities. It is recognized that a wide audience including project management, the U.S. Department of Energy (DOE), the U.S. Nuclear Regulatory Commission (NRC), and others are interested to various levels of detail in the design methods. It is expected that project technical information used as input to design documents will be verified and taken from the latest versions of reference sources given herein.

The design methodology is intended to provide designs that satisfy the safety and operational requirements of the YMP. Three waste package configurations have been selected to illustrate the application of the methodology during the licensing process. These three configurations are the Transportation, Aging and Disposal (TAD) canister bearing waste package, the 5–Defense High-Level Waste/DOE Spent Nuclear Fuel short (5–DHLW/DOE SNF Short) co-disposal waste package, and the naval canistered SNF long (Naval SNF Long) waste package.

Design work for the other three waste packages will be completed at a later date using the same commensurate design methodology. These include the 5–DHLW/DOE SNF Long co-disposal waste package, the DOE 2–Multi-Canister Overpack/2–DHLW co-disposal (2–MCO/2–DHLW) waste package, and the naval canistered SNF short (Naval SNF Short) waste package.

The methodology report has evolved with changes in the waste package, emplacement pallet, and drip shield designs over many years and will be further revised as the design is finalized. This revision should be considered a “snapshot in time”. It incorporates changes in design methodology resulting from the baseline change to a TAD based repository. The various systems, structures and components and analyses are at different stages of development. Some parts of the report are detailed, while other less detailed parts will undergo further refinement.

This report is only part of the complete design description. Other documents related to the design include the requirement documents, design reports, design drawings and specifications, manufacturing specifications, and numerous documents for the many detailed calculations. The relationship between the *Waste Package Component Design Methodology Report* and other project documents is shown in Figure 1.

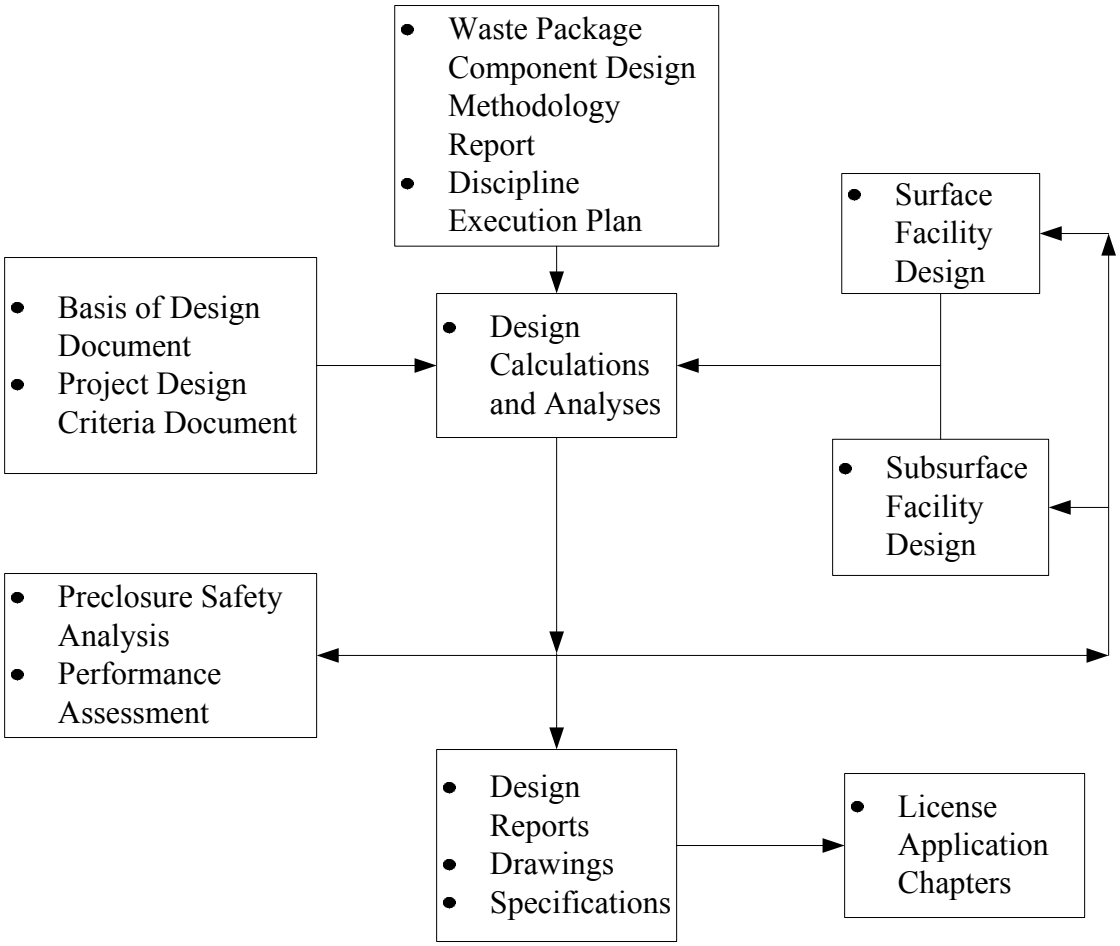

Figure 1. Relationship between Methodology Report and other Design Documents

Figure 2 shows a typical cutaway emplacement drift view in the repository with different waste packages beneath drip shields sitting on emplacement pallets, which rest on the steel invert structure. The invert structure will be packed with crushed tuff ballast (not shown in Figure 2). This report applies to six specific waste package configurations and ancillary components. Different waste package configurations accommodate different waste forms and canisters and have different diameters, lengths, and internal structural arrangements. The internal structures, if present, separate waste form and provide structural support. The waste packages are supported by emplacement pallets and protected from post-closure dripping water and rock fall by drip shields.

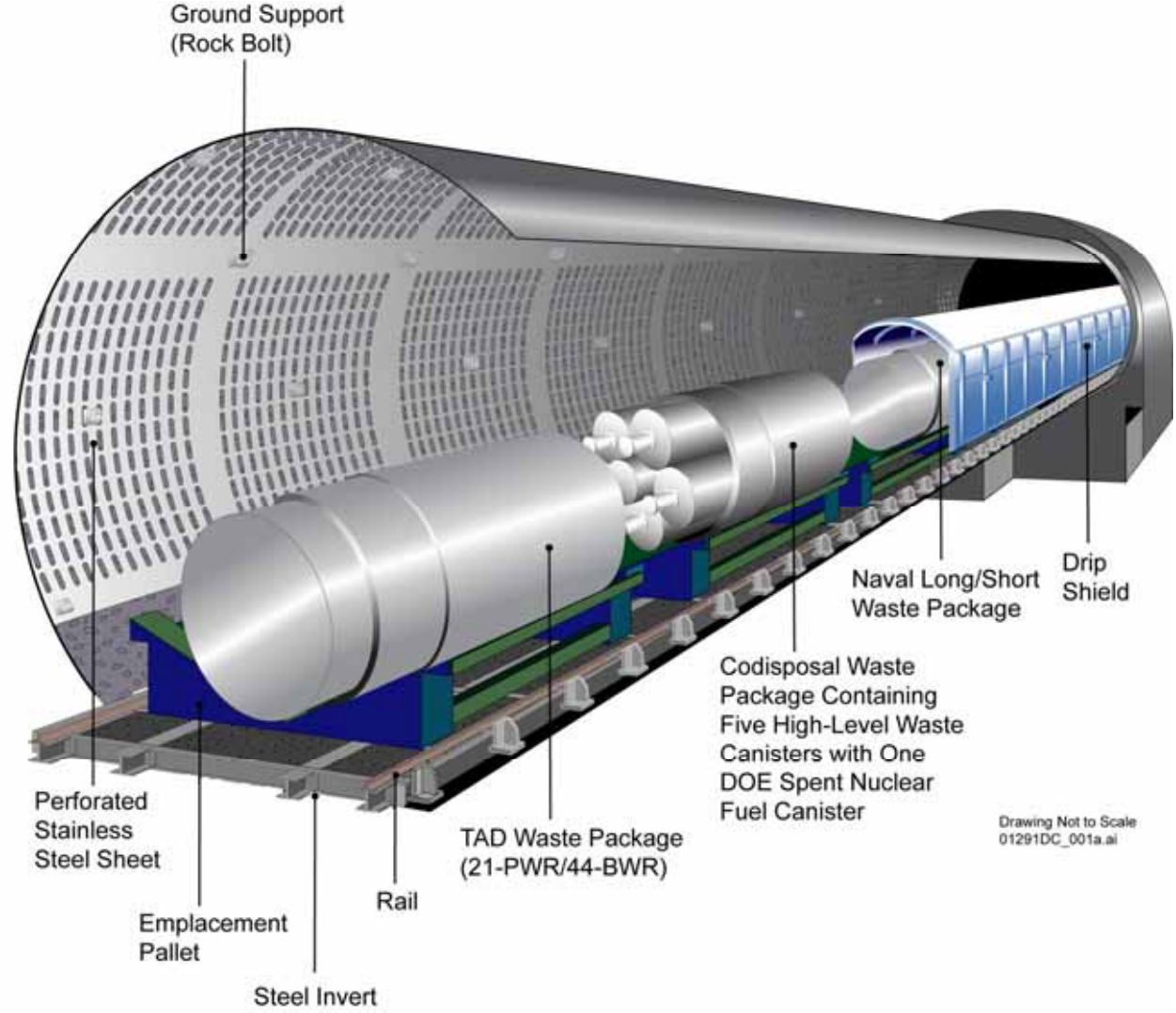

Figure 2. Cutaway View of Different Waste Packages in a Repository Drift

The fundamental design of the waste packages is a canistered waste form inside a dual cylinder comprised of an inner vessel and an outer corrosion barrier. Each end of the waste package has two lids, one for the inner vessel and one for the outer corrosion barrier. Sleeves at the ends of the waste package provide for structural rigidity as a bearing point for handling operations.

Design methodology can be viewed as: (1) considering the requirements imposed on the design, (2) formation of design concepts, (3) gathering all the design input information, (4) making defensible assumptions, (5) selecting analyses methods and computational tools, and (6) defining how design requirements are satisfied. Some iteration of this process occurs if compliance to the requirements cannot be comprehensively demonstrated, or if the inputs to the design process change, particularly those involving constraints imposed by other SSCs. Each of these parts of design methodology is extensive and discussed in detail in this report. The results of specific

calculations and analyses performed using the design methodology are summarized in the specific design reports.

The scope of this report includes computational methods for determining the source term, structural performance, thermal conditions, and shielding protection. The design inputs, assumptions, methods, and tools have been chosen to obtain designs that ensure defense-in-depth as well as satisfy requirements on system performance. Such requirements include those imposed by federal regulations from the DOE and the NRC, and those imposed by the YMP to meet repository performance goals.

The design methods and techniques described in this report are to be used in design activities producing input to the License Application of all waste package components. These include all waste package configurations, the emplacement pallets, and drip shields.

Waste package components are evaluated for the preclosure period. During preclosure the current requirements levied on the waste packages include prevention of breach during structural events and maintaining an environment for physical and chemical stability of the waste. Various structural and thermal analyses are performed to assure performance for normal operations and Category 1 and Category 2 event sequences. These analyses provide confidence that the waste packages will survive hazards such as external object impacts, drops, transport events, rock fall, seismic motion, and fires without breaching during preclosure. Evaluations of postclosure events are generally performed by the YMP Lead Laboratory.

2. QUALITY ASSURANCE

This document was prepared in accordance with PA-PRO-0313, *Technical Reports*. The waste package is classified as a safety category item (important to safety and important to waste isolation, ITS/ITWI) in the *Basis of Design for the TAD Canister-Based Repository Design Concept (*BOD*)* (BSC 2006 [DIRS 177636], Sections 11.1.2 and 12.1.2). The waste package emplacement pallet and the drip shield are also classified as safety category items (ITS/ITWI, and ITWI, respectively) in the BOD (BSC 2006 [DIRS 177636], Section 8.1.2). Therefore, this document is subject to the requirements of the *Quality Management Directive* (BSC 2007 [DIRS 180474], Sections 2.1.C.1.1.a.i., ii. and 17.E.) and the approved version is designated as QA:QA.

3. COMPUTER SOFTWARE AND MODEL USAGE

The only computational software used in this report is the commercially available Microsoft Office Excel 2003 (11.8117.8122) SP2 spreadsheet code (STN: 610236-2003-00), which is part of Microsoft Office Professional, hereinafter referred to as “Excel” in Appendix I. Excel was used to compute average values and to plot data. The results are verified by visual inspection. Excel was executed on an IBM Compatible PC running Microsoft Windows XP Professional operating system Version 2002 Service Pack 2.

No other computational software or models were used in the generation of this report; however, computer software that is used to implement the methodology presented in this report is described in detail in Section 7.

Design methods use several computer software packages, including:

- ANSYS V. 8.0. (HP-UX 11.0, HP-UX 11.22, Sun OS (operating system) OS 5.8. Software Tracking Number, STN: 10364-8.0-00), for many structural and thermal analysis calculations ([DIRS 170070])

- LS-DYNA V. 970.3858 D MPP. 2003. HP-UX 11.22. STN: 10300-970.3858 D MPP-00), for structural dynamic analysis calculations ([DIRS 166918]).

- TRUEGRID 2.3.0. STN: 610418-2.3.0-00, a general purpose mesh generation program

- LS-PREPOST 2.1. STN: 610463-2.1-00, for preparing input data for and processing the result from LS-DYNA

- Microsoft Excel 2000 (PC Windows 2000 OS, STN: 610236-2000-00).

- Microsoft Excel 2003 (PC Windows XP OS, STN: 610236-2003-00).

- Mathcad (PC Windows 2000/XP OS, STN: 611161-13-00), for solving systems of equations.

- FLUENT V. 6.0.12. 2003. HP-UX 11.00. STN: 10550-6.0.12-00, for convective flow and heat transfer calculations (Fluent, Inc. 2003 [DIRS 163001]).

- DriftFlow V. 1.0. 2002. Windows 2000. STN: 10722-1.0-00, for ventilation calculations [DIRS 163090].

- WPLOAD V. 2.0. 2007. Windows 2000 & Windows XP. STN: 11131-2.0-00. [DIRS 182947]

- SCALE V. 4.4A. 2000. HP. STN: 10129-4.4A-00, for shielding [DIRS 154394]

    - SAS2 module, for depletion analysis
    - ORIGEN-S module, for decay calculations

- MCNP V. 4B2LV. 1998. HP-UX 9.07 & 10.20, Windows 95, Solaris 2.6. CSCI: 30033-V4B2LV, for neutron/photon/electron transport for shielding calculations [DIRS 154060]

- MCNP V. 4B2LV. 2002. WINDOWS 2000. STN: 10437-4B2LV-00, for neutron/ photon / electron transport for shielding calculations [DIRS 163407]

The computer codes listed above (except Mathcad, Excel, TrueGrid, and LS-PREPOST which are exempt from qualification) are qualified under YMP Software Configuration Management (SCM) to assure quality of the software used in performing design calculations. These are the latest, but not only, versions of the software packages under SCM. Some calculations use earlier versions of the codes and other operating systems, and individual calculations document the actual version used. In the remainder of this document, the software is referred to by name only,

without specific version numbers and operating systems, but the controlled code versions at the time of the calculations are the only code versions used.

4. WASTE PACKAGE COMPONENT DESIGN REQUIREMENTS

The first levels of input to waste package component design are requirements established through a process starting with the *Nuclear Waste Policy Amendments Act of 1987. Public Law No. 100-203, 101 Statute 1330* [DIRS 100016]. These requirements are further developed into design requirements in upper tier requirement documents and assigned to SSCs through the BOD (BSC 2006 [DIRS 177636]).

4.1 REQUIREMENTS

Requirements for the repository originate within the DOE and are presented in the *Basis of Design for the TAD Canister-Based Repository Design Concept* (BOD) (BSC 2006 [DIRS 177636]). Laws and statutes, such as 10 CFR Part 63 [DIRS 176544], are included in these project level requirements. The BOD decomposes these requirements to the point that each can be assigned to SSCs as appropriate. An organization uses the requirement or further breaks it down by deriving daughter requirements. The BOD generates requirements based on functions of the repository. Some of these requirements will point to criteria in the *Project Design Criteria Document* (PDC) (BSC 2006 [DIRS 178308]). Criteria are the numerical values and other measures whereby satisfaction of the design requirements is demonstrated. Identifying criteria in the PDC assign the criteria to individual SSCs. Design criteria consist of the codes, standards, and general discipline design criteria that are specified for use on the project. SSCs of the repository are designed to specified requirements and derived internal constraints (e.g., *Postclosure Modeling and Analyses Design Parameters* (BSC 2007 [DIRS 179342]). These requirements will be incorporated in future revisions of the BOD.)

4.1.1 Design Philosophy

Requirements drive the design of the waste package, drip shield, and waste package emplacement pallet. There are two primary conditions or periods of concern. These are the preclosure period and the postclosure period. For preclosure, the waste package is relied on to contain the waste form within its boundary, support the prevention of nuclear criticality, and preserve the physical and chemical stability of the waste form. For postclosure, the waste package is relied on to restrict the transport of radionuclides to the outside of the waste package, greatly decrease the likelihood of criticality, and delay the degradation of the waste form. This document only addresses the preclosure period, except for the postclosure degraded emplacement pallet static analysis.

In order to show that the waste packages will perform their required functions adequately, many analyses must be performed. The design philosophy requires that the waste package survive external hazards such as object impacts, drops, transport events, rock fall, seismic motion, and fire without breaching. It must also show that the waste form stays within specified thermal limits throughout its life. A calculation is done in accordance with the *ASME Boiler and Pressure Vessel Code (includes 2002 addenda) (ASME B&PV)* (ASME 2001 [DIRS 158115]) to account for the pressure retention by the inner vessel under normal operations. Most calculations

are performed for conditions identified as beyond the design basis for the inner vessel and assure survivability of the outer corrosion barrier until replacement of the waste package following the accepted event sequence.

Structurally, waste packages consist of an *American Society of Mechanical Engineers (ASME) Nuclear Code* (NC), (ASME 2001 [DIRS 158115], Section III, Stamped Class 2) inner vessel (IV) of ASME SA-240 [UNS S31600] with additional controls on nitrogen and carbon, hereinafter termed as 316 SS, and an outer corrosion barrier (OCB) made of ASME SB-575 [UNS N06022], hereinafter referred to as Alloy 22 with limited constituents of 20.0 to 21.4 % Cr, 12.5 to 13.5 % Mo, 2.5 to 3.0 % W, and 2.0 to 4.5 % Fe (BSC 2007, [DIRS 179342], Table 1, Item 03-19) where Cr, Mo, W, Fe are Chromium, Molybdenum, Tungsten , and Iron respectively.

Shielding calculations determine ionizing radiation dose rates on waste package surfaces and in the vicinity of these surfaces. Radiation dose rate is a function of the radiation type, radiation energy spectrum and intensity, radiation interaction information, material compositions and densities, system geometry, and flux-to-dose rate conversion factors. Additionally, the radiation dose rate is dependent on the location of the detector.

The radiation source terms of the waste forms are an important input to shielding calculations. The radiation source terms consist of neutron and photon intensities as functions of their energies. The radiation source terms for commercial SNF have been generated for PWR and BWR fuel designs. These are contained in the following documents:

- *PWR Source Term Generation and Evaluation* (BSC 2004 [DIRS 169061])
- *BWR Source Term Generation and Evaluation* (BSC 2003 [DIRS 164364])

For HLW glass, photon and neutron, source terms are generated using the design basis glass developed at the Savannah River Site Defense Waste Processing Facility (SRS) and are provided in *Source Terms for HLW Glass* Canisters (BSC 2007 [DIRS 183163]). The SRS source terms are used in shielding evaluations because they are the highest of all HLW glass. If future changes result in a higher-level radioactive waste glass canister, it will be evaluated.

DOE SNF has been categorized into nine fuel groups:

1. Uranium Metal Fuels (N-Reactor fuel)
2. Uranium-Zirconium/Uranium-Molybdenum Fuels (Fermi Liquid Metal Reactor fuel)
3. Uranium Oxide Fuels (high enriched uranium fuels—Shippingport PWR fuel)
4. Uranium Oxide Fuels (low enriched uranium fuels—Three Mile Island-2 PWR fuel)
5. Uranium-Aluminum Fuels (Advanced Test Reactor)
6. Uranium/Thorium/Plutonium Carbide Fuels (Ft. St. Vrain Gas Cooled Reactor fuel)
7. Mixed Oxide Fuels (Fast Flux Test Facility Reactor fuel)
8. Uranium/Thorium Oxide Fuels (Shippingport Light Water Breeder Reactor fuel)
9. Uranium-Zirconium-Hydride Fuels (TRIGA fuel).

A representative fuel type is chosen as a bounding case for each group. Burnup, fissile enrichments, and total fuel mass determine the selection of the representative fuel used for shielding and criticality analysis.

The bounding source terms for each fuel group are provided in the following documents.

- *Evaluation of Codisposal Viability for Th/U Oxide (Shippingport LWBR) DOE-Owned Fuel* (CRWMS M&O 2000 [DIRS 151743])
- *Evaluation of Codisposal Viability for MOX (FFTF) DOE-Owned Fuel* (CRWMS M&O 1999 [DIRS 125206])
- *Evaluation of Codisposal Viability for U-Zr/U-Mo Alloy (Enrico Fermi) DOE-Owned Fuel* (CRWMS M&O 2000 [DIRS 151742])
- *Evaluation of Codisposal Viability for HEU Oxide (Shippingport PWR) DOE-Owned Fuel* (CRWMS M&O 2000 [DIRS 147651])
- *Evaluation of Codisposal Viability for UZrH (TRIGA) DOE-Owned Fuel* (CRWMS M&O 2000 [DIRS 147650])
- *Evaluation of Codisposal Viability for U-Metal (N Reactor) DOE-Owned Fuel* (CRWMS M&O 2001 [DIRS 154194])
- *Evaluation of Codisposal Viability for Th/U Carbide (Fort Saint Vrain HTGR) DOE-Owned Fuel* (BSC 2001 [DIRS 157734])
- *Specification for Advanced Test Reactor Mark VII Zone Loaded Fuel Elements* (INEEL 2003 [DIRS 171506])
- *TMI Fuel Characteristics for Disposal Criticality Analysis* (DOE 2003 [DIRS 164970], Table D-1)

4.1.2 Codes and Standards

Some codes and standards are imposed through the *Project Design Criteria Document* (BSC 2006 [DIRS 178308]), while the design engineer selects others. Codes and standards include industry codes such as the *ASME B&PV* (includes 2002 addenda) (ASME 2001 [DIRS 158115]) and standards such as those published by American National Standards Institute (ANSI). Publications by the NRC are included, which consist of:

- Regulatory Guides—Rules for specific areas of concern that if followed are acceptable ways to meet NRC requirements
- NRC Regulation Reports (NUREGs)—Guidance documents from the NRC

- NUREG/Contractor Reports (NUREG/CRs)—Information published by the NRC. For example, *Yucca Mountain Review Plan, Final Report*. NUREG-1804 (NRC 2003 [DIRS 163274]) is used to ensure that items identified by the NRC are addressed.

- "Interim Staff Guidance (ISG)", which are treated as De Facto regulatory guides.

4.1.2.1 Commitment Codes and Standards

- *ASME B&PV* (ASME 2001 [DIRS 158115], Section III, Division 1) is used for construction of the inner vessel.

- ANSI N14.6-1993 [DIRS 102016] addresses lifting devices for large radioactive packages (Note that this standard has been withdrawn, pending revision; however, it still provides guidance for acceptable performance).

- ANSI/ANS-6.1.1-1977 [DIRS 107016] presents flux-to-dose rate conversion factors for neutron and gamma radiation.

4.1.2.2 Accepted Source or Guidance

Structural:

- NUREG-0612 (NRC 1980 [DIRS 104939]) describes the requirements for lifting and handling large packages such as waste packages.

Thermal:

- *ASME B&PV* (ASME 2001 [DIRS 158115], Section III, Division 1, Subsection NB–1120) sets temperature limits for structural alloys.

Source Term and Shielding:

- NUREG/CR-5625 (Hermann et al. 1994 [DIRS 154045]) provides technical support for the NRC decay heat guide using the SAS2H and ORIGEN-S analysis sequence of the SCALE system

- NUREG-1536 (NRC 1997 [DIRS 101903]) provides guidance for evaluating shielding of SNF packages

- NUREG-1617 (NRC 2000 [DIRS 154000]) provides guidance for evaluating shielding of SNF packages

- NUREG-1567 (NRC 2000 [DIRS 149756]) provides guidance for evaluating shielding of SNF packages

4.1.3 Use of Codes and Standards

4.1.3.1 Structural Codes and Standards

The *ASME B&PV (includes 2002 addenda)* (ASME 2001 [DIRS 158115]) is used for design and fabrication of the inner vessel. This is consistent with the NRC requirements to use codes and standards based on accepted industry technology (NRC 2003 [DIRS 163274]).

The Yucca Mountain Project waste package inner vessel (IV) thickness is determined by the postulated accident loads. Therefore it will satisfy the ASME B&PV Code Design Loads that are based on pressure and loaded dead weight. The IV will be fabricated in accordance with all provisions of the *ASME B&PV* (ASME 2001 [DIRS 158115]), Section III, Division 1, Class 2 Code requirements including application of the ASME Nuclear Code Symbol Stamp (ASME 2001 [DIRS 158115]). The ASME design work will be performed by an ASME Designer of Record, and not by Bechtel SAIC Company, LLC.

The outer vessel made of Alloy 22 specifically included as a corrosion barrier and is not a pressure vessel; however it does possess inherent capabilities for pressure retention. Nevertheless, it will be constructed in accordance with specific applicable *ASME B&PV* (ASME 2001 [DIRS 158115]) Section III technical requirements including the material, fabrication, and examination requirements and in accordance with selected administrative requirements of the *ASME B&PV* (ASME 2001 [DIRS 158115]). The postulated loads from the nuclear safety design basis will be evaluated against appropriate criteria. For example, the stress intensity (SI) limits of Appendix F of the *ASME B&PV* (ASME 2001 [DIRS 158115]) are used for a deterministic calculation of failure margin under extreme loads. The OCB will be fabricated in accordance with the applicable specified provisions of ASME *B&PV* (ASME 2001 [DIRS 158115]) NC-2000 (Materials), NC-4000 (Welding), and NC-5000 (Nondestructive Examination).

The waste form is placed within the inner vessel (IV), which in some configurations is partitioned by divider plates to separate and isolate waste in canisters. Where present, divider plates facilitate loading of the canistered waste forms and aid in transferring heat from the fuel to the outside and support the canisters during structurally dynamic event sequences.

The *ASME B&PV* (ASME 2001 [DIRS 158115], Section III, Division I), Subsection NC was selected for the code-compliant design and fabrication of the waste packages. The implementation of the ASME Code [DIRS 158115] is described in *BSC Position on the Use of the ASME Boiler and Pressure Vessel Code for the Yucca Mountain Waste Packages* (BSC 2007 [DIRS 182357]). For the code design, the only part of the waste package considered to be a pressure vessel is the stainless steel type 316 [UNS S31600] with additional controls on nitrogen and carbon, hereinafter referred to as 316 SS, inner vessel. For all other components of the waste package, the *ASME B&PV* (ASME 2001 [DIRS 158115]) is used as guidance, either through the use of conservative material properties or conservative stress intensity (SI) limits.

While the seal welds are anticipated to be sound welds, at present no credit for resistance against dynamic events is taken. Therefore, for dynamic structural events, where the inner vessel in the vicinity of the seal welds may be reasonably anticipated to experience considerable loads, these

welds are not credited to maintain the hermeticity of the inner vessel. It is anticipated that future development of this report will introduce techniques for taking credit for these welds. To maintain containment of the waste form, it must be shown that the OCB not breach.

A passive component reliability evaluation is also conducted on the waste package and ancillary components for severe events. This is described in Section 7.1.7 of this report.

The waste package emplacement pallet is considered as a Class 2 vessel plate-type support. The ASME B&PV Code (ASME 2001 [DIRS 158115]) Subsection NF-3000 governs the code compliance design of the emplacement pallet. An elastic analysis based on the maximum stress intensity and allowable limits contained in NF-3220 is performed.

The following are specific applications of structural standards used in the design.

ASME B&PV Code Case N-621 (ASME 2001 [DIRS 158115]) provides the material allowables for the emplacement pallet. Specifically, this code case provides the values of the Class 1 design stress intensity (S_m).

NUREG-0612 (NRC 1980 [DIRS 104939]) describes the requirements for lifting and handling of heavy loads such as the waste packages. The standard explicitly applies to heavy loads lifted near or over spent fuel pools at nuclear reactor facilities but is also applied to aging and transport cask lifting devices. Thus, the standard can be applied to the waste package. NUREG-0612 specifies that all components that participate in the load path must be designed to a safety factor of six against the yield and a factor of ten against the ultimate stress. The standard implicitly includes a dynamic factor to account for "bounce" when lifting and lowering large objects. The standard permits load splitting between redundant load paths, so that if a redundant lifting yoke is used, a factor of three against yield strength is used for each separate yoke and a factor of five against ultimate strength is applied. These factors ensure that structural failure of lifting components will not occur in normal conditions, but it is the responsibility of the facility personnel to ensure that the lifting attachments are securely engaged to the large package. A positive means of verification of lifting fixture engagement is necessary, and in general, it is necessary to provide a flat surface to set the package on. Guide plates to center a waste package in a specific location in a pool or dry location are not recommended as such guide devices have caused disengagement of the lifting fixtures for aging cask systems. The particular form of engagement of the lifting fixtures and the waste package is not specified by the standard; only the structural load path requirements are specified.

4.1.3.2 Thermal Codes and Standards

Methods of thermal analysis are discussed in various standard review plans. NUREG-1536 (NRC 1997 [DIRS 101903]) and NUREG-1567 (NRC 2000 [DIRS 149756]) discuss aging, and NUREG-1617 (NRC 2000 [DIRS 154000]) discusses transportation.

A reference relevant to SNF aging at the repository surface facility is *Recommended Temperature Limits for Dry Storage of Spent Light Water Reactor Zircaloy-Clad Fuel Rods in Inert Gas* (Levy et al. 1987 [DIRS 144349]). This publication provides methods for evaluation of fuel rod pressure at elevated temperatures and provides temperature limits for a desired forty-year aging period. The ability of irradiated Zircaloy cladding to provide a barrier against the

release of radioactive material is evaluated as a function of thermal damage to the cladding. Damage is expressed in terms of diffusion-controlled cavity growth of micro-flaws in the Zircaloy matrix. *Interim Staff Guidance – 11* (ISG-11) Rev 3. "*Cladding Considerations for the Transportation and Storage of Spent Fuel*" (NRC 2003 [DIRS 170332]) provides guidance on use of fixed cladding temperature limits for SNF.

The thermal design of the waste packages is based on temperature limits given in the BOD (BSC 2006 [DIRS 177636]) and other documents (BSC 2007 [DIRS 179342], and DOE 2007 [DIRS 178792]).

DOE SNF must remain below 350°*C* and 400°*C* for zircaloy and stainless steel claddings, respectively (BSC 2006 [DIRS 177636], Section 11.2.2.18). Commercial spent nuclear fuel (CSNF) cladding must remain below 350°*C* upon emplacement (BSC 2006 [DIRS 179342], Item 04-05) and below 400°*C* (BSC 2006 [DIRS 177636], Section 11.2.3.4.3) during normal operations. For off-normal conditions CSNF cladding must remain below 570°*C* (BSC 2006 [DIRS 177636], Section 11.2.3.4.3). HLW (vitrified) glass must remain below 400°*C* (BSC 2007 [DIRS 179342], Items 04-06 and 06-05). DOE standard canisters must remain below 148.9°*C* in an open environment and below 315.5°*C* in a closed environment (DOE 2007 [DIRS 178792], Section 10.1.3). MCO canisters must remain below 132°*C* for either enclosed or open environments (DOE 2007 [DIRS 178792], Section 10.2.3).

4.1.3.3 Source Term and Shielding Codes and Standards

Standards for performing shielding and source term calculations include Code of Federal Regulations, American National Standards Institute standards, and NRC Regulatory Guides and NUREG reports. The nuclear engineering codes and standards applicable to the YMP are listed in the *Project Design Criteria Document* (BSC 2006 [DIRS 178308], Section 4.10.1). Shielding and source term methodologies follow the recommendations of appropriate NUREG's to ensure compliance with applicable American National Standards Institute (ANSI) standards and NRC Regulatory Guides.

Flux-to-dose rate conversion factors are taken from ANSI/ANS-6.1.1-1977 [DIRS 107016] for Monte-Carlo N-Particle (MCNP) shielding calculations (Section 7.4.1.3). For SAS1 shielding calculations (Section 7.4.1.4), the flux-to-dose rate conversion factors are contained in the computer code packages (the default neutron and photon-to-dose rate conversion factors comes from ANSI/ANS-6.1.1-1977 [DIRS 107016]).

4.2 INTERFACE WITH OTHER PROJECT ORGANIZATIONS

Waste package, emplacement pallet, and drip shield design inputs are dependent on several parallel tasks including facility design, preclosure safety analysis, and fabrication methods. Interface Exchange Drawings (IED) define the interfaces with the Lead Laboratory.

4.2.1 Configuration Interfaces

Interface control drawings define the interfaces for waste package components with facilities and the engineered barrier system. Interface controls that delineate the design responsibilities of the

Thermal/Structural Analysis Discipline and Subsurface Design Project and other organizations are developed as necessary.

5. MATERIAL PROPERTIES INFORMATION AND PARAMETERS

In order to develop the necessary design output, additional information and parameters are required, including radionuclide parameters and structural and thermal properties of materials. Finally, inputs are developed through interfaces with equipment and processes assigned to other organizations. The next three subsections will describe the source of the requirements, information and parameters, and interface inputs.

The contents of this section provide references to sources identifying the various input parameters. The versions of references are appropriate for use. More recent versions of these references may be acceptable. The TSA DEM will make a determination of suitability as required. Often the given reference is preferable over the more recent due to ease of availability of the reference in the project systems.

A considerable amount of technical information and parameters are needed as input to waste package, emplacement pallet, and drip shield design. The inputs are used in structural, thermal, source term, and shielding analyses.

5.1 STRUCTURAL

The technical data and parameters for structural calculations include the mechanical properties of the selected materials based on the configuration of the surface facility and engineered barrier systems. The geometry of the waste package, emplacement pallet, and drip shield are used in the process. These structural parameters are varied appropriately to assure that designs comply with the governing requirements.

5.1.1 Mechanical Material Properties

Sources for values of the mechanical material properties used in the deterministic structural analyses are listed in Table 1. Discussions on the use of some of the material properties listed in this table are provided in Section 6. Other mechanical material properties used in the passive component reliability methodology are discussed separately in Section 7.1.7 and Appendix I. ASME stress compliance material properties are given in a document entitled *Material Properties for Waste Package ASME Stress Compliance*, (BSC 2007 [DIRS 182724]).

5.1.2 Dimensional and Material Variability

Most structural calculations assume the nominal or minimum thicknesses for the inner vessel and outer corrosion barrier. A few calculations evaluate the sensitivity of the end products to fabrication variability.

Available minimum material strength properties are used to ensure conservative deterministic assessments due to material variability. Passive component reliability assessments are based on average material strength properties with a material variability factored into the assessment.

When available, material properties that are temperature dependent are used for variable temperature environment calculations.

Table 1. Sources of Material Properties for Structural Analyses

Material Property	Source
316 SS with modified carbon and nitrogen (IV, spread and interface rings, purge port cap, lids, EP tubes)	
Density (ρ)	*Standard Practice for Preparing, Cleaning, and Evaluating Corrosion Test Specimens* (ASTM G 1-90 1999 [DIRS 103515], Table X1.1)
Yield Strength (S_y)	*2001 ASME Boiler and Pressure Vessel Code (includes 2002 addenda)* (ASME 2001 [DIRS 158115], Section II, Part D, Table Y-1) *Corrosion. Volume 13 of Metals Handbook* (ASM International 1987 [DIRS 103753], p. 931). This document is used to determine chemical composition of 316 Stainless Steel
Ultimate Tensile Strength (S_u)	*2001 ASME Boiler and Pressure Vessel Code (includes 2002 addenda)* (ASME 2001 [DIRS 158115], Section II, Part D, Table U) *Corrosion. Volume 13 of Metals Handbook* (ASM International 1987 [DIRS 103753], p. 931). This document is used to determine chemical composition of 316 Stainless Steel
Percentage Elongation	*2001 ASME Boiler and Pressure Vessel Code (includes 2002 addenda)* (ASME 2001 [DIRS 158115], Section II, Part A, SA-240, Table 2), which presents specifications for heat-resisting chromium and chromium-nickel SS plate, sheet, and strip for pressure vessels *Technical Data Blue Sheet, Stainless Steels, Chromium-Nickel-Molybdenum, Types 316 (S31600), 316L (S31603), 317 (S31700), 317L (S31703)* (Allegheny Ludlum 1999 [DIRS 151409], p. 8)
Elastic Modulus (E)	*2001 ASME Boiler and Pressure Vessel Code (includes 2002 addenda)* (ASME 2001 [DIRS 158115], Section II, Part D, Table TM-1)
Mean Coefficient of Thermal Expansion	*2001 ASME Boiler and Pressure Vessel Code (includes 2002 addenda)* (ASME 2001 [DIRS 158115], Section II, Part D, Table TE-1)
Poisson's Ratio (v)	*Properties and Selection: Stainless Steels, Tool Materials and Special-Purpose Metals. Volume 3 of Metals Handbook* (ASM 1980 [DIRS 104317], Figure 15, p. 755)
TSw2 Rock	
Density (ρ)	Reference Information Base Data Item: *IED Geotechnical and Thermal Parameters IV [Sheet 1 of 1]* (BSC 2007 [DIRS 179808], Table 1).
ASME SA-240 [UNS S31603] (316L SS) (Naval and DOE Canisters)	
Density (ρ)	*Standard Practice for Preparing, Cleaning, and Evaluating Corrosion Test Specimens* (ASTM G 1-90 1999 [DIRS 103515], Table X1.1)
Yield Strength (S_y)	*2001 ASME Boiler and Pressure Vessel Code (includes 2002 addenda)* (ASME 2001 [DIRS 158115], Section II, Part D, Table Y-1)
Ultimate Tensile Strength (S_u)	*2001 ASME Boiler and Pressure Vessel Code (includes 2002 addenda)* (ASME 2001 [DIRS 158115], Section II, Part D, Table U)
Percentage Elongation	*2001 ASME Boiler and Pressure Vessel Code (includes 2002 addenda)* (ASME 2001 [DIRS 158115], Section II, Part A, SA-240. Table 2)
Elastic Modulus (E)	*2001 ASME Boiler and Pressure Vessel Code (includes 2002 addenda)* (ASME 2001 [DIRS 158115], Section II, Part D, Table TM-1)
Poisson's Ratio (v)	*Properties and Selection: Stainless Steels, Tool Materials and Special-Purpose Metals*. Volume 3 of *Metals Handbook* (ASM 1980 [DIRS 104317], Figure 15, p. 755). Poisson's ratio for 316 SS will be used for 316L SS (Assumption 6.1.1.9).

Table 1. Sources of Material Properties for Structural Analyses (Continued)

Material Property	Source
ASME SA-516 [UNS K02700] (A 516, Grade 70) (WP Guides)	
Density (ρ)	*2001 ASME Boiler and Pressure Vessel Code (includes 2002 addenda)* (ASME 2001 [DIRS 158115], Section II, Part A, SA-20, Section 14.1), which presents specifications for pressure vessel plates, carbon steel, for moderate- and lower-temperature service
Yield Strength (S_y)	*2001 ASME Boiler and Pressure Vessel Code (includes 2002 addenda)* (ASME 2001 [DIRS 158115], Section II, Part D, Table Y-1)
Ultimate Tensile Strength (S_u)	*2001 ASME Boiler and Pressure Vessel Code (includes 2002 addenda)* (ASME 2001 [DIRS 158115], Section II, Part D, Table U)
Percentage Elongation	*2001 ASME Boiler and Pressure Vessel Code (includes 2002 addenda)* (ASME 2001 [DIRS 158115], Section II, Part A, SA-516, Table 2)
Elastic Modulus (E)	*2001 ASME Boiler and Pressure Vessel Code (includes 2002 addenda)* (ASME 2001 [DIRS 158115], Section II, Part D, Table TM-1)
Mean Coefficient of Thermal Expansion	*2001 ASME Boiler and Pressure Vessel Code (includes 2002 addenda)* (ASME 2001 [DIRS 158115], Section II, Part D, Table TE-1)
Poisson's Ratio (v)	*Properties and Selection: Irons and Steels*. Volume 1 of *Metals Handbook* (ASM 1978 [DIRS 102018], p. 393), which provides Poisson's ratio for cast carbon steel that will be used for SA-516 carbon steel (Assumption 6.1.1.8)
ASME SB-265 [UNS R52400] (Ti Grade 7) (Drip Shield)	
Density (ρ)	*2001 ASME Boiler and Pressure Vessel Code (includes 2002 addenda)* (ASME 2001 [DIRS 158115], Section II, Part D, Table NF-2) *Properties and Selection: Nonferrous Alloys and Special-Purpose Materials. Volume 2 of ASM Handbook* (ASM International 1990 [DIRS 141615], Table 20, p. 620)
Yield Strength (S_y)	*2001 ASME Boiler and Pressure Vessel Code (includes 2002 addenda)* (ASME 2001 [DIRS 158115], Section II, Part D, Table Y-1)
Ultimate Tensile Strength (S_u)	*2001 ASME Boiler and Pressure Vessel Code (includes 2002 addenda)* (ASME 2001 [DIRS 158115], Section II, Part B, SB-265, Table 1), which provides specifications for titanium and titanium alloy strip, sheet, and plate
Percentage Elongation	*2001 ASME Boiler and Pressure Vessel Code (includes 2002 addenda)* (ASME 2001 [DIRS 158115], Section II, Part B, SB-265, Table 1), which provides specifications for titanium and titanium alloy strip, sheet, and plate
Elastic Modulus (E)	*2001 ASME Boiler and Pressure Vessel Code (includes 2002 addenda)* (ASME 2001 [DIRS 158115], Section II, Part D, Table TM-5)
Mean Coefficient of Thermal Expansion	*2001 ASME Boiler and Pressure Vessel Code (includes 2002 addenda)* (ASME 2001 [DIRS 158115], Section II, Part D, Table TE-5)
Poisson's Ratio (v)	*2001 ASME Boiler and Pressure Vessel Code (includes 2002 addenda)* (ASME 2001 [DIRS 158115], Section II, Part D, Table NF-1) *Properties and Selection: Nonferrous Alloys and Special-Purpose Materials*. Volume 2 of *ASM Handbook* (ASM International 1990 [DIRS 141615], Table 21, p. 621)

Table 1. Sources of Material Properties for Structural Analyses (Continued)

Material Property	Source
ASME SB-265 [UNS R56404] (Ti Grade 29) (Drip Shield Structural Members)	
Density (ρ)	*Properties and Selection: Nonferrous Alloys and Special-Purpose Materials*. Volume 2 of *ASM Handbook* (ASM International 1990 [DIRS 141615], Table 20, p. 620).
Yield Strength (S_y)	*2001 ASME Boiler and Pressure Vessel Code (includes 2002 addenda)* (ASME 2001 [DIRS 158115], Section II, Part B, SB-265, Table 3), which provides specifications for titanium and titanium alloy strip, sheet, and plate
Ultimate Tensile Strength (S_u)	*2001 ASME Boiler and Pressure Vessel Code (includes 2002 addenda)* (ASME 2001 [DIRS 158115], Section II, Part B, SB-265, Table 1), which provides specifications for titanium and titanium alloy strip, sheet, and plate
Percentage Elongation	*2001 ASME Boiler and Pressure Vessel Code (includes 2002 addenda)* (ASME 2001 [DIRS 158115], Section II, Part B, SB-265, Table 1)
Elastic Modulus (E)	*Properties and Selection: Nonferrous Alloys and Special-Purpose Materials*. Volume 2 of *ASM Handbook* (ASM International 1990 [DIRS 141615], Table 21, p. 621)
Mean Coefficient of Thermal Expansion	*Properties and Selection: Nonferrous Alloys and Special-Purpose Materials*. Volume 2 of *ASM Handbook* (ASM International 1990 [DIRS 141615], Table 20, p. 620)
Poisson's Ratio (v)	*Properties and Selection: Nonferrous Alloys and Special-Purpose Materials*. Volume 2 of *ASM Handbook* (ASM International 1990 [DIRS 141615], Table 21, p. 621).
Alloy 22 (OCB, EP Plates, Drip Shield Base and Stabilization Pin)	
Density (ρ)	*2001 ASME Boiler and Pressure Vessel Code (includes 2002 addenda)* (ASME 2001 [DIRS 158115], Section II, Part B, SB-575, Section 7.1), which provides specifications for low-carbon nickel-molybdenum-chromium, low-carbon nickel-chromium-molybdenum, low-carbon nickel-chromium-molybdenum-copper, and low-carbon nickel-chromium-molybdenum-tungsten alloy plate, sheet, and strip
Yield Strength (S_y)	*2001 ASME Boiler and Pressure Vessel Code (includes 2002 addenda)* (ASME 2001 [DIRS 158115], Section II, Part D, Table Y-1) Hastelloy C-22 Alloy (Haynes International 1997 [DIRS 100896], p. 15) INCONEL Alloy 22. (Special Metals Corporation 2006, Publication Number SMC-049 [DIRS 182449] p. 2, Table 4) INCONEL Alloy 622. (Inco Alloys International 1995. Product Handbook. [DIRS 182441], p. 1, Table 3)
Ultimate Tensile Strength (S_u)	*2001 ASME Boiler and Pressure Vessel Code (includes 2002 addenda)* (ASME 2001 [DIRS 158115], Section II, Part D, Table U) Hastelloy C-22 Alloy (Haynes International 1997 [DIRS 100896], p. 15) INCONEL Alloy 22. (Special Metals Corporation 2006, Publication Number SMC-049 [DIRS 182449] p. 2, Table 4) INCONEL Alloy 622. (Inco Alloys International 1995. Product Handbook. [DIRS 182441], p. 1, Table 3)

Table 1. Sources of Material Properties for Structural Analyses (Continued)

Material Property	Source
Percentage Elongation	*2001 ASME Boiler and Pressure Vessel Code (includes 2002 addenda)* (ASME 2001 [DIRS 158115], SB-575, Table 3), which provides specifications for low-carbon nickel-molybdenum-chromium, low-carbon nickel-chromium-molybdenum, low-carbon nickel-chromium-molybdenum-copper, and low-carbon nickel-chromium-molybdenum-tungsten alloy plate, sheet, and strip Hastelloy C-22 Alloy (Haynes International 1997 [DIRS 100896], p. 15) INCONEL Alloy 22 (Special Metals Corporation 2006, Publication Number SMC-049 [DIRS 182449] p. 2, Table 4) INCONEL Alloy 622 (Inco Alloys International 1995. Product Handbook. [DIRS 182441], p. 1, Table 3)
Elastic Modulus (E)	Hastelloy C-22 Alloy (Haynes International 1997 [DIRS 100896], p. 14)
Mean Coefficient of Thermal Expansion	Hastelloy C-22 Alloy (Haynes International 1997 [DIRS 100896], p. 13)
Poisson's Ratio (v)	*Properties and Selection: Stainless Steels, Tool Materials and Special-Purpose Metals*. Volume 3 of *Metals Handbook* (ASM 1980 [DIRS 104317], p. 143). Poisson's ratio for Alloy 625 is used for Alloy 22 (Assumption 6.1.1.7)
ASME SA-240 [UNS S30400] 304 SS properties used for 304L SS (MCO/DHLW Canister)	
Density (ρ)	*Standard Practice for Preparing, Cleaning, and Evaluating Corrosion Test Specimens* (ASTM G 1-90 1999 [DIRS 103515], Table X1.1)
Yield Strength (S_y)	*2001 ASME Boiler and Pressure Vessel Code (includes 2002 addenda)* (ASME 2001 [DIRS 158115], Section II, Part D, Subpart 1, Table Y-1)
Ultimate Tensile Strength (S_u)	*2001 ASME Boiler and Pressure Vessel Code (includes 2002 addenda)* (ASME 2001 [DIRS 158115], Section II, Part D, Table U)
Percentage Elongation	*2001 ASME Boiler and Pressure Vessel Code (includes 2002 addenda)* (ASME 2001 [DIRS 158115], Section II, Part A, SA-240, Table 2)
Elastic Modulus (E)	*2001 ASME Boiler and Pressure Vessel Code (includes 2002 addenda)* (ASME 2001 [DIRS 158115], Section II, Part D, Subpart 2, Table TM-1)
Mean Coefficient of Thermal Expansion	*2001 ASME Boiler and Pressure Vessel Code (includes 2002 addenda)* (ASME 2001 [DIRS 158115], Section II, Part D, Table TE-1)
Poisson's Ratio (v)	*Properties and Selection: Stainless Steels, Tool Materials and Special-Purpose Metals*. Volume 3 of *Metals Handbook* (ASM 1980 [DIRS 104317], p. 755).

5.2 THERMAL

As is the case for structural analyses, the engineering designs of the waste package, emplacement pallet, drip shield, and surface facilities are also input to the thermal analyses. In addition, the thermal properties for the design materials and the configuration of the natural system are needed for thermal analyses. Waste stream arrival scenarios are needed for loading simulations.

5.2.1 Thermal Material Properties

The material properties used in thermal analyses are from references listed in Table 2.

5.2.2 Dimensional and Material Variability

Most thermal calculations assume the nominal thicknesses for the inner vessel and outer corrosion barrier.

Table 2. Sources of Material Properties for Thermal Analyses

Material Property	Source
316 SS with modified nitrogen and carbon (IV) & 316L SS (DOE Canister)	
Density (ρ)	*Standard Practice for Preparing, Cleaning, and Evaluating Corrosion Test Specimens* (ASTM G 1-90 1999 [DIRS 103515], Table X1.1)
Emissivity (ε)	*Marks' Standard Handbook for Mechanical Engineers* (Avallone and Baumeister 1987 [DIRS 103508], p. 4-68, Table 4.3.2)
Thermal Conductivity (k)	*2001 ASME Boiler and Pressure Vessel Code (includes 2002 addenda)* (ASME 2001 [DIRS 158115], Section II, Part D, Table TCD (Material Group K))
Specific Heat (c_p)	*2001 ASME Boiler and Pressure Vessel Code (includes 2002 addenda)* (ASME 2001 [DIRS 158115], Section II, Part D, Table TCD (Material Group K))—computed from the thermal diffusivity
Alloy 22 (Outer Corrosion Barrier)	
Density (ρ)	*2001 ASME Boiler and Pressure Vessel Code (includes 2002 addenda)* (ASME 2001 [DIRS 158115], Section II, Part B, SB-575, Section 7.1), which provides specifications for low-carbon nickel-molybdenum-chromium, low-carbon nickel-chromium-molybdenum, low-carbon nickel-chromium-molybdenum-copper, and low-carbon nickel-chromium-molybdenum-tungsten alloy plate, sheet, and strip
Emissivity (ε)	*CRC Handbook of Chemistry and Physics76th Edition, 1995-1996* (Lide 1995 [DIRS 101876], p. 10-297) for nickel-chromium alloy
Thermal Conductivity (k)	Hastelloy C-22 Alloy (Haynes International 1997 [DIRS 100896], p. 13)
Specific Heat (c_p)	Hastelloy C-22 Alloy (Haynes International 1997 [DIRS 100896], p. 13)
Ti Grade 7 and Ti Grade 29 (Drip Shield)	
Density (ρ)	*2001 ASME Boiler and Pressure Vessel Code (includes 2002 addenda)* (ASME 2001 [DIRS 158115], Section II, Part D, Table NF-2)
Emissivity (ε)	*CRC Handbook of Chemistry and Physics, 76th Edition, 1995-1996* (Lide 1995 [DIRS 101876], p. 10-298)
Thermal Conductivity (k)	*2001 ASME Boiler and Pressure Vessel Code (includes 2002 addenda)* (ASME 2001 [DIRS 158115], Section II, Part D, Table TCD)
Specific Heat (c_p)	*2001 ASME Boiler and Pressure Vessel Code (includes 2002 addenda)* (ASME 2001 [DIRS 158115], Section II, Part D, Table TCD) computed from the thermal diffusivity

Table 2. Sources of Material Properties for Thermal Analyses (Continued)

Material Property	Source
Helium (Waste Package Fill Gas)	
Density (ρ)	*2001 ASHRAE Handbook, Fundamentals* (ASHRAE 2001 [DIRS 157789], p. 20.55)
Thermal Conductivity (k)	*2001 ASHRAE Handbook, Fundamentals* (ASHRAE 2001 [DIRS 157789], p. 20.55)
Specific Heat (c_p)	*2001 ASHRAE Handbook, Fundamentals* (ASHRAE 2001 [DIRS 157789], p. 20.55)
Crushed Tuff (Invert Ballast)	
Density (ρ)	*Estimation of Mechanical Properties of Crushed Tuff for Use Ballast Material in Emplacement Drifts.* 800-CYC-SSE0-00100-000-00A. [DIRS 168138], Section 7.2 (Using the equation for total density and ignoring moisture content)
Emissivity (ε)	*Introduction to Heat Transfer.* (Incropera and DeWitt 1996 [DIRS 107784], p. 768, Table A.8). Use quartz sand as surrogate.
Thermal Conductivity (k)	Thermal Properties Measured 12/01/99 to 12/02/99 Using the Thermolink Soil Multimeter and Thermal Properties Sensor on Selected Potential Candidate Backfill Materials Used in the Engineered Barrier System (DTN: GS000483351030.003 [DIRS 152932])–average for 4-10 crushed tuff. GS000483351030.003 [DIRS 152932] is referenced on *IED Emplacement Drift Invert.* 800-IED-MGR0-00601-000 REV 00A. [DIRS 179897]
Specific Heat (c_p)	Thermal Properties Measured 12/01/99 to 12/02/99 Using the Thermolink Soil Multimeter and Thermal Properties Sensor on Selected Potential Candidate Backfill Materials Used in the Engineered Barrier System (DTN: GS000483351030.003 [DIRS 152932])—average for 4-10 crushed tuff. GS000483351030.003 [DIRS 152932] is referenced on *IED Emplacement Drift Invert.* 800-IED-MGR0-00601-000 REV 00A [DIRS179897]
Air	
Density (ρ)	*2001 ASHRAE Handbook, Fundamentals* (ASHRAE 2001 [DIRS 157789], p. 20.59)
Thermal Conductivity (k)	*2001 ASHRAE Handbook, Fundamentals* (ASHRAE 2001 [DIRS 157789], p. 20.59)
Specific Heat (c_p)	*2001 ASHRAE Handbook, Fundamentals* (ASHRAE 2001 [DIRS 157789], p. 20.59)
304L SS (MCO/DHLW Canister)	
Density (ρ)	*Standard Practice for Preparing, Cleaning, and Evaluating Corrosion Test Specimens* (ASTM G 1-90 1999 [DIRS 103515], Table X1.1)
Emissivity (ε)	*Marks' Standard Handbook for Mechanical Engineers* (Avallone and Baumeister 1987 [DIRS 103508], p. 4-68, Table 4.3.2)
Thermal Conductivity (k)	*2001 ASME Boiler and Pressure Vessel Code (includes 2002 addenda)* (ASME 2001 [DIRS 158115], Section II, Part D, Table TCD (Material Group J))
Specific Heat (c_p)	*2001 ASME Boiler and Pressure Vessel Code (includes 2002 addenda)* (ASME 2001 [DIRS 158115], Section II, Part D, Table TCD (Material Group J))—computed from the thermal diffusivity
516 CS (Waste Basket Guides)	
Density (ρ)	*2001 ASME Boiler and Pressure Vessel Code (includes 2002 addenda)* (ASME 2001 [DIRS 158115], Section II, Part A, SA-20, 14.1)
Emissivity (ε)	*Marks' Standard Handbook for Mechanical Engineers* (Avallone and Baumeister 1987 [DIRS 103508], p. 4-68, Table 4.3.2)
Thermal Conductivity (k)	*2001 ASME Boiler and Pressure Vessel Code (includes 2002 addenda)* (ASME 2001 [DIRS 158115], Section II, Part D, Table TCD (Material Group B))
Specific Heat (c_p)	*2001 ASME Boiler and Pressure Vessel Code (includes 2002 addenda)* (ASME 2001 [DIRS 158115], Section II, Part D, Table TCD (Material Group B))—computed from the thermal diffusivity
Concrete (Surface Facility Structures)	
Density (ρ)	*Introduction to Heat Transfer.* (Incropera and DeWitt 1996 [DIRS 107784], p. 755, Table A.3).
Emissivity (ε)	*Introduction to Heat Transfer.* (Incropera and DeWitt 1996 [DIRS 107784], p. 768, Table A.8).
Thermal Conductivity (k)	*Introduction to Heat Transfer.* (Incropera and DeWitt 1996 [DIRS 107784], p. 755, Table A.3).
Specific Heat (c_p)	*Introduction to Heat Transfer.* (Incropera and DeWitt 1996 [DIRS 107784], p. 755, Table A.3).

5.2.3 Configuration and Thermal Transport Properties of the Natural System

The footprint layout of the subsurface area is shown in Figure 3, taken from *Subsurface-Underground Layout Configuration for LA General Arrangement* (BSC 2007 [DIRS 182932]) and modified to fit for this document. The emplacement drifts will be located within the lower part of the lithophysal zone of the densely welded devitrified lithophysal-rich tuff (TSw1) unit and the entire densely welded devitrified lithophysal-poor tuff (TSw2) unit of the Topopah Spring Tuff (BSC 2003 [DIRS 165572], Table II-2). The rock layer thicknesses are measured at the location of N233, 760 *m* and E170, 750 *m*; the ground surface elevation is 4,663 *ft* (1421.3 *m*).

The stratigraphy of the major geologic units near the center of the repository, and characteristic thermal transport properties rock, are taken from:

Updated Heat Capacity of Yucca Mountain Stratigraphic Units (DTN: SN0307T0510902.003 [DIRS 164196]) for specific heat of all rock layers

Revised Thermal Conductivity of the Non-Repository Layers of Yucca Mountain (DTN: SN0303T0503102.008 [DIRS 162401]) for density and thermal conductivity of non-repository layers

Thermal Conductivity of the Potential Repository Horizon Rev 3 (DTN: SN0404T0503102.011 [DIRS 169129]) for density and thermal conductivity of Repository Layers

5.2.4 Waste Stream Arrival Sequence

The detailed waste package arrival sequence will not be known until the repository is in operation. Hypothetical arrival sequences are simulated based on expected waste forms, inventories, expected future inventories and transport capabilities. A range of potential waste stream arrival sequences is used to analyze throughput and emplacement capability.

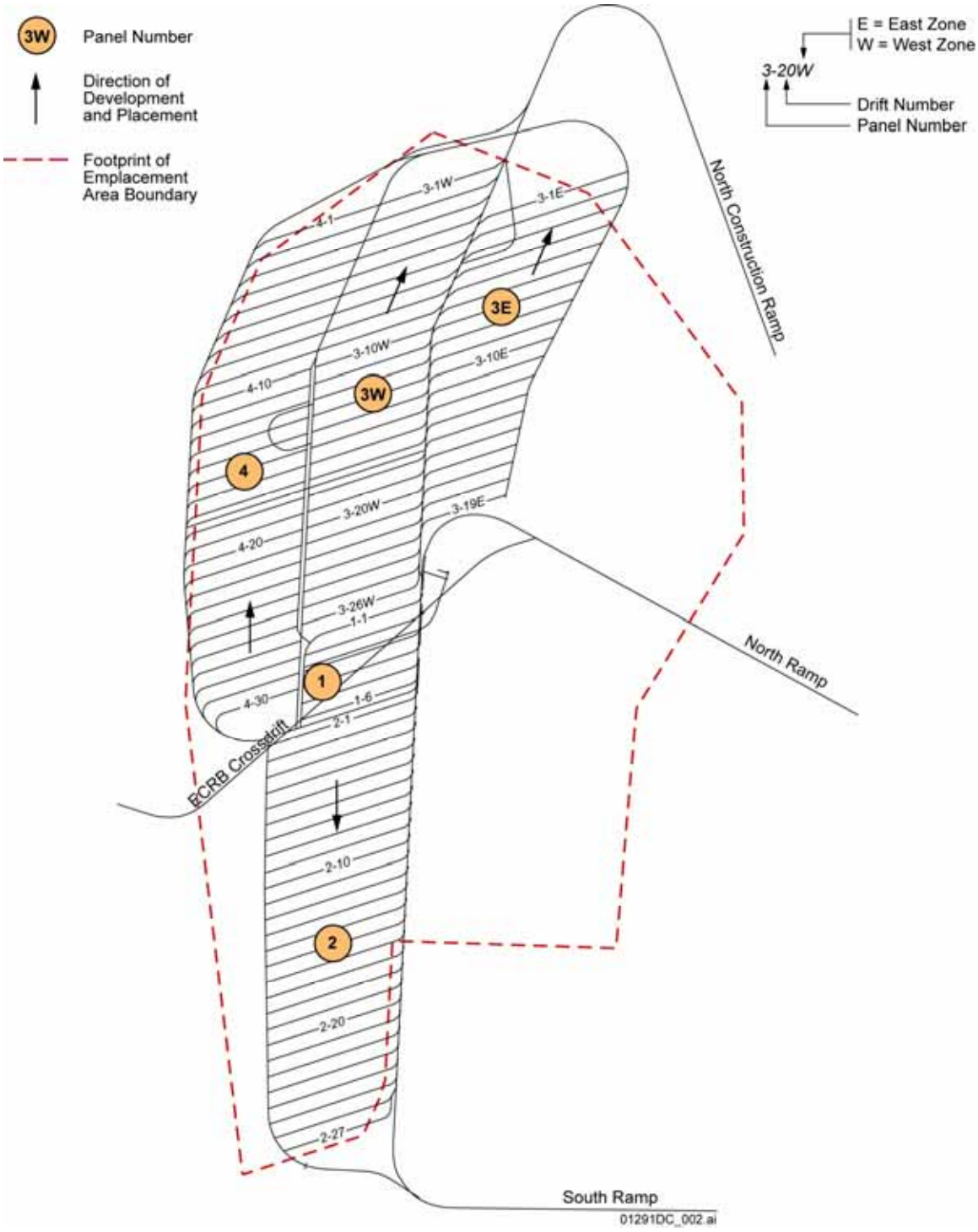

Figure 3. Underground Layout Configuration

5.3 SOURCE TERM

The decay of radionuclides in SNF and HLW is the source of decay thermal energy and ionizing radiation. Source term calculations are performed to determine radionuclide concentrations, radiation fields, and decay thermal power. Differences in the physical forms among the various waste forms (e.g., commercial SNF, DOE SNF, and DOE HLW) lead to very different input requirements for generating the source terms for the representative waste forms. Similarities between PWR's and BWR's result in common input requirements; geometric and operational differences between the two reactor types also create input requirements that are uniquely applicable to each.

5.3.1 Inputs for CSNF Source Term Determinations

Sources for material compositions (other than uranium dioxide) used to determine CSNF source terms are listed in Table 3. For each material, the maximum permissible amount of cobalt is incorporated. For the Stainless Steels, if cobalt impurity is not specified, a cobalt impurity of 0.08 weight percent (wt %) is used (Ludwig and Renier 1989 [DIRS 146398], p. 45). The maximum amount of tin, nickel, and niobium are used because it leads to larger gamma sources. The remaining elements are representative of the material compositions for each material.

Table 3. Sources of Material Compositions Used in Source Term Determinations

Material	Source
UNS R60802 (Zircaloy-2)	*Standard Specification for Wrought Zirconium Alloy Seamless Tubes for Nuclear Reactor Fuel Cladding.* Philadelphia, Pennsylvania: American Society for Testing and Materials (ASTM B 811-90. 1991 [DIRS 131753], Table 2)
UNS R60804 (Zircaloy-4)	*Standard Specification for Wrought Zirconium Alloy Seamless Tubes for Nuclear Reactor Fuel Cladding.* Philadelphia, Pennsylvania: American Society for Testing and Materials (ASTM B 811-90. 1991 [DIRS 131753], Table 2)
UNS S30400 (SS-304)	*2004 ASME Boiler and Pressure Vessel Code* (ASME 2004 [DIRS 171846], Section II A, SA-240, Table 1)
UNS S30403 (SS-304L)	*2004 ASME Boiler and Pressure Vessel Code* (ASME 2004 [DIRS 171846], Section II A, SA-240, Table 1)
UNS S30200 (SS-302)	*2004 ASME Boiler and Pressure Vessel Code* (ASME 2004 [DIRS 171846], Section II A, SA-240, Table 1)
Inconel-718	Product Handbook (Inco Alloys International 1988 [DIRS 130835], p. 11)
Inconel-X-750	Product Handbook (Inco Alloys International 1988 [DIRS 130835], p. 11)
Stainless Steel CF3M	*Properties and Selection: Stainless Steels, Tool Materials and Special-Purpose Metals*. Volume 3 of *Metals Handbook* (ASM 1980 [DIRS 104317], p. 95)

Elemental impurities in the uranium dioxide of the fuel are given in *Standard- and Extended-Burnup PWR and BWR Reactor Models for the ORIGEN2 Computer Code* (Ludwig and Renier 1989 [DIRS 146398], Table 5.4).

The isotopic composition of commercially available uranium is provided by the empirical relationships in *Sequoyah Unit 2, Cycle 3* - Volume 2 of *Scale-4 Analysis of Pressurized Water Reactor Critical Configurations* (Bowman et al. 1995 [DIRS 123796], p. 20).

Neutron flux scaling factors are also required for regions outside the active fuel in order to determine neutron-activated gamma source terms. These scaling factors are 150 percent of those provided by *Activation Measurements and Comparison with Calculations for Spent Fuel Assembly Hardware.* Volume 1 of *Spent Fuel Assembly Hardware: Characterization and 10 CFR 61 Classification for Waste Disposal* (Luksic 1989 [DIRS 120506], Table S.1, p. vi).

The presence of corrosion products (crud) on the fuel is also accounted for in the source term determination. This is obtained from:

- *Standard Review Plan for Spent Fuel Dry Storage Facilities* (NRC 2000 [DIRS 149756], Table 9.2)
- *Spent Fuel Corrosion Product and Fuel Cleaning Assessment (*Jones, R. H. 1992 [DIRS 146405], Tables 1 and 2).
- The half-life of the radionuclides used in the crud source calculations are provided by *Nuclides and Isotopes*, Chart of the Nuclides (Baum et al. 2002 [DIRS 175238]).

PWR Lattice—For the PWR commercial SNF, the Babcock & Wilcox (B&W) Mark B 15 × 15 PWR fuel assembly is selected as the generic PWR lattice for analysis. This lattice has a high initial heavy metal loading and large amounts of Stainless Steel and Inconel assembly hardware, maximizing fission product generation and activation of structural hardware. While a typical B&W Mark B assembly has an initial heavy metal loading of 464 *kg* of uranium (Punatar 2001 [DIRS 155635], Table 3.1), this is increased to 475 *kg* to provide coverage of all commercial SNF waste streams (Assumption 6.3.1.4). Source terms for a generic stainless-steel-clad fuel assembly and for a longer South Texas assembly are also generated in PWR Source Term Generation and Evaluation (BSC 2004 [DIRS 169061]). For the longer South Texas assembly, a uranium metal mass of 550 *kg* is used.

The additional uranium mass is accommodated by increasing the fuel length of a B&W Mark B assembly, rather than by increasing the fuel density. This is consistent with the demonstration of previous calculations that a lower fuel density generates higher gamma and neutron sources described in BWR Source Term Generation and Evaluation (BSC 2003 [DIRS 164364], pp. 48 and 49). A longer active fuel length and a lower density decrease the fuel self-shielding. This results in a higher flux and consequently higher source intensities.

The physical characteristics and operating conditions of the B&W Mark B 15 × 15 PWR fuel assembly are obtained from:

- *Summary Report of Commercial Reactor Criticality Data for Crystal River Unit 3* (Punatar 2001 [DIRS 155635], Table 2-2, Figure 2-2, Table 2-9)
- *Operational Data—B&W NSS* (Framatome Cogema Fuels 1999 [DIRS 146419], p. 3)

The Mark B and the South Texas assemblies are used in the evaluation of the crud activity on the assembly surface. The larger fuel rod surface area in the South Texas assembly is used as the

bounding case because crud activity is directly proportional to the surface area in the assembly exposed to the coolant.

BWR Lattice—For BWR commercial SNF, a General Electric (GE) 8 × 8 BWR fuel assembly is used as the generic fuel design for BWR source term determination (BSC 2003 [DIRS 164364], p. 6). This design has a high initial heavy metal loading and an adequate amount of fuel assembly hardware data. The initial heavy metal loading is conservatively increased from 184 kg (Larsen et al. 1976 [DIRS 146576], p. A-2) to 200 *kg* to provide coverage of the actual waste stream (Assumption 6.3.1.4). In cases where the hardware for the assembly is not conservative, substitutions and approximations are made to increase conservatism. The stainless-steel-clad fuel assembly is also considered because it presents higher gamma source intensity due to activation.

As was the case for PWR fuel, the additional fuel mass is added as increased length, rather than as increased density.

The crud activity is directly proportional to the surface area in the assembly components exposed to coolant. Therefore, an assembly that has a higher surface area is used to conservatively evaluate the crud activity.

The physical characteristics and operating conditions for the GE 8 × 8 fuel assembly are obtained from the following sources:

- *Summary Report of Commercial Reactor Criticality Data for Quad Cities Unit 2* (CRWMS M&O 1999 [DIRS 134660])

- *Core Design and Operating Data for Cycles 1 and 2 of Quad Cities 1* (Larsen et al. 1976 [DIRS 146576], pp. A-1, A-8, and C-12)

- *Appendix 2A. Physical Descriptions of LWR Fuel Assemblies*. Volume 3 of *Characteristics of Spent Fuel, High-Level Waste, and Other Radioactive Wastes Which May Require Long-Term Isolation* (DOE 1987 [DIRS 132333], pp. 2A-16 and 2A-158).

Additional information required to perform the *BWR Source Term Generation and Evaluation* (BSC 2003 [DIRS 164364]) is taken from:

- *CRC Depletion Calculations for Quad Cities Unit 2* (CRWMS M&O 1999 [DIRS 134650], p. 50–55) for dimensions and materials for PATH B geometric descriptions of the SAS2H code.

- *SCALE, RSIC Computer Code Collection* (NRC 1997 [DIRS 122675], Table S2.6.4, p. S2.6.12) for clad temperature during operation.

5.3.2 Inputs for DOE SNF and HLW Source Term Determinations

The DOE SNF and HLW source term calculations rely on the input of initial radionuclide inventories and, in the case of HLW, chemical compositions of the glass waste forms. The initial radionuclide inventories for DOE SNF are taken from *General Description of Database Information Version 5.0.1* (DOE 2004 [171271]).

The volume, mass, and canister quantities for the HLW have historically been taken from *Final Environmental Impact Statement for a Geologic Repository for the Disposal of Spent Nuclear Fuel and High-Level Radioactive Waste at Yucca Mountain, Nye County, Nevada* (DOE 2002 [DIRS 155970], Volume II, Appendices A through O, p. A-39 to A-43, A-48, A-55, and A-56). As inventories are better quantified, the canister quantities are taken from updated references. (See listed references below).

Chemical compositions and initial radionuclide inventories are provided by:

- *Projected Glass Composition and Curie Content of Canisters from Savannah River Site (U)*. X-ESR-S-00015, Rev. 1. (Ray, J.W. 2007 [DIRS 181690]).

- WVNS (West Valley Nuclear Services Company) 2001. *WVDP Waste Form Qualification Report - Canistered Waste Form Specifications, Chemical Specification.* Chapter 1 of *Waste Form Qualification Report (WQR).* WVDP-186. [DIRS 157559]

- WVNS (West Valley Nuclear Services) 2003. "Radionuclide Scaling factors." Addendum 1 of *WVDP Waste Form Qualification Report - Waste Form Specifications, Radionuclide Inventory Specification.* WVDP-186, Rev. 0. [DIRS 168547]

- "Response to Repository Environmental Impact Statement Data Call for High-Level Waste." Memorandum from K.G. Picha, Jr. (DOE) to W. Dixon (YMSCO), September 5, 1997, with attachments. (Picha, K.G., Jr. 1997. [DIRS 104406])

- *Waste Treatment and Immobilization Plant (WTP) High-Level Waste (HLW) Canister Production Estimates to Support Analyses by the Yucca Mountain Project.* DOE/ORP-2004-03, Rev. 0. (DOE 2004 [DIRS 172092])

- *Recommended Values for HLW Glass for Consistent Usage on the Yucca Mountain Project*. (BSC 2007 [DIRS 182239]).

- *Source Terms for HLW Glass Canisters* (BSC 2007 [DIRS 183163])

6. WASTE PACKAGE COMPONENT DESIGN ASSUMPTIONS

The assumptions involved in performing calculations or analytical work may be divided into two categories. The first category consists of generic assumptions that can be part of a calculation process or computational tool. Appropriate generic assumptions are addressed in this report that relate to the processing and disposal of the range of waste forms in the repository.

The second category of assumptions is specific assumptions related to a particular analysis or calculation. An example of a specific assumption is an assumption necessary to perform a drop calculation for a particular waste package. Some, but not all, specific assumptions are addressed in this report. Each individual calculation report describes all assumptions pertaining to the specific calculation.

The generic assumptions appropriate to the methodology are listed in the following sections. None of these assumptions require verification. The basis for each assumption is included.

6.1 STRUCTURAL CALCULATION ASSUMPTIONS

6.1.1 Material Property Assumptions

6.1.1.1 Contact Stiffness between Waste Package Impact Surface and Emplacement Pallet

For ANSYS calculations, the assumption is made that the contact stiffness between the waste package and the impact surface and waste package and emplacement pallet can be determined iteratively. The rationale for this assumption is explained in the following paragraph. LS-DYNA calculations do not require this assumption.

The magnitude of the contact stiffness (between surfaces used in the simulation) is a parameter that influences the resulting stresses. If the stiffness value is very large, stiffness matrix ill-conditioning and divergence will occur. Similarly, an extremely small stiffness value results in compatibility violations. Therefore, an optimum value for the contact stiffness is one that is between the two and is arrived at iteratively. Therefore, an iterative process to determine the value of contact stiffness used in the finite element simulation is deemed acceptable for static solutions.

6.1.1.2 Strain Rate Effect on Material Properties

Strain-rate-dependent material properties are not published in traditional sources (e.g., the ASTM, ASME and ASM standards, codes and metal property data) for waste package and auxiliary component materials. The material properties obtained under static loading conditions are assumed for these materials. The maximum element wall-averaged (EWA) strain rates reached at the governing stress locations during the calculations are evaluated to determine that the impact of using material properties obtained under static loading conditions is minor.

6.1.1.3 Room Temperature Uniform Strain of SA-516 Carbon Steel

The Room Temperature (RT) uniform strain (the strain corresponding to the uniaxial tensile strength) of SA-516 [UNS K02700] carbon steel (CS) is not available in traditional sources (ASME Code). Therefore, it is conservatively assumed that the uniform strain is 50 percent of the elongation. The rationale for this assumption is based on measurements of the engineering stress-strain curves for SA-36 CS (Boyer 2000 [DIRS 152656], p. 189; Bowles 1980 [DIRS 153409], Figure 1-3, p. 11), which has a similar chemical composition as SA-516 CS (ASME 2001 [DIRS 158115], Section II, Part A, SA-516/SA-516M, Table 1 and SA-36/SA-36M, Table 2).

6.1.1.4 Room Temperature Uniform Strain of 316L Stainless Steel

The RT uniform strain of 316L [UNS S31603] stainless steel (SS) is not listed in traditional sources. Therefore, it is assumed that the RT uniform strain is 60 percent of the RT elongation. The rationale for this assumption is based on measurements of the engineering stress-strain curves for "as-received" 316L SS material at moderate strain rate (8 s^{-1}) (Boyer 2000 [DIRS 152656], page 305).

6.1.1.5 Room Temperature Uniform Strain of Alloy 22 and 316 SS

The RT uniform strain of Alloy 22 and 316 SS is not listed in traditional sources. Therefore, it is assumed that the RT uniform strain is 90% of the RT elongation for both materials. The rationale for this assumption is based on measurements of the RT engineering stress-strain curves of Alloy 22 (DTN: LL020603612251.015 [DIRS 160430]), S02234_001 Mechanical Deformation, file: LL020603612251.015 Instron Data yr 2002, and 316 SS (Boyer 2000 [DIRS 152656], p.304). The use of DTN: LL020603612251.015 [DIRS 160430] was approved as the appropriate data for the intended use in an Information Exchange Document (BSC 2005 [DIRS 173627]).

6.1.1.6 Room Temperature Uniform Strain of 304 SS

The RT uniform strain of 304 SS is not available in traditional sources. Therefore, it is conservatively assumed that the uniform strain is 75 percent of the elongation. The rationale for this assumption is based on measurements of the engineering stress-strain curves for 304 SS (Boyer 2000 [DIRS 152656], p. 294).

6.1.1.7 Room Temperature Poisson's Ratio for Alloy 22

The RT Poisson's ratio of Alloy 22 is not published in traditional sources. Therefore, the RT Poisson's ratio of ASME SB-443 [UNS N06625], hereinafter termed Alloy 625, is assumed for Alloy 22. The chemical compositions of Alloy 22 and Alloy 625 are similar since they are both 600 Series nickel-base alloys (ASME 2001 [DIRS 158115], Section II, Part B, SB-575, Table 1 and ASM 1980 [DIRS 104317], p. 143, respectively). Therefore, the difference in their Poisson's ratio is expected to be small. The rationale for this expectation is that ASM 1980 [DIRS 104317], pages 141, 143 and 145 indicate small differences in RT Poisson's ratio values for the 600 Series nickel-base alloy family:

Alloy 600 [UNS N06600] = 0.290

Alloy 625 [UNS N06625] = 0.278

Alloy 690 [UNS N06690] = 0.289

The impact on stress results of small differences in Poisson's ratio is anticipated to be negligible.

6.1.1.8 Room Temperature Poisson's Ratio for SA-516 CS

The RT Poisson's ratio is not available for SA-516 CS in traditional sources. Therefore, Poisson's ratio of cast carbon steel is assumed for SA-516 CS. The rationale for this assumption is that the elastic constants of cast carbon steels are only slightly affected by changes in composition and structure (ASM 1978 [DIRS 102018], p. 393). Hence, the impact of this assumption is minimal.

6.1.1.9 Room Temperature Poisson's Ratio of 316L SS

The RT Poisson's ratio of 316L SS is not published in traditional sources. Therefore, the RT Poisson's ratio of 316 SS is assumed for 316L SS. The chemical compositions of 316L SS and 316 SS are similar (ASME 2001 [DIRS 158115], Section II, Part A, SA-240, Table 1) because they are both 300 Series (austenitic) SS's. Therefore, the difference in their Poisson's ratio is expected to be small. The rationale for this expectation is that ASM 1980 ([DIRS 104317], page 755 Figure 15) indicates small differences in RT Poisson's ratio values for the 300 Series SS family:

Type 304 SS [UNS S30400] = 0.290

Type 316 SS [UNS S31600] = 0.298

Type 310 SS [UNS S31000] = 0.308

The impact on stress results of small differences in Poisson's ratio is anticipated to be negligible.

6.1.1.10 Room Temperature Poisson's Ratio for 304L SS

The RT Poisson's ratio for 304L SS is not available in traditional sources. Therefore, it is assumed to be the same as Poisson's ratio for 304 SS. The rationale for this assumption is that the chemical compositions of 304L SS and 304 Stainless Steel are similar (ASME 2001 [DIRS 158115], Section II, Part A, SA-240, Table 1). Hence, the impact of this assumption is minimal.

6.1.1.11 Elevated Temperature Poisson's Ratio and Density

The Poisson's ratio and density at elevated temperatures are not published in traditional sources for Alloy 22, 316 SS and 316L SS. The RT Poisson's ratio and density are assumed for these materials. The impact of using RT Poisson's ratio and density is anticipated to be small. The rationale for this assumption is that temperature sensitivities of these material properties are expected to be small and small variations will have negligible affect on the calculation's stress

results. The change in density will be downward as the material expands, inversely related to the volumetric expansion term $(1+\Delta T\alpha)^3$, where ΔT is the temperature increase above RT and α is the relative (to RT) coefficient of thermal expansion. The total mass will remain unchanged, so the effect of density change on stress is unclear, however even in the unlikely event that the resulting stress effect is a magnitude greater than the density change, it will be negligible.

6.1.1.12 Elevated Temperature Elongation Properties

The elongation properties of Alloy 22 and 316 SS at elevated temperatures are not available in traditional sources. However, vendor data is available for the typical elongation of Alloy 22 and 316 SS (Haynes International 1997 [DIRS 100896], p. 15; Allegheny Ludlum 1999 [DIRS 151409], p. 8, respectively). The percent difference between typical elongation at room temperature and elevated temperatures is normalized and applied to the minimum elongation data available from accepted codes. The rationale for this assumption is to be as accurate as possible in establishing this value which influences the slope of the elastic-plastic stress strain curve.

6.1.1.13 Material Properties for Titanium

The temperature-dependent tensile and yield strength of Ti-29 (Titanium Grade 29) are not available in traditional sources. However, vendor data for these material properties are available (TIMET 2000 [DIRS 160688], Figure 1). Therefore, the tensile and yield strengths of Ti-29 from TIMET at elevated temperatures will be normalized and used with the room temperature values from ASME to calculate the tensile and yield strength of Ti-29 at elevated temperatures. The rationale for this assumption is that the ASME B&PV Code (ASME 2001 [DIRS 158115]) states the minimum material properties. Therefore, calculating the minimum properties at elevated temperatures with this method provides a bounding value of tensile and yield strength of Ti-29 for this calculation.

The temperature-dependent modulus of elasticity of Ti-29 is not available through the ASME Code or through the *ASM Metals Handbook* (ASM International 1990 [DIRS 141615]). However, vendor data are available for this material property (TIMET 2000 [DIRS 160688], Table 2). Therefore, the modulus of elasticity of Ti-29 from TIMET at elevated temperatures will be normalized and used with room temperature values from the *ASM Metals Handbook* (ASM International 1990 [DIRS 141615], Table 21, p. 621) to calculate the modulus of elasticity of Ti-29 at elevated temperatures. The rationale for this assumption is that the room temperature data is only adjusted by the trend in the vendor data and not by the absolute values in the vendor data.

Temperature-dependent Poisson's ratio is not available for Ti-7 (Titanium Grade 7) and Ti-29. Therefore, the room temperature Poisson's ratio is assumed for these materials. The impact of using Poisson's ratio at room temperature is anticipated to be small. The rationale for this assumption is twofold: first, for the subject materials, this property does not change significantly at the temperature of interest in this calculation; secondly, the material property in question does not have dominant impact on the calculation results.

The rate-dependent material properties obtained under the static loading conditions are used for dynamic loading of Ti-7 and Ti-29. The impact of using material properties obtained under static loading conditions is anticipated to be small. The rationale for this assumption is that the mechanical properties of subject materials do not significantly change at the peak strain rates.

6.1.1.14 Friction Coefficient between 316 SS and 316L SS

The friction coefficient for contact between 316 SS and 316L SS is not available in traditional sources. It is, therefore, assumed that the dynamic (sliding) friction coefficient for this contact is 0.4. The rationale for this assumption is that this friction coefficient represents the lower bound for the steel-on-steel contacts (Avallone and Baumeister 1987 [DIRS 103508], Table 3.2.1, p. 3-26; Meriam and Kraige 1987 [DIRS 104306], p. 441).

6.1.1.15 Friction Coefficients for Drop Contacts Involving Alloy 22

The friction coefficients for contacts involving Alloy 22 are not available in traditional sources. It is, therefore, assumed that the dynamic (sliding) friction coefficient for all contacts is 0.4. The rationale for this assumption is that this friction coefficient represents the lower bound for most dry contacts involving steel and nickel (Meriam and Kraige 1987 [DIRS 104306], p. 441; Avallone and Baumeister 1987 [DIRS 103508], Table 3.2.1, p. 3-26), nickel being the dominant component in Alloy 22 (ASME 2001 [DIRS 158115], Section II, Part B, SB-575, Table 1).

6.1.1.16 Variation of Functional Friction Coefficient

The variation of functional friction coefficient between the static and dynamic values as a function of relative velocity between the contact surfaces is not available in traditional sources for the materials used in this report. Therefore, the effect of relative velocity of the surfaces in contact is not included in this report by assuming that the functional friction coefficient and static friction coefficient are equal to the dynamic friction coefficient. The impact of this assumption is anticipated to be negligible. The rationale for this conservative assumption is that it provides the bounding set of results by minimizing the friction coefficient within the given finite element analysis framework.

6.1.1.17 Material Properties for TSw2 Rock

Temperature-dependent material properties are not available for TSw2 (Topopah Spring Welded) rock. Hence, room temperature material properties are assumed for this material. The impact of using constant material properties is anticipated to be small. The rationale for this assumption is that the material properties of the rock do not have dominant impact on the calculation results. The likely exception is the yield strength of the rock, which decreases with the increasing temperature. Thus, the representation of the rock as an elastic-ideally-plastic solid with room temperature yield strength is conservative.

6.1.1.18 Compressive Strength of TSw2 Rock

A recommended unconfined compressive strength of the TSw2 is available (*IED Geotechnical and Thermal Parameters IV* (BSC 2007 DIRS [179808], Figure 1). The scatter of data is large as expected for rocks and brittle materials in general. For the purpose of the rock fall

calculations, the unconfined compressive strength of the TSw2 is assumed to be 70 *MPa*. The rationale for this assumption is based on the recommended compressive strength value for nonlithophysal of significant size (3000 *mm*) (BSC 2007 [DIRS 179808], Figure 1).

6.1.1.19 Young's Modulus and Poisson's Ratio of TSw2 Rock

The modulus of elasticity and Poisson's ratio of the TSw2 are characterized by significant scatter of data, *IED Geotechnical and Thermal Parameters IV [Sheet 1 of 1]* (BSC 2007 [DIRS 179808], Table 2). For the purpose of rock fall calculations, modulus of elasticity is assumed to be 33.6 *GPa*, and Poisson's ratio 0.20. The rationale for this assumption is that these values agree well with typical values of said properties for most rocks of interest (BSC 2007 [DIRS 179808], Table 2).

6.1.1.20 Density of TSw2 Rock

The density of the TSw2 is assumed to be 2411 kg/m^3 The rationale for this assumption is that this value agrees well with the mean density of the sample Topopah Spring Welded rocks, *IED Geotechnical and Thermal Parameters IV [Sheet 1 of 1]* (BSC 2007 [DIRS 179808], Table 1). This assumption has no effect on the calculation results because the important input parameter is rock mass, regardless of the density.

6.1.1.21 Friction Coefficients for Contacts Involving Seismic Rock fall Analysis

The friction coefficient for contacts occurring between the rock and Ti-7 or invert and Alloy 22 is not available in literature. It is, therefore, assumed that the dynamic (sliding) friction coefficient for this contact is 0.525. The rationale for this assumption is that this friction coefficient represents the upper bound of the range kinetic friction values for metal-on-stone contacts (Beer and Johnston 1977 [DIRS 145138], Table 8.1, p. 306).

6.1.2 Representation of Waste Package Loaded Internals Assumptions

6.1.2.1 Commercial Waste Form Geometry

The exact geometry of the waste form is simplified in such a way that its total mass is assumed to be distributed within a bar of square cross section with uniform mass density. The rationale for this assumption is to provide a simplified finite element representation without affecting computational results.

6.1.2.2 Commercial Waste Form Material

The waste form is assumed to be made of 304 SS. The rationale for this assumption is that the end fittings of the form are made of 304 SS (Punatar 2001 [DIRS 155635], Section 2.1, p. 2-4 [for PWR]; Stout and Leider 1997 [DIRS 100419], p. 2.1.2.3 [for BWR])**,** and these are the parts that will come in contact with other components.

6.1.2.3 TAD Canister

The TAD canister includes a canister shell, lid(s) and component (e.g., baskets for holding fuel assemblies, thermal shunts and neutron absorbers, etc) needed to perform its function. The TAD canister shall be a right circular cylinder with a nominal diameter of 66.5 *in*. The TAD canister shall not be less than 186.0 *in* and not greater than 212.0 *in*. including the lifting features. The TAD canister loaded weight shall be consistent with the above dimensions (*Transportation, Aging and Disposal Canister System Performance Specification* WMO-TADCS-000001 DOE/RW-0585 [DIRS 181403], Section 3.1).

6.2 THERMAL ANALYSIS ASSUMPTIONS

Thermal analyses are performed at different geometric scales including repository scale, drift scale, and waste package scale. Assumptions appropriate to each scale of thermal analysis are presented in the following sections.

6.2.1 Assumptions for Repository-Scale Thermal Analysis

6.2.1.1 Pillar Representation of Repository

In the pillar representation of the repository, the problem domain is represented as a rectangular parallelepiped (Section 7.2.2.4) or rectangular cross-section (Section 7.2.2.3). Vertically, it ranges downward from the top of the mountain to well into the saturated zone. Laterally, the representation is bounded by vertical planes parallel to the drifts and centered at the midpoint between the drifts. The thermal boundary conditions at these locations are adiabatic surfaces. For the three-dimensional pillar representation, the axial boundaries are placed perpendicular to the drift axis, either between waste packages or axially bisecting one or both of the waste packages at the end of the drift segment. Again, the thermal boundary conditions at these planes are adiabatic surfaces. The rationale for this assumption is that it approximates a drift segment at or near the geometric center of the repository. The assumption of no lateral heat transfer is appropriate because it maximizes the temperatures within the pillar; however, it is a good assumption only from emplacement to about 1,000 years after, at which time appreciable cooling begins from the edges of the repository (CRWMS M&O 1994 [DIRS 142611], p. 7).

6.2.1.2 Omission of Gross Water Movement

The effect of water mobilization into the repository from the surrounding rock matrix, as well as that from percolation flux that reaches the repository horizon from the surface, is neglected in thermal evaluations of the waste package. The rationale for this assumption is that it is conservative (higher peak temperatures) because it neglects thermal energy transport away from the drifts by the gross movement of this water. For the first few decades after repository closure, the thermal pulse penetrates only a few meters into the host rock and little water will be mobilized and a peak temperature occurs in this same short time period. Neglecting the movement of water has little effect on thermal calculations.

While gross water movement within the host rock fracture network is not represented, the thermal transport properties include the effect of entrapped water. For instance, rock strata specific heats (DTN: SN0307T0510902.003 [DIRS 164196]) are represented as constant values.

Near the boiling temperature in the host rock, the specific heat is adjusted upward to account for the latent heat of vaporization of water in the host rock (Figure 4(a)). The thermal conductivity is also reduced at rock temperatures above boiling to represent the loss of aqueous water (Figure 4(b)).

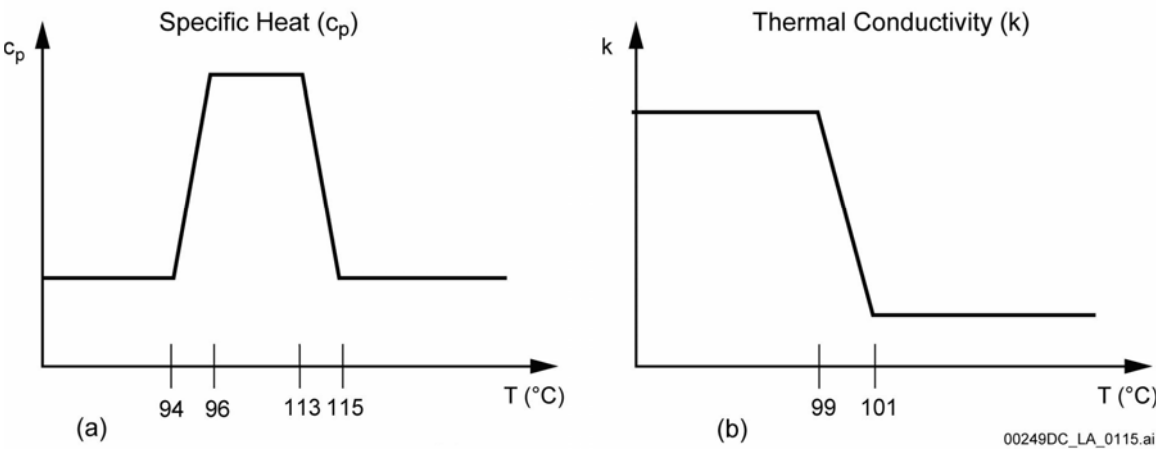

Figure 4. Adjustments of Host Rock Thermal Transport Properties

6.2.1.3 Treatment of Waste Package Internals

The waste form, basket, and basket support structure within the waste package are represented in repository-scale calculations as a homogeneous, smeared-property, heat-generating cylinder. The length of the cylinder corresponds to the inside length of the inner vessel, and the diameter of the cylinder corresponds to the inner diameter of the inner vessel. The rationale for this assumption is that the internal temperatures are not of immediate interest in repository-scale calculations, provided that the thermal transport properties for the internals are correct in an average sense.

6.2.1.4 Fixed Temperature at the Surface of the Mountain

The boundary condition at the top of the two- and three-dimensional repository representations is a fixed temperature, the value of which is taken from the Technical Data Management System. The rationale for this assumption is that while climatic changes affect the temperature distribution a few meters into the mountain, the rock acts as a thermal capacitor, and the annual averaged surface temperature is adequate for determining temperatures at the repository horizon.

6.2.1.5 Initial Temperature Gradient in the Mountain

Based on the values of rock temperature and depth for the USW SD-12 borehole given in DTN: GS031208312232.003 ([DIRS 171287], file: TEMPERATURE.txt), the initial thermal gradient in the rock (before waste emplacement) is determined to be 0.02°*C/m*.

GS031208312232.003 is cited in *IED Geotechnical and Thermal Parameters II* (BSC 2007 [DIRS 178277]). Since the variation in thermal conductivity of the rock layers is small, and

since the heat flux across layers is constant, it is reasonable to assume that this initial thermal gradient extends to the maximum depth of the typical ANSYS pillar representation (1085 *m*). Since the lower boundary is far from the emplacement drifts, this assumption will not significantly affect the temperature calculation.

6.2.1.6 Modes of Heat Transfer within the Drift

All three modes of heat transfer (conduction, convection and radiation) occur in the drift. During the preclosure period, most of the heat is removed by mixed (forced and natural) convection. This heat is removed by the ventilation system and the heat transfer to the rock is reduced. The method of calculating convection effects during preclosure is described in Section 7.2.

During postclosure, convective heat transfer is neglected, and heat transfer is represented by radiation and conduction only. The rationale for this assumption is that neglecting convective heat transfer will result in a conservative calculation of waste form peak temperatures. Calculations in a drift above borehole-emplaced waste packages have shown that radiative heat transfer is an order of magnitude greater than the convective heat transfer (Gartling et al. 1981 [DIRS 142640], p. 59). The dominance of radiation heat transfer can also be shown by simple analytic solutions. Neglecting convection gives conservative (high) values for waste package and cladding temperatures and only slightly lower rock temperatures.

The conductive heat transfer between the waste package and the emplacement pallet, and hence through the pallet into the invert, is neglected. The rationale for this assumption is that the emplacement pallet contacts the waste package in only a few places, and conduction is necessarily limited. An effective thermal conductivity with directional dependence is used to represent the invert.

6.2.1.7 Approximation of Heat-Removal by Ventilation

For repository-scale thermal analysis, the ventilation system is not explicitly represented in the drift. Heat is transferred from the waste package to the drift wall by thermal radiation. During postclosure, all heat transfer is by thermal radiation. During preclosure, heat loss from the waste package and drift wall to the ventilation system is represented by a convective coefficient and a sink temperature. An alternative, simplified method to account for heat removal by the ventilation system is to directly remove a fraction (termed ventilation efficiency) of the heat from the drift wall surface.

6.2.2 Assumptions for Drift-Scale Thermal Analysis

All of the assumptions for repository-scale analysis are also applicable to drift-scale analysis. In addition, drift-scale analysis assumes uniform temperature around a circumference 16 *ft* (5 *m*) into the drift rock surface. Note drift-scale analysis is valid only for the same linear heat load as used to determine the 16 *ft* (5 *m*) rock temperature in the corresponding pillar analysis. The rationale for this assumption is drift internal structures have little impact on rock temperatures at this location (BSC 2006 [DIRS 179686], Tables 53, 54, 61-66, and 95).

6.2.3 Assumptions for Waste Package-Scale Thermal Analysis

6.2.3.1 Two-dimensional Representation of Waste Package Internals

Two-dimensional representations of the waste form and waste package components are used for the purpose of defining the peak-fuel cladding temperatures. Inherent to this assumption is that axial heat transfer does not significantly affect the solution. The rationale for this assumption is that the metal thermal conductivities and heat generation rate distributions are such that axial heat transfer is negligible. This characteristic behavior is shown in *The TN-24P PWR Spent-Fuel Storage Cask: Testing and Analyses* (Creer et al. 1987 [DIRS 136937]) and *Repository Twelve Waste Package Segment Thermal Calculation,* (BSC 2006 [DIRS 179686], Figure 21).

6.2.3.2 Omission of Convection within the Waste Package

Convective heat transfer through the waste package fill gas (within the basket gaps and all other waste package vacancies) is neglected. Considering only conduction and radiation heat transfer provides conservative results for peak fuel cladding temperature. The rationale for this assumption is as follows: some convective heat transfer will occur in the waste package fill gas; however, in a horizontal emplacement configuration, convection is minor compared to thermal radiation (at the expected temperatures), and stable convection cells either do not develop or are difficult to predict. Also, some fill gases, such as helium, are neutrally buoyant relative to their thermal conductivity (unlike air, for example), and natural convection has a negligible contribution to total heat transfer. An extensive discussion of natural convection heat transfer is contained in *Introduction to Heat Transfer*, 3rd Edition (Incropera and DeWitt 1996 [DIRS 107784], p. 448–478).

6.2.4 Assumptions for Waste Package Fire Analyses

Calculations for fire analyses are performed parametrically, assuming the worst fire conditions will not exceed those defined in the NRC regulations for transportation casks. Fire prevention controls that will be implemented at the repository are anticipated to result in far less severe fire conditions. A 2-D finite element representation (FER) of the waste package is used. The waste package inner components are integrally connected and fuel assemblies are modeled with an effective thermal conductivity. The integral connection minimizes thermal resistance to the fire and is therefore conservative in estimating waste package internal temperatures (from a fire). More detailed assumptions are given in reports for fire analysis of each type of waste package.

6.2.5 Assumptions for Waste Package in Surface Facilities and Transporter

Prior to emplacement, a loaded waste package is located in various surface facilities (including the weld cell) and the transporter. At times, axisymmetric geometries are used as conservative representations of rectangular rooms to simplify the calculation. Only radiation heat transfer is used when convection is unimportant to the calculated temperatures. Off-normal transients are often calculated as adiabatic heat up of a system with no heat rejection to the outside environment. The effects of temperature and surface condition on emissivity are ignored because surface condition is unknown and limited temperature range data are available. Since radiation heat transfer is proportional to fourth power of temperature this has small impact.

6.2.6 Assumptions for DriftFlow Calculations

DriftFlow is used to determine the effect of ventilation in the repository drifts. All modes of heat transfer (conduction, radiation, and convection) are considered. An overall convection heat transfer coefficient is used. Conduction is calculated by superimposing temperature responses to yearly pulses of heat. The temperature responses are based on ANSYS results for a "pillar" analysis. The rationale is that mathematical solutions for conduction heat transfer assuming Fick's law can be superimposed and overall heat transfer coefficients are common practice in heat transfer calculations.

6.2.7 Assumptions for FLUENT Calculations

Convection heat transfer coefficients are calculated by Computational Fluid Dynamics analysis. Ventilation flow rates are specified and a uniform rock temperature 5 *m* (16 *ft*) from the surface is taken from ANSYS calculations. The rationale for this is that previous calculations have shown that drift internal structures have little impact on rock temperatures at this location (BSC 2006 [DIRS 179686], Tables 53, 54, 61-66, and 95).

6.2.8 Assumptions for WPLOAD Calculations

In WPLOAD, it is assumed all naval canisters have the same thermal power history. Thermal power for DOE-SNF canisters is neglected and all DHLW canisters have the same thermal power history. Only one waste package of each type will be open at a time. Waste packages will be loaded only one emplacement drift at a time. These assumptions are conservative since they limit operating flexibility to less than may be available and are reasonable for the intended use of WPLOAD to study loading strategies.

6.3 SOURCE TERM GENERATION ASSUMPTIONS

Source term calculations provide heat generation rates, photon and neutron spectra and intensities, and radionuclide inventories of commercial SNF assemblies, DOE SNF, and HLW. The heat generation rates are used in thermal evaluations of the waste packages and the host rock of the repository. The photon and neutron sources are used to determine the radiation level surrounding a waste package. The radionuclide inventories are used to determine dose rates due to the release of radionuclides from the waste packages.

6.3.1 Commercial Spent Nuclear Fuel Waste Forms Assumptions

Assumptions related to the evaluation of source terms from commercial SNF waste forms are discussed in the following sections.

6.3.1.1 Generic Fuel Assemblies and Burnup Histories

It is assumed that the commercial SNF waste stream can be approximated by calculating source terms for generic PWR and BWR assemblies at incremental enrichments and burnups and that a generic burnup history (without the modeling of outages, intermittent down times, etc.) can be used for the depletion calculations. The rationale for this assumption is based on the analysis provided in NUREG/CR-5625 (Hermann et al. 1994 [DIRS 154045]), which shows that the heat

generation rates of generic PWR and BWR SNF assemblies, in *watts per kg U*, do not vary significantly with details of irradiation history for a given burnup and cooling time between 5 and 100 years. Design basis values of fuel parameters (enrichment, burnup, and aging) can be different for shielding analysis and thermal analysis.

The decay heat rates include the contributions from the radiation generated by the fission products and from the radiation generated by the actinides. The fission product contribution dominates the decay heat generation initially, but its importance decreases with time relative to the actinide contribution. Fission product generation is sensitive to the assembly burnup, which is determined by the total number of fissions. It is less sensitive to the neutron spectra or actinide compositions because the fission yields vary slowly with these variables. While the irradiation history, especially for the last reactor cycle, will greatly influence the short-lived fission products, the dependence of the decay heat rate on the specific power exists only for the first five years of cooling. There is a mandatory five-year cooling period before waste acceptance, per 10 CFR 961.11 [DIRS 182678], which will aid in decreasing the dependence of the heat generation rate on the short-lived fission products. Therefore, generic burnup histories can be used for the depletion calculations.

6.3.1.2 Uniform Specific Power

An average uniform specific power over the entire length of the assembly is assumed, and the total irradiation interval is determined as the ratio of the assembly burnup to the specific power. The actual axial burnup profile is accounted for in the subsequent shielding and thermal evaluations.

6.3.1.3 Interpolation in Arrays of Results (Decay Heat Source)

It is assumed that the source terms can be generated for an array of various enrichments, burnups, and decay times and that interpolation can then be used to obtain the source terms of any specific assemblies in the waste stream without requiring explicit modeling of the assemblies. The rationale for this assumption is that, as described in Section 6.3.1.1, for a given burnup and cooling time during the repository preclosure period, the decay heat rate, in watts per kg U, is relatively constant for different fuel assembly types. For a sufficient number of enrichments, burnups, and decay times, the source term error resulting from interpolation is on the order of the resolution of the calculation methods.

6.3.1.4 Assembly Mass Loading

As discussed in Section 5.3.1, the B&W Mark B assembly is used as the generic PWR fuel lattice for analysis due to its high initial heavy metal loading and large amount of SS and Inconel hardware. It is assumed that the initial heavy metal loading of a PWR assembly is 475 *kg* of heavy metal, instead of the 464 *kg* of a typical B&W Mark B assembly (Punatar 2001 [DIRS 155635], Table 3.1). For a BWR assembly, the initial heavy metal loading is assumed to be 200 *kg*, instead of the 184 *kg* for a typical GE 8 × 8 BWR fuel assembly (Larsen et al. 1976 [DIRS 146576], p. A-2). The rationale for these assumptions is that a higher initial uranium loading leads to a proportionally higher source term, which is conservative for design considerations.

Design basis values of fuel parameters (enrichment, burnup, and aging) can be different for shielding analysis and thermal analysis.

6.3.2 Non-Commercial Spent Nuclear Fuel Waste Forms Assumptions

Assumptions related to evaluation of source terms from non-commercial SNF waste forms are discussed in the following sections.

6.3.2.1 U.S. Department of Energy Spent Nuclear Fuel Waste Forms

For DOE SNF, it is assumed that the total initial radionuclide inventory provided by *General Description of Database Information Version 5.0.1* (DOE 2004 [DIRS 171271]) is adequate for the analyses of the repository at Yucca Mountain. The rationale for this assumption is that the Idaho National Laboratory (INL) formerly Idaho National Engineering and Environmental Laboratory (INEEL) has generated inventories for several representative fuel types in the DOE SNF waste stream, which are used to generate radionuclide inventories for the rest of the waste stream.

6.3.2.2 Defense High-Level Radioactive Waste

For HLW in borosilicate glass logs, the defense HLW historical information regarding the inventory at the various sites is used in decay calculations to generate initial radionuclide inventories (originally DOE 2002 [DIRS 155970], Appendix A, and later DOE 2004 [DIRS 172092], Ray 2007 [DIRS 181690], WVNS 2001 [DIRS 157559], and BSC 2007 DIRS [182239]). These inventories are then used in ORIGEN-S decay calculations to obtain source terms over time. The ORIGEN-S code is described in Section 7.3.1.2. It is assumed that the information for the material planned for disposal at Yucca Mountain is adequately represented by the radionuclide inventories provided by the sites. The rationale for this assumption is that the information provided represents an average of the material, not the bounding.

6.4 SHIELDING ANALYSES ASSUMPTIONS

6.4.1 Use of an Axial Peaking Factor or Axial Burnup Profile

Because the radiation source terms are generated with the assumption that the burnup is uniformly distributed within a SNF assembly, an axial power peaking factor or axial burnup profile is used to develop neutron and photon source strengths in the active fuel region. The rationale for this assumption is to conservatively account for the maximum values of the actual axial source distributions. In the event an axial power peaking factor is used, the value for a PWR SNF assembly is 1.25 (BSC 2004 [DIRS 172227], Section 5.2.1). This value is based on the predicted axial decay heat rate profile of a PWR SNF assembly provided in *Testing and Analyses of the TN-24P PWR Spent-Fuel Dry Storage Cask Loaded with Consolidated Fuel* (EPRI 1989 [DIRS 101947], p. 3-26). The axial power peaking factor of a BWR SNF assembly is 1.25 (BSC 2003 [DIRS 166596], Section 3.5, page 9). This peaking factor has been determined from the axial burnup profile of a BWR SNF assembly as a function of average assembly burnup (BSC 2003 [DIRS 164364], p. 47). The rationale for using this value is that it is conservative for an assembly average burnup of 40 GWd/MTU or higher. In the event an axial

burnup profile is used, a typical axial gamma and neutron source profile for PWR or BWR assembly are used to account for the axial distribution of gamma and neutron sources in active fuel. Typical gamma and neutron axial source profiles are provided in *Users Manual for SCALE-4.4A* (CRWMS M&O 2000 [DIRS 153872], Table S4.4.5).

6.4.2 Homogenization of the Radiation Source Region for CSNF

In a three-dimensional shielding analysis for the waste packages containing commercial SNF, the contents and radiation sources of each SNF assembly region (i.e., plenum, end fitting, and active fuel) are uniformly homogenized. The rationale for this assumption is based upon a study of the effect of source geometry on the waste package surface dose rates described in *Calculation of the Effect of Source Geometry on the 21-PWR WP Dose Rates* (CRWMS M&O 1998 [DIRS 102134], p. 22 to 26). The results of the study indicate that identical dose rates on the external surfaces of a waste package are obtained for two different source geometry representations: a detailed geometric representation, and a representation in which the contents and radiation sources are homogenized inside region dimensions. Note that the use of a detailed assembly description is acceptable.

6.4.3 Homogenization of the DOE SNF Canister

The contents and radiation source of the DOE SNF canisters are homogenized inside the cavity of the DOE SNF canister. However, if the DOE SNF canister contains one intact SNF assembly (e.g., Shippingport Light Water Breeder Reactor SNF), the assembly contents and radiation sources are homogenized inside the assembly dimensions. The rationale for this assumption is that the homogenization process decreases the fuel self-shielding and moves the radiation source closer to the outer surfaces of the waste package, allowing more particles to reach the outer surface and, hence, increasing the dose rate. Note that the use of a detailed assembly description is acceptable.

6.4.4 Omission of Waste Package Internals

For the one-dimensional shielding analysis of waste package radial dose rates, the fuel region of the waste package, which consists of the waste form, neutron absorber plates, thermal shunts, and other structural members, is radially homogenized inside the waste package cavity with some internal components omitted. The rationale for this assumption is that it is conservative for calculating dose rates on the surfaces of the waste package because the structure components that would otherwise attenuate neutrons and photons are not represented.

6.4.5 Use of a Watt Fission Spectrum

A Watt fission spectrum (Briesmeister 1997 [DIRS 103897], Appendix H, pp. H-2 and H-3) is used for the neutron source energy distribution of DOE SNF because the actual neutron spectra are not available for most of the DOE fuels. The rationale for this assumption is that the dose rate evaluation is not sensitive to the neutron spectrum because the neutron dose rate contribution to the total dose rate outside of the waste package is negligible for the repository preclosure period.

6.4.6 Fresh Fuel Assumption

The composition of fresh fuel is used to represent the attenuation properties of spent fuel in the shielding calculations. The rationale for this assumption is that, while photon attenuation properties of spent fuel and fresh fuel are similar, fresh fuel has a conservatively higher neutron dose rate, due to greater production of fission neutrons. This is not due to the fission yield for neutrons, but rather to the greater abundance of fissile constituents. The neutron and gamma ray sources in the actinides and fission products are derived from the spent fuel composition and are represented as fixed sources in the shielding calculations. Therefore, the radiation sources are not affected by this assumption.

6.4.7 Treatment of Material Composition Variations

For material compositions having elements with specified ranges, (i.e. weight percentages of each constituent) the midpoint value is used and the abundance of the most abundant element is adjusted to maintain the material density. The rationale for this assumption is that small weight percentage variations of each element constituent do not affect the accuracy of dose results, as long as the density is maintained. This assumption is used to model the analyzed system.

6.4.8 High-Level Radioactive Waste Glass Source Terms

The source terms utilized for the short HLW calculation features the SRS HLW and the Hanford HLW, which are the bounding cases (BSC 2007, [DIRS 183163], Attachment C). However, it should be mentioned that the HLW sources should not be compared strictly by intensity for SRS and Hanford. Therefore, selection of either SRS or Hanford is based on specific application.

6.4.9 Infinite Cylinder Representation of a Waste Package in SAS1 Analyses

For waste package shielding analysis, SAS1 is an effective tool for evaluating the radiation levels on and beyond the radial outer surface of a waste package. SAS1 assumes a waste package to be an infinite cylinder with a homogenized fuel region in the center, enclosed by the IV and OCB. The rationale for this assumption is that, because the length of a waste package is approximately three times the diameter, the infinite cylinder representation of the waste package should yield accurate dose results for the radial direction.

7. WASTE PACKAGE COMPONENT ANALYSIS METHODS AND COMPUTATIONAL TOOLS

This section describes the analytical methodology and computational tools used in each of the design disciplines. For each discipline, reference is made to specific computational tools, to demonstrate that qualified computer codes or commercial off the shelf software embodying these methodologies exist. However, this should not be construed to limit subsequent analyses and calculations to only versions listed in Section 3. New versions are not listed in this Section of these computer codes can and will be qualified for future analyses and calculations.

It should be noted that this report may describe methods not for calculations and analyses beyond those cited in the LA.

7.1 STRUCTURAL DESIGN

Structural design uses the computational tools discussed in Section 7.1.1 to perform various analyses discussed in Section 7.1.2. A discussion of the mesh used for structural calculations is given in Section 7.1.3. Design stress limits are presented in Section 7.1.4. Construction of nonlinear material behavior curves is presented in Section 7.1.5, fracture considerations given in Section 7.1.6 and reliability methodology for waste packages is in Section 7.1.7.

7.1.1 Computational Tools

Structural calculations are performed using ANSYS, LS-DYNA, Mathcad and Excel.

7.1.1.1 ANSYS

ANSYS is a finite-element software package that can be used to solve a variety of problems. Waste packages, emplacement pallets and drip shields can be represented as two-dimensional or three-dimensional finite-element geometries, depending on the symmetry of the design or the loading. ANSYS is widely used for structural evaluations of static and dynamic problems. Materials can be represented with elastic or elastic-plastic temperature-dependent properties. Dynamic evaluations can be performed, such as real-time events with gravitational acceleration acting on component masses. Interfaces between components are represented with contact elements that incorporate interface stiffness and friction. Seismic evaluations can be performed as frequency domain analyses using a response spectrum or can be solved as time-domain analyses using time histories (acceleration, velocity, or displacement). Thermal expansion and stress can be calculated by combining thermal and structural representations into a single analysis.

7.1.1.2 LS-DYNA

LS-DYNA is a finite element program for nonlinear dynamic analysis of structures in three dimensions. Livermore Software Technology Corporation is the development source for the LS-DYNA finite element analysis software program. LS-DYNA is capable of simulating complex real world problems and is widely accepted as the premier analysis software package for a vast number of engineering applications. LS-DYNA analysis capabilities include, but are not limited to, nonlinear dynamics, rigid multi-body dynamics, quasi-static simulations, thermal analysis, fluid analysis, fluid-structure interactions, and finite element method-rigid multi-body dynamics coupling. LS-DYNA is well suited for performing dynamic impact analyses of the waste packages, drip shields, and emplacement pallets.

7.1.1.3 Mathcad

Mathcad can solve systems of equations, allowing the user to evaluate the impact of parameter variance quickly.

7.1.1.4 Excel

Excel can solve systems of equations, and plot a group of data.

7.1.2 Description of Pertinent Analyses

Structural calculations demonstrate that the waste package, drip shield, and emplacement pallet meet the requirements for normal operations and event sequences. These fall into the following broad groups:

- Normal Operations
- Internal Pressurization
- External object Impacts on Waste Package
- Dynamic Impacts on the Waste Package
- Seismic Evaluations
- Residual Stress Reduction

7.1.2.1 Geometric Design Calculations

Geometric design calculations are primarily sizing calculations to verify that each component is designed to accept the waste form with the dimensions given in the BOD (BSC 2006 [DIRS 177663]). Additionally, external features and features that interface with the Facilities Design Project are discussed and demonstrated to show compliance with the proper criteria. These calculations are written as sections of the analysis of the appropriate component design, rather than as stand-alone calculations.

7.1.2.2 Normal Operations Calculations

Normal operating loads are those associated with expected normal operations, such as loading, maneuvering, and emplacing the waste packages.

Emplacement Pallet Lift — A static, elastic analysis was performed for the EP while loaded with the heaviest WP using ANSYS. A quarter-symmetry, three-dimensional, FER of the EP with brick elements is used in the analysis. The exact mass and geometry of the WP is represented by simplified model. A quarter model of the OCB is used to represent the WP. The density of the OCB model is then back calculated using the quarter mass of the WP and the volume of the OCB model. This approach preserves all features of the problem relevant to the structural analysis.

Static Loading of Waste Package on Emplacement Pallet—The stresses in the EP, due to the static loading of the waste package on the pallet, are assessed using a quarter-symmetric, three-dimensional, static, finite-element analysis in ANSYS. The waste package is represented as a simple hollow cylinder with brick elements and the density of the model is modified to account for the weight of the non-represented parts of the WP and internals mass.

Residual and Differential Thermal Expansion Stresses—Residual and differential thermal expansion stresses are evaluated in the axial and radial directions for all waste packages. This stress is evaluated parametrically using the highest projected surface temperature of the waste package near 200°*C* (BSC 2006 [DIRS 179686], Tables 49, 50). The IV and OCB are designed with radial and axial gaps to prevent contact that would result from thermal expansion. These gaps are toleranced such that the nominal dimension is the minimum gap allowed.

7.1.2.3 Internal Pressurization Calculations

The pressurization of the waste package is assumed to occur due to the rupture of all fuel rod cladding or other primary barriers contained in the waste package, provided the waste form retains an intact pressure boundary before being loaded into the waste package. The calculation uses a closed-form solution to the problem of a cylindrical shell subject to internal pressure load to determine the maximum stresses in the waste package. In this evaluation, the inner vessel lid is assumed to fail before the outer lid; however, no structural credit is assumed for the outer lid. Evaluations are performed over uniform waste package temperatures ranging from 20°*C* to 600°*C*. The peak stresses (membrane and bending) at the junction of the cylinder and lid from these evaluations are obtained and shown to be less than the ultimate tensile stress.

7.1.2.4 Static Load of Collapsed Drift on Drip Shield

The stress and buckling within the drip shield, due to static load of the rock from the collapsed drift, is evaluated using a quarter-symmetric, three-dimensional, static, finite-element LS-DYNA analysis. The drip shield connector plates, connector plate guides, and lifting plates are not included in this representation. This slightly conservative approach has a negligible effect on calculated results. The overburden pressure, which takes into account the masses of the loose rock, is applied statically on appropriate structural members.

7.1.2.5 Impacts on Waste Package

Rock fall on Waste Package — The waste package rock fall is evaluated as a three-dimensional, transient dynamic, elastic-plastic finite-element analysis using LS-DYNA. The interaction of the waste package internals, inner vessel, and outer corrosion barrier is conservatively assumed to maximize the stress on the inner vessel and outer corrosion barrier. A realistic representation of rock geometry is assumed for this evaluation. The rock shape and dimensions are based on rock fracture characteristics, and static material properties are conservatively used due to the unavailability of dynamic material properties.

The rock may have an initial velocity due to a seismic event and then be accelerated due to gravitational forces until it strikes the waste package surface. The simulation is continued throughout the impact until the rock begins to rebound at which time the induced stresses reach peak values.

For multiple rock fall scenarios the subsequent rock impacts are of average expected size and kinetic energy (BSC 2007 [DIRS 180415], Table 6 and Appendix A). A complementary cumulative distribution function comparison for rock fall masses of a two-block rock fall configuration shows that one block carries most of the weight (several metric tons) and the second block will be of typical rock fall size (a few hundred kilograms) ((BSC 2007 [DIRS 180415], Section 6.4.5.2.4). The maximum effective strain rates that typically occur during rock fall events are not high enough to produce significant material property changes. The impact of using material properties obtained under static loading conditions for the multiple rock fall event scenario is anticipated to be small.

7.1.2.6 Dynamic Waste Package Impacts

Oblique Impact on TEV Lifting Feature — The impact evaluation is a bounding case for other impact events and is performed for a waste package as a three-dimensional, transient dynamic, elastic-plastic finite element analysis using LS-DYNA. A representation of the waste package is positioned to impact the TEV lifting rail in a worst case orientation. The interaction of the waste package internals and waste package is conservatively assumed to maximize the stress on the inner vessel and outer corrosion barrier.

Vertical Impact on Invert Steel — The vertical impact evaluation is a bounding case for other impact events and is performed for a waste package as a three-dimensional, transient dynamic, elastic-plastic finite element analysis using LS-DYNA. A representation of the waste package is positioned to impact the invert steel in a worst case orientation. The interaction of the waste package internals and waste package is conservatively assumed to maximize the stress on the IV and OCB.

Vertical Impact with Emplacement Pallet — The vertical impact with emplacement pallet evaluation is performed as a three-dimensional, transient dynamic, elastic-plastic finite element analysis using LS-DYNA. A full three-dimensional representation of the waste package and emplacement pallet is positioned above an unyielding surface and the invert steel in a worst case orientation for stresses at the OCB to emplacement pallet contact.

Transporter Runaway TEV — Events resulting in a transporter runaway are not credible (BSC 2005 [DIRS 174467], Section 4.1.17), but transporter accidents may occur. For these events, if identified, evaluations will be performed as a three-dimensional, transient dynamic, elastic-plastic finite-element analysis using LS-DYNA, in a manner similar to the vertical and horizontal drops.

Sliding and Inertial Effects of Waste Package Contents — Inertial effects of the waste package contents are an intrinsic part of dynamic structural calculations performed explicitly by finite element codes. Sliding effects of waste package internal contents during impacts are evaluated in calculations where specific answers about stresses in the waste package contents are to be determined. Coefficients of friction are used based on the materials and situation. When the waste package contents are not specifically under evaluation, those contents are often simplified so that the mass and inertial effects are accounted for but geometry is simplified. A rationale for simplifying waste package contents is to decrease computer execution time and size of the finite element representation. Another rationale is that for evaluation of the outer corrosion barrier, waste package contents need not be modeled in detail to get an accurate answer.

7.1.2.7 Seismic Evaluations

Evaluation of Waste Package Component Exposed to Vibratory Ground Motion — The motion of preclosure repository components (namely waste package and pallet) due to a seismic event is evaluated using a three-dimensional finite element representation with an acceleration time history as an externally applied load. Because these repository components are not anchored to the drift invert or to each other, in case of an extremely intense seismic event they

are free to move and impact each other, generating considerable contact forces as well as material and structural (geometrical) nonlinearities. The nonlinearity of the problem is further exacerbated by an essential role played by friction. The primary objective of these simulations is to evaluate the impact velocities at the waste package outer corrosion barrier in the course of seismic events of various intensities and frequencies of occurrence. The predicted impact velocities are used in conjunction with the bounding dynamic impact events to evaluate the seismic response.

7.1.3 Mesh Discretization

The purpose of mesh refinement is to ensure the mesh objectivity of the finite element analyses, i.e., that the results obtained are not mesh-sensitive. The mesh-refinement study consists of the development of an optimum (cost-effective) mesh that is believed to give mesh-objective (mesh-insensitive) results. That mesh is then refined again and computational results for the two mesh sizes are compared. The finite-element representation is considered mesh-objective if the relative difference in results between the two meshes is approximately an order of magnitude smaller than the relative difference in mesh size in the region of interest; otherwise further mesh refinement is needed. The mesh density, as used throughout this section, refers to the volume or the area of the representative (3-dimension or 2-dimension, respectively) element in the region of interest (for example, the element characterized by the highest stresses or strains).

The optimum mesh is created by the following sequence of steps:

- The initial mesh is created by pursuing the customary engineering practices: the element type is appropriately chosen; the mesh is refined in the regions of interest (the highest stress/strain regions, initial impact regions, stress concentration regions, etc.); the mesh is mapped whenever possible; and the aspect ratio of elements is kept reasonable.

- In the region of interest, the initial mesh is refined in one direction while the element size in the other two directions is kept unchanged (for example, the mesh is refined across the thickness while kept unchanged in the hoop and axial directions). The mesh-refinement procedure is repeated in this manner until the relative difference in results between the two successive meshes is acceptable (i.e., approximately an order of magnitude smaller than the relative difference in the mesh size). The mesh dimension in this direction is then fixed at the largest value that satisfied the previously mentioned criterion.

- The same procedure is consecutively repeated in the remaining two directions.

- The intention of this one-direction-at-a-time mesh refinement is to create, in a consistent and systematic manner, a mesh that is cost-effective and objective.

- Whether the created mesh meets the latter requirement is verified by the final step: the simultaneous mesh refinement in all three directions. The level of this mesh refinement should be similar in all three directions. In this final step, the same mesh-acceptance criterion is evoked: the mesh is considered objective if the relative difference in results between the two meshes is approximately an order of magnitude smaller than the relative difference in mesh size in the region of interest.

It should be emphasized that the mesh objectivity is verified by the final step regardless of whether the final mesh is arrived at by the described one-direction-at-a-time mesh refinement or not. The one-direction-at-a-time mesh refinement is optional because its only purpose is to develop a cost-effective mesh (that satisfies the objectivity requirement).

7.1.4 Waste Package Component Design Stress Limits and Failure Criteria

For structural analyses of preliminary designs that consider material nonlinear behavior, the maximum-shear-stress or Tresca (strength of materials) criterion is used in determining stress limits. In general terms, this criterion assumes that the design is safe as long as stress intensity (the difference between maximum and minimum principal stress) remains below a certain limit. In particular, the failure criterion chosen was the acceptance criteria for plastic analysis (ASME 2001 [DIRS 158115] Section III, Division 1, Appendix F, F-1341.2). This is an acceptable vessel designer choice of ASME Code acceptance criteria for service loadings with Level D service limits for vessel designs in accordance with NC-3200 (Safety Class 2 vessels) when a complete stress analysis is performed (ASME 2001 [DIRS 158115], NC-3211.1(c), Appendix XIII and Note (4) to Table NC-3217-1).

The ASME Code suggests the following primary stress intensity limits for plastic analyses (ASME 2001 [DIRS 158115], Section III, Division 1, Appendix F, F-1341.2):

- The general primary membrane stress intensity shall not exceed 0.7 S_u for ferritic steel materials included in Section II, Part D, Subpart 1, Table 2A and the greater of 0.7 S_u and $S_y + {}^1/_3 (S_u - S_y)$ for austenitic steel, high-nickel alloy, and copper-nickel alloy materials included in Section II, Part D, Subpart 1, Table 2A, where S_u and S_y are tensile strength and yield strength, respectively.

- The maximum primary stress intensity at any location shall not exceed 0.9 S_u.

- The average primary shear across a section loaded in pure shear shall not exceed 0.42 S_u.

The Pressure Vessel Research Council of the Welding Research Council provides guidelines (Hechmer and Hollinger 1998 [DIRS 166147]) to the ASME B&PV Code Rule Committees for assessing stress results from three-dimensional finite element analysis in terms of stress limits in the design-by-analysis rules (ASME 2001 [DIRS 158115], Section III [Class 1, NB] and Section VIII, Division 2). These guidelines were developed for linear analyses and Pressure Vessel Research Council recommends that future research work should be conducted to generate state-of-the-art guidelines for applying inelastic, large-deformation analyses. Therefore, a cautious use of the Pressure Vessel Research Council recommendations was made in developing methodologies for post-processing LS-DYNA nonlinear plastic simulations to assure conservative representations of the general primary membrane stress intensity and maximum primary stress intensity.

The Pressure Vessel Research Council recommendations also refer to an earlier Pressure Vessel Research Council (Phase 1) report (Hechmer and Hollinger 1998 [DIRS 166147]), which recommended that the ASME Code (ASME 2001 [DIRS 158115], Appendix F) "should be revised to provide a limit on effective plastic strain which is more appropriate for events that are

energy controlled, rather than load controlled, which is all that was considered when ASME B&PV Code Appendix F was written." The YMP recognizes that strain-based or energy-based criterion may be more appropriate than stress-based limits for evaluation of the credible preclosure event sequences, (see Section 4.1.3.1). However, the project is also committed to applying the ASME Code for structural analyses, and until the ASME B&PV Code Rule Committees prepare rules in the ASME Code, Appendix F (ASME 2001 [DIRS 158115], Appendix F) for using strain energy limits, primary stress intensity limits will be used.

The ASME Code design-by-analysis guidance recognizes the differences in importance of different types of stresses and provides guidance on their correct assignment to the different categories of stress intensity used to evaluate different types of failure modes (ASME 2001 [DIRS 158115]). The three types of stresses are membrane, bending and peak stresses. The three categories of stress intensity are primary (P_m, P_L and P_b [general primary membrane, local primary membrane, and primary bending, respectively]), secondary (Q), and peak (F).

A primary stress is defined as "a normal stress developed by the imposed loading which is necessary to satisfy the laws of equilibrium of external and internal forces and moments. The basic characteristic of a primary stress is that it is not self-limiting. Primary stresses which considerably exceed the yield strength will result in failure or, at least, in gross distortion" (ASME 2001 [DIRS 158115], Section III, Division 1, Appendix XIII, XIII-1123(h)).

A secondary stress is defined as "a normal or a shear stress developed by the constraint of adjacent parts or by self-constraint of the structure. The basic characteristic of a secondary stress is that it is self-limiting. Local yielding and minor distortions can satisfy the conditions which cause the stress to occur and failure from one application of the stress is not expected" (ASME 2001 [DIRS 158115], Section III, Division 1, Appendix XIII, XIII-1123(i)). A cited example of a secondary stress is "bending stress at a gross structural discontinuity." A gross structural discontinuity is defined as "a source of stress or strain intensification which affects a relatively large portion of a structure and has a significant effect on the overall stress or strain pattern or on the structure as a whole" (ASME 2001 [DIRS 158115], Section III, Division 1, Appendix XIII, XIII-1123(b)). Cited examples of gross structural discontinuities are head-to-shell junctions and junctions between shells of varying thickness.

A local primary membrane stress is defined as "a membrane stress produced by pressure or other mechanical loading and associated with a discontinuity [that] would, if not limited, produce excessive distortion in the transfer of load to other portions of the structure. Conservatism requires that such a stress be classified as a local primary-membrane stress even though it has some characteristics of a secondary stress" (ASME 2001 [DIRS 158115], Section III, Division 1, Appendix XIII, XIII-1123(j)). The other differentiating feature of a local primary membrane stress is that it is localized, and guidance is provided (ASME 2001 [DIRS 158115]) for evaluating if membrane stress fields are adequately "local" to be assigned a P_L classification rather than a more restrictive P_m classification.

The failure mode being addressed by the general primary membrane stress intensity (P_m) limit is "collapse" in the sense that collapse includes tensile instability and ductile rupture under short term loading (Hechmer and Hollinger 1998 [DIRS 166147], Guideline 1). The principal (main) failure mode being addressed by the maximum primary stress intensity ($P_L + P_b$) is excessive.

The event sequences considered in this report are not repetitive where fatigue cracking or incremental collapse might be an issue. It follows that evaluation of secondary stress intensities (Q) or maximum total stress intensities ($P_L + P_b + Q + F$) are not appropriate. Brittle fracture is also precluded by the high ductility of the outer boundary material, Alloy 22, at the temperatures experienced after waste form loading. Although the high-stress areas are comprised of primary, secondary, and peak stresses, only the primary stress intensities (P_m, P_L, and P_b) contribute to plastic instability (tensile tearing) or excessive plastic deformation, and therefore, only the primary stress intensities are evaluated for the event sequences.

The ASME Code was used to determine which stress fields should be classified as primary and which should be classified as secondary when evaluating the event sequences (ASME 2001 [DIRS 158115], Section III, Division 1, Appendix XIII, Table XIII-1130-1). All membrane stress fields were conservatively classified as primary. Classification of the bending stresses was more involved.

Review of representative analyses for the event sequences indicated that the most important wall-bending stresses in the outer corrosion barrier occurred near gross structural discontinuities. Some of these gross structural discontinuities were integral to the outer boundary and some were introduced by the constraint of adjacent parts or impact surfaces.

The integral gross discontinuities in the outer corrosion barrier are similar to ASME Code vessel details such as shell-to-lid junctures and step-changes in wall thickness. The bending stresses are being created by self-constraint, and the ASME Code classifies these bending stresses as secondary (ASME 2001 [DIRS 158115], Section III, Division 1, Appendix XIII, Table XIII-1130-1). The only exception is at the shell-lid junction, where concern about the predictability of the central stresses of the lid leads the ASME Code to caution the designer to consider classifying the bending stresses as P_b (ASME 2001 [DIRS 158115], Section III, Division 1, Appendix XIII, Table XIII-1130-1, Note (4)). However, this is not appropriate guidance for inelastic analyses because the increased flexibility of the juncture caused by inelastic behavior is correctly captured and the central stresses of the lid are accurately predicted.

The bending stresses created by the constraint of adjacent parts or impact surfaces (which can be considered [temporary] "adjacent parts") were reviewed on individual cases with attention to the amount and type of constraint introduced. In the design analyses to date, the constraint of the adjacent part (e.g., sleeves) or impact surface (e.g., emplacement pallet, rock) created local yielding and minor localized distortions in the OCB. The outer corrosion barrier distorted shape reduced the outer corrosion barrier bending stresses while increasing the OCB membrane stresses. The bending stresses in these locally yielded regions are therefore self-limiting and satisfy the basic characteristic of a secondary stress.

Two special reduced modulus studies were conducted on the stress classifications for a horizontal drop event (*Stress Intensity Classification: Waste Package Outer Corrosion Barrier Stresses due to Horizontal Drop Event* BSC 2004 [DIRS 173389]) and a waste package on an emplacement pallet drop ~~(*Drop of Waste Package on Emplacement Pallet - A Mesh Study* BSC 2003 [DIRS 165497])~~. These studies support the above classification.
(Stress Intensity Classification: Waste package Outer Corrosion Barrier Stresses due to Drop with Emplacement Pallet. BSC 2007 [DIRS 184420])

004 na 12/18/07

The structural criterion developed for the OCB for the event sequences was to directly address the dominant failure mode, ductile tearing, and limit the membrane stress intensities, which include average section shear stresses, to acceptable limits. The use of inelastic analyses ensures that local thinning or shape changes that could increase membrane stress intensities are properly accounted for.

Inelastic analyses were conducted using true stress and true strain based constitutive relationships, therefore for Alloy 22, the limit on P_m is $0.7\sigma_u$, the limit on P_L is $0.9\sigma_u$ (where $P_b = 0$), where σ_u is the true tensile strength at temperature (ASME 2001 [DIRS 158115], Section III, Division 1, Appendix F, F-1322.3(b) and F-1341.2).

As stated earlier, P_L must be "local" to not be classified as a more restrictive general primary membrane stress intensity, P_m (ASME 2001 [DIRS 158115], Section III, Division 1, Appendix XIII, XIII-1123(j)). Interpretation of this guidance with respect to the ASME B&PV Code Appendix F (ASME 2001 [DIRS 158115]) limits results in requiring P_L values exceeding $0.77\sigma_u$ to not extend for greater than $\sqrt{R \cdot t}$ in any direction, where R is the midsurface radius and t is the thickness of the OCB.

Rigorously performed, calculation of the primary membrane stress intensities involves:

- Identifying the governing wall location, which may not necessarily contain the maximum stressed point (Hechmer and Hollinger 1998 [DIRS 166147], Guidelines 3 and 4)
- Identifying the orientation of the stress classification line, typically normal to the mid-plane of the shell or lid thickness (Hechmer and Hollinger 1998 [DIRS 166147], Guideline 4d).
- Identifying the stress component ($\sigma_x, \sigma_y, \sigma_z, \tau_{xy}, \tau_{yz}, \tau_{zx}$) fields across the wall of the outer corrosion barrier
- Averaging the stress component fields to create wall-averaged stress components
- Translating the wall-averaged stresses to principal stress directions by solving a cubic equation
- Calculating the difference between the maximum (σ_1) and minimum (σ_3) stress direction values.

To simplify the calculation, the wall-average of the element total stress intensity (twice the maximum shear stress) values through the outer corrosion barrier is used to define the primary membrane stress intensities. This is a conservative representation because it ignores possibly changing principal stress planes through the wall, and it includes the secondary and peak stress contributions.

The failure criterion used is broken into tiered screening criteria shown in Table 4. The easiest to apply and most conservative criteria are applied initially. If these can not be met, less conservative screening criteria are imposed that require more calculations. These screening

criteria in decreasing order of conservatism are listed below. An element's total stress intensity, σ_{int}, is equal to twice the element's maximum shear stress (ASME 2001 [DIRS 158115], Section III, Division 1, NB-3000).

Table 4. Outer Corrosion Barrier Tiered Screening Criteria

Criteria	Condition of Acceptance
Maximum $\sigma_{int} < 0.7\sigma_u$? No.	Yes: Meets P_m and P_L limits without the need for wall averaging.
Maximum $\sigma_{int} < 0.77\sigma_u$? No.	Yes: Meets P_L limit without the need for wall averaging, but the stress field must not be uniform around the entire circumference (only a concern for vertical drop events).
Maximum wall-averaged $\sigma_{int} < 0.7\ \sigma_u$? No.	Yes: Meets P_m and P_L limits.
Maximum wall-averaged $\sigma_{int} < 0.77\sigma_u$? No.	Yes: Meets P_L limit if the stress fields are not uniform around the entire circumference (only a concern for vertical drop events).
Maximum wall-averaged $\sigma_{int} < 0.9\ \sigma_u$ and wall-averaged $\sigma_{int} < 0.77\ \sigma_u$ at $\sqrt{R \cdot t}$ surrounding maximum location? No: Fails simplified screening criterion.	Yes: Meets P_L

Note: P_m is the general primary membrane stress intensity

P_L is the local primary membrane stress intensity

P_b is the primary bending stress intensity

R is the median wall radius

t is the wall thickness

If the wall-averaged σ_{int} limits can not be met, perform a more rigorous evaluation using all six stress components (and solve the cubic equation for principal stress direction values) or use multiple stress classification lines to extrapolate to governing wall locations when they have significant non-membrane stress contributions.

If the screening criteria can not be met, perform a rigorous Code evaluation using quantitative instead of bounding stress classifications. This will require additional elastic finite element analysis with variable Modulus of Elasticity and time-slicing.

For lifting analyses, the acceptance criteria are outlined in *American National Standard for Radioactive Materials—Special Lifting Devices for Shipping Containers Weighing 10000 Pounds (4500 kg) or More* (ANSI N14.6-1993 [DIRS 102016], Section 4.2.1.1). The load-bearing members of the lifting device shall be capable of lifting three times the combined weight

of the shipping container, plus the weight of the intervening components of the lifting device, without generating a combined shear stress or maximum principal stress at any point in the device in excess of S_y. The lifting device shall also be capable of lifting five times the weight without exceeding S_u. This has been withdrawn pending revision, but is still used for guidance.

7.1.5 Calculations for True Measures of Ductility

The material properties in the engineering handbooks and vendor catalogs refer to engineering stress and strain definitions: $s = P/A_0$ and $e = L/L_0 - 1$ (Dieter 1976 [DIRS 118647], Chapter 9), where P is the force applied during a static tensile test, L is the length of the deformed specimen, and L_0 and A_0 are the original length and cross-sectional area of the specimen, respectively. The engineering stress-strain curve does not give a true indication of the deformation characteristics of a material during plastic deformation because it is based entirely on the original dimensions of the specimen. In addition, ductile metal that is pulled in tension becomes unstable and necks down in the course of the test. Hence, LS-DYNA finite element code requires input in terms of true stress and strain definitions: $\sigma = P/A$ and $\varepsilon = \ln(L/L_0)$.

The true stresses and strains (σ, ε) are calculated by using their engineering counterparts (s, e) based on the following relations:

$$\sigma = s \cdot (1 + e) \qquad \text{Equation 1}$$

$$\varepsilon = \ln(1 + e) \qquad \text{Equation 2}$$

Equations 1 and 2 can be readily derived based on constancy of volume ($A_0 \cdot L_0 = A \cdot L$) and strain homogeneity during plastic deformation (Dieter 1976 [DIRS 118647], Chapter 9). These expressions are applicable only in the hardening region of the stress-strain curve that is limited by the onset of necking.

Equations 1 and 2 are used to calculate true tensile strength and true uniform strain (the strain corresponding to tensile strength). These material properties are then used to calculate the hardening (tangent) modulus, E_1 (Figure 5).

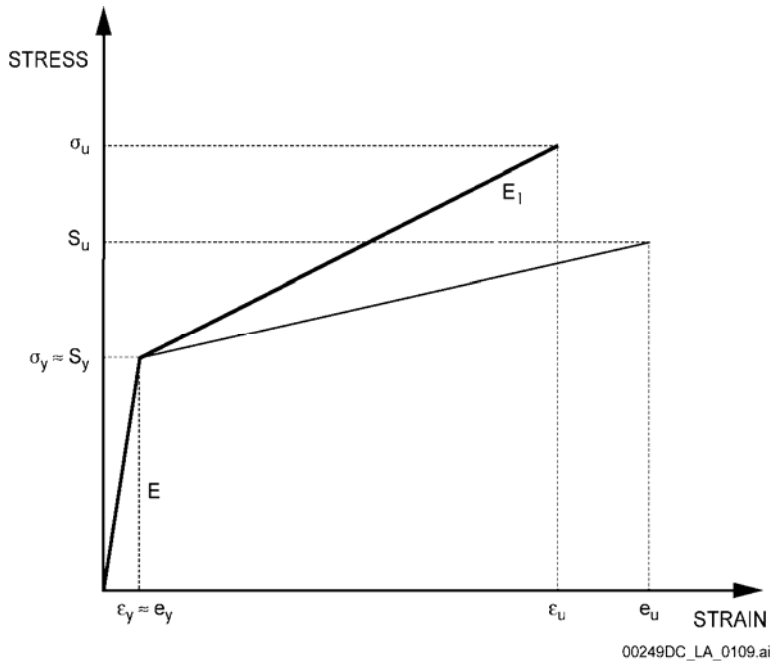

Figure 5. Key Attributes of Bi-linear Stress-Strain Curves

7.1.6 Fracture Mechanics Analyses

The structural analysis methods discussed so far predict margin to failure by ductile collapse. Fracture Mechanics may be used to analyze the potential for brittle fracture. Depending on the material properties, a combination of ductile and brittle failure may need to be considered. The waste package and the drip shield materials, in general, possess ductile behavior. Specific material properties for specific structural calculations may show that only ductile collapse must be considered. For such cases, no further investigation of brittle fracture is required. However, any potential brittle behavior due to environmental conditions in the repository, such as the hydrogen embrittlement of titanium or fabrication effects/defects on titanium and Alloy 22 may require further investigation of these materials. For these cases, fracture mechanics calculations can be performed using either the stress intensity factor or the J-integral at the crack tip, depending on the extent of plasticity that results from the impact. If these fracture parameters exceed the material limits, the crack propagation will be evaluated. Otherwise, the crack growth is arrested and there is no failure. Hence, a rigorous analysis of the crack propagation scheme may determine the consequence of such an event.

The specific problem of crack propagation in the waste package and drip shield materials involves low-velocity impact of two structural components. Existing cracks (manufacturing flaws) on metallic plates may be analyzed. The crack propagation or arrest, under dynamic loads due to rock impacts or handling accidents may be investigated using the commercially available software. This problem may require elastic-plastic material properties and large deformation simulations in addition to the contact between the impacting object and the metal plate.

7.1.7 Passive Component Reliability Methodology for Waste Packages and Ancillary Components

The NRC has provided draft guidance on how the DOE may demonstrate the safety of the waste packages in a risk-informed framework (BSC 2007 [DIRS 181782]), as well as accompanying guidance for seismically initiated event sequences (NRC 2006 [DIRS 178130]). An approach is advanced, working in concert with the Preclosure Safety Analysis Organization, to apply the guidance embodied in the following sections to the evaluation of waste package and ancillary component performance.

The methodology in this subsection specifically addresses dynamic structural performance of the waste package and ancillary components. Thermal performance is excluded since the limits associated with thermal performance are specified as simple temperature limits that are not amenable to inclusion in the passive-component reliability framework.

7.1.7.1 Risk-informed Approach for Passive Components

In the NRC draft guidance for assessing the reliability of passive components, such as waste packages, an approach is advocated where the statistical distribution of the structural capability of the component is compared with the statistical distribution of the loads that might be imposed on the component (BSC 2007 [DIRS 181782]). This is illustrated in Figure 6, where the convolution of these two curves estimates the risk of "failure" for the component in this context. (Note that the structural performance of the waste packages is approximated to be a log-normal distribution, consistent with reliability data for engineered structures.) The risk-informed approach follows this guidance and places it in terms of the unique characteristics of the waste packages and the expected operations at the repository.

Preclosure Safety Analysis has offered the opinion, based on previous analyses of the waste package structural performance, that the waste package is a very robust structure and implementation in accordance with Appendix B of HLWRS-ISG-02 (BSC 2007 [DIRS 181782]) is sufficient. This is because, for credible event sequences, previous structural analyses using a code compliance-based approach (See Section 7.1.7.2.1) suggest that there should be large margin to breach of the waste package OCB.

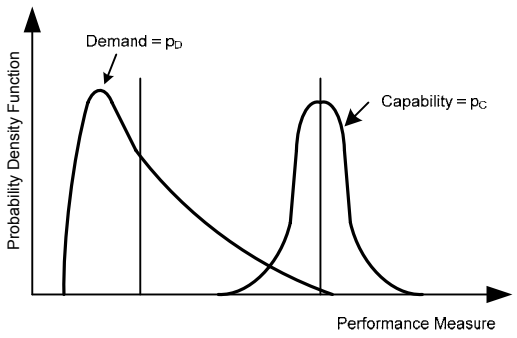

Figure 6. Demand and Capability Curves

7.1.7.2 Structural Analysis Approach (Non-Seismic)

The basic approach for the analysis of event sequences involving dynamic structural analysis is outlined in this sub-section. Extensions to address the effects of vibratory ground motion are described in the sequel sub-section.

7.1.7.2.1 Current Deterministic Approach

In the current deterministic approach to the structural analysis of waste package performance, net conservative material properties and performance limits are used to assess margin to waste package OCB breach for a fixed limiting condition (e. g., drop height). The conservatism in the current approach for structural analyses may be summarized as follows:

- Code minimum structural properties (when the term "Code" is used, it refers to the ASME B&PV (ASME 2001 DIRS [158115]) as applied to the waste package (BCS 2007 [DIRS 182357])
- Code allowable structural limits
- Margin against failure by ductile rupture
- Net conservative structural analysis treatment (strain rate effects neglected, etc.)
- Worst geometry and orientation for event
- Range of temperatures studied (20°*C* to 300°*C*)

7.1.7.2.2 Prospective Risk-informed Approach

For the event sequence evaluations for the LA, expected material properties will be assumed and the performance of Alloy 22 will be extended to defensibly higher values based on the anticipated structural failure mechanism (i.e. ductile tearing). The new approach for structural analyses may be summarized as follows:

- Consider a credible range for the independent variable that controls the event (e. g., over a range of impact velocities).
- Nominal (typical) properties obtained from metals vendors (affects Demand and Capability in terms of the NRC guidance.
- Adjusted multi-axial tensile instability corresponding to more realistic material structural performance (affects Capability in terms of the NRC guidance)
- Failure by void formation under primary loading versus safety factors on ductile rupture (affects Capability in terms of the NRC guidance)
- Net conservative structural analysis treatment (strain rate effects neglected, etc.) (affects Capability in terms of the NRC guidance)

- Worst geometry and orientation for event—which is not fully compliant with a risk-informed approach, subject to the logic stated in initial discussion of Section 7.1.7.1 (affects Demand in terms of the NRC guidance)

- Relatively low operational temperatures, but not as low as for transportation analyses of shipping casks (affects Capability in terms of the NRC guidance)

For the actual Finite Element Analysis (FEA), the average of the vendor structural properties (e. g., Young's modulus, yield strength, elongation, etc.) will be used to establish nominal response. The variability of Toughness Index (a measure of the material energy absorbing capacity) will be used to establish the off-nominal capability distribution that addresses material property scatter. The Toughness Index, I_T, is the flow stress multiplied by the uniform strain, ε_u. The flow stress is the average of the yield strength, σ_y, and the ultimate strength, σ_u, and the uniform strain is the strain at the ultimate strength. I_T is defined in terms of true stress and strain values with triaxiality adjustments.

$$I_T = \frac{1}{2} \cdot \varepsilon_u \left(\sigma_y + \sigma_u \right) \qquad \text{Equation 3}$$

The basis for this definition is illustrated in Figure 7. A uniaxial stress-strain curve can be approximated by a bi-linear (see Section 7.1.5 Figure 5) or tri-linear representation (see Section 7.1.7.2.4, Figure 9). Appendix I, Figure I-6 provides a true stress-strain curve for Alloy 22 (see the red curve in that figure) that illustrates that these linearizations are very close the actual curve, up the uniform strain value.

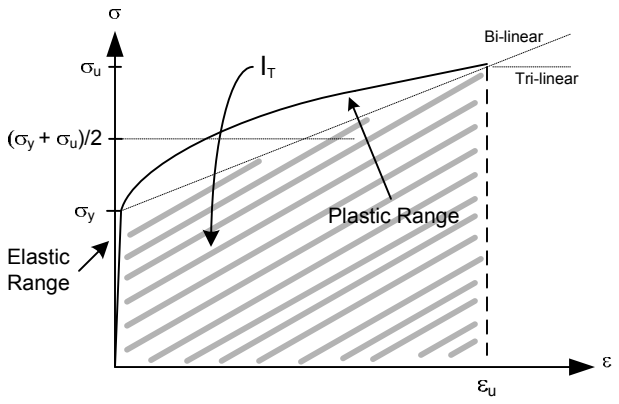

Figure 7. Illustration of Physical Basis for Toughness Index

The elastic strains are very small and the approximate area under the stress-strain curve that represents I_T is computed as:

$$\text{Area} = I_T = \left(\sigma_y \cdot \varepsilon_u\right) + \frac{\varepsilon_u\left(\sigma_u - \sigma_y\right)}{2} = \sigma_y \cdot \varepsilon_u + \frac{\sigma_u \cdot \varepsilon_u}{2} - \frac{\sigma_y \cdot \varepsilon_u}{2} = \frac{1}{2} \cdot \varepsilon_u\left(\sigma_y + \sigma_u\right) \qquad \text{Equation 4}$$

This may be seen to be equivalent to the energy absorption capacity by the following observations. This is illustrated in Figure 8, where a normal force imposed on an element is result in deformation along a single axis (i. e., plane strain).

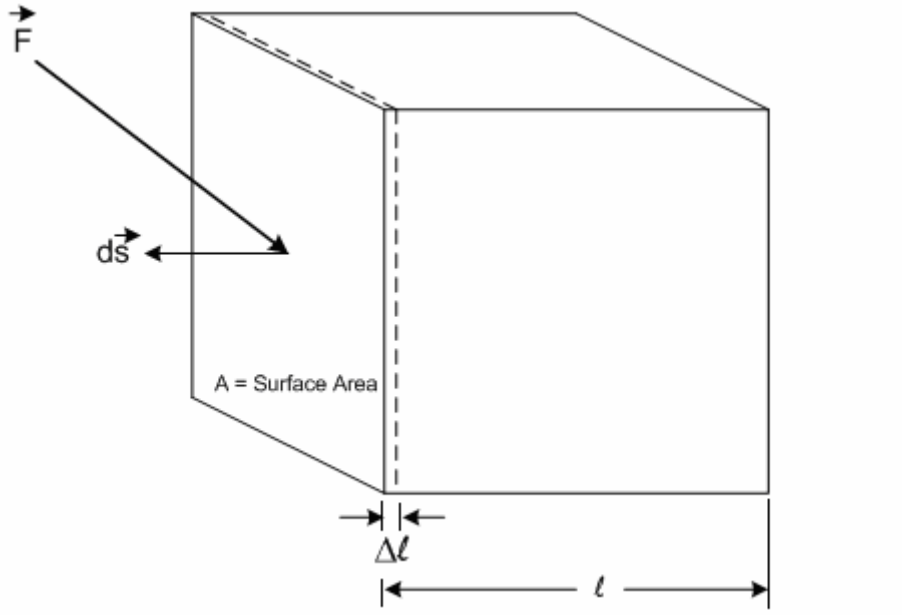

Figure 8. Forces on Element inducing Deformation

First the change in energy, ΔE, due to deformation of a given volume of the material is the work, W, done upon that volume:

$$\Delta E = W = \int_C \vec{F} \bullet d\vec{s} \qquad \text{Equation 5}$$

Considering the normal force against the face of the element,

$$\vec{F} \bullet d\vec{s} = F_n \cdot d\ell = A \cdot \sigma \cdot d\ell \qquad \text{Equation 6}$$

Here A, is the surface area of the element upon which the force is impressed. From the engineering definition of strain,

$$\varepsilon = \frac{\Delta \ell}{\ell}$$ Equation 7

Taking the limit as $\Delta\ell$ goes to zero:

$$d\varepsilon = \frac{d\ell}{\ell} \Rightarrow d\ell = \ell \cdot d\varepsilon$$ Equation 8

The work is computed as the force applied along a path. Noting that the stress that produces the strain is along the displacement path, the work equation for loadings that induce strain equal to the uniform strain may be re-cast as:

$$W = \int_{o}^{\varepsilon_u} A \cdot \ell \cdot \sigma \, d\varepsilon = A \cdot \ell \cdot \int_{0}^{\varepsilon_u} \sigma \, d\varepsilon$$ Equation 9

Ignoring elastic strains, and for the bi-linearization shown in Figure 7,

$$\sigma = E_1 \cdot \varepsilon + \sigma_y$$ Equation 10

Where E_1 is the slope of the bi-linear curve in the plastic range; therefore,

$$\frac{\Delta E}{A \cdot \ell} = \frac{W}{A \cdot \ell} = \int_{\varepsilon_y}^{\varepsilon_u} \sigma \, d\varepsilon = \frac{\varepsilon_u}{2}\left(\sigma_u + \sigma_y\right)$$ Equation 11

It may be seen from this equation that the energy change normalized by the volume is the same as the Toughness Index. For this reason, the area under the engineering stress-strain curve is sometimes termed the strain energy density.

The variability of the three-dimensional stress-strain state (the triaxiality) affects the failure behavior in metals. Ductile failure theories have been developed based on the stress triaxiality term, $\eta = \sigma_m/\sigma'$ and a deviatoric state parameter, ξ. The hydrostatic, or mean, stress, σ_m, is defined below in Equation 12, while σ' is the effective stress—usually the Von Mises stress.

$$\sigma_m = \frac{\sigma_1 + \sigma_2 + \sigma_3}{3}$$ Equation 12

Appendix I discusses the selection of the triaxiality adjustment based on an Alloy 22 representative tensile Forming Limit Diagram (FLD) at the membrane strain Triaxiality Ratio ($TR = \varepsilon_2/\varepsilon_1$).

Due to the established characteristics of Alloy 22, the NRC has concluded that it is not necessary to treat the welds and the heat-affected zones of the welds differently from the base metal—such as by fast fracture (Kokajko 2005, DIRS [182443], enclosure Section 4.2, p. 4). This conclusion is also supported by the results of a material variability study conducted by BSC (Allegheny Technologies 2004 [DIRS 182446]). The failure mode of ductile rupture is conservatively

bounded by void formation. Ductile rupture has been recognized by the NRC as the failure mode for Alloy 22 for such events (Reamer 2004 [DIRS 182440], Enclosure, Section 4.2).

The toughness (strain energy) expended versus toughness available at the governing wall section is used as a measure of damage. The Von Mises effective stress and strain time histories are used to compute a wall-averaged toughness expended, I_T', (approximate area under a constructed stress-strain response curve) from initiation of loading to the time of unloading. An expended toughness fraction, ETF, defined as I_T'/I_T is a measure of damage and when ETF equals 1.0, failure is defined.

Conservative analysis assumptions, such as neglecting strain rate effects, are retained since they are small contributors to the conservative margin. The current mesh-discretization procedure will be retained as it is used to ensure a numerically convergent FEA mesh and has been reviewed by the NRC (Reamer 2004 [DIRS 182440], Section 4.1). Friction coefficients will continue to be taken from the lower end of the representative range for the various material contacts. This is generally a small effect or is conservative, but not overly so. The current approach to stiffness and contact damping will be retained, as the effect of varying these values is small and is done for numerical convergence reasons. Finally, the bi-linear true stress-strain curve definition of material structural properties (Section 7.1.5) will be modified for a more appropriate failure behavior treatment described in Section 7.1.7.2.4.

The worst geometry and orientation will be retained for many of the analyses. This is because the current state of the design of the various facilities and transportation equipment is insufficient to define a range or even an "average" orientation for the event sequences. This will be changed to an average orientation, or a range of orientations, as such information becomes available after the initial submittal of the LA.

For deterministic calculations, lower temperatures are slightly more challenging to the structural performance of the waste packages than higher temperatures. This is due to the increased elongation and disproportionate reduction in yield versus ultimate strength at elevated temperature. For risk-informed calculations, RT will be used. Initial risk informed calculations indicate only a small temperature dependence of the results. ETF values are typically within 10% for equivalent RT and 300°*C* event sequences with RT more damaging at high load levels and 300°*C* more damaging at low load levels. (It should be noted for some extreme-temperature event sequences, notably the drift collapse, that other temperature treatments must be used). It should also be noted that a companion calculation using the deterministic methodology will be performed to estimate the gain in perceived margin from the risk informed approach.

7.1.7.2.3 Unrealized Conservatisms

There are several underlying conservatisms that cannot be realized by the proposed approach. These will remain as unquantified defense-in-depth. Some of these are: (1) the structural performance of the inner vessel of the waste package, including the seal welds that close the inner vessel closure lid; (2) the structural performance of the canisters that enclose the waste forms; and (3) the structural capability of the waste forms and the capability of those waste forms to retain the radionuclides.

7.1.7.2.4 Treatment of Structural Properties

Appendix I discusses the selection of the OCB Capacity calculation approach and provides more details of the approach. It will use an LS-DYNA explicit dynamics solver with modified structural properties (Hallquist 1998 [DIRS 155373]).

A precursor analysis and a material representative cold forming limit diagram (FLD) will be used to adjust the OCB uniaxial uniform strain value for triaxiality effects. Alternatively, a worst-case triaxiality can be used. Triaxiality is the effect of two or three dimensions in the structural response of a homogeneous material. The material structural properties are obtained from uniaxial tension tests, which leads to both underestimating and overestimating the strength of the material in two and three dimensional stress/strain fields, depending on the ratios (triaxiality) of the stress-strain fields.

The use of FLD's is appropriate for dynamic structural event sequences involving the OCB since, in the abstract, it is a relatively thin plate with a finite radius of curvature. In this sense, the structural response of the OCB to the impact against a stiffer surface is essentially a metal forming process.

A precursor analysis may be performed that uses a best-estimate bi-linear true stress-strain curve (Section I-3, Figure I-6) for all waste package components at a loading that results in the OCB governing location's effective (Von Mises) element-wall-averaged (EWA) strain nearly equal to the triaxiality-adjusted true uniform strain value (tensile instability level). A wall-averaged strain value is used since the margin to the through-wall breach of the OCB is sought. This approach will require an iterative calculational procedure. (N. B., if a worst-case triaxiality value is assumed, then this precursor analysis is unnecessary.)

The term "best-estimate" refers to the use of the average of published "typical" plate material strength and elongation values for the OCB material Alloy 22, from three vendors (Haynes 1997 [DIRS 100896], Inco 1995 [DIRS 182441], Special Metals 2006 [DIRS 182449]). The term "best estimate" for the other waste package materials will be based on a simplified 10% increase in ASME B&PV Code (ASME 2001 DIRS [158115]) minimum strength and elongation values. The wall membrane strains with increased loading at the governing OCB location will be reviewed between the yield and tensile instability level for strain path linearity (i. e., proportional loading).

A best-estimate tri-linear material model for the OCB will be conservatively developed using the worst-case triaxiality or based on the actual triaxiality of the governing location in the final (tensile instability level) bilinear precursor analysis. The OCB uniaxial uniform strain (and bilinear curves) can be adjusted during precursor analyses using a factor, "ADJ," based on the precursor analysis Triaxiality Ratio (TR). The methodology for developing this adjustment is provided in Appendix I, with values provided in Table I-3 and Figure I-7. The value for TR is based on the ratio of minimum to maximum membrane strains. If the actual triaxiality is sought, the value of TR used in the final precursor analysis and in subsequent analyses will be justified based on the TR values at the governing stress location.

The last stage of the OCB material model, at true strains above the triaxiality-adjusted true uniform strain, will be modified to have no strain hardening. The remaining waste package components will continue to use best-estimate bilinear material models. The true stress–true strain curve in this region will be horizontal, which introduces a tensile instability if an entire wall section is loaded to this level (Jones & Holliday 2000 [DIRS 182173]). This will be evidenced by computationally large deformations for a small increase in loading, large-scale load redistributions or solution failure due to numerical instability. This type of stress-strain relationship is depicted schematically in Figure 9.

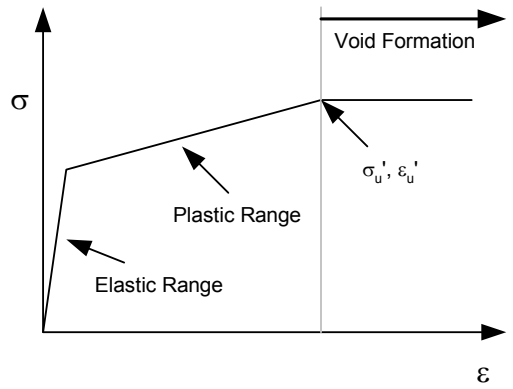

Figure 9. Tri-linear Stress-Strain Curve

The specific strain-based FLD that is used (Shi & Gerdeen 1991 [DIRS 182447]) to define the triaxiality adjustment on the uniaxial uniform strain value is valid provided that the strain path of the governing location is reasonably linear (i.e., is characterized by proportional loading — see Figure 10). If the strain path is highly nonlinear, an alternate stress-based FLD triaxiality adjustment will be developed and used (Stoughton & Zhu 2004 [DIRS 182453]).

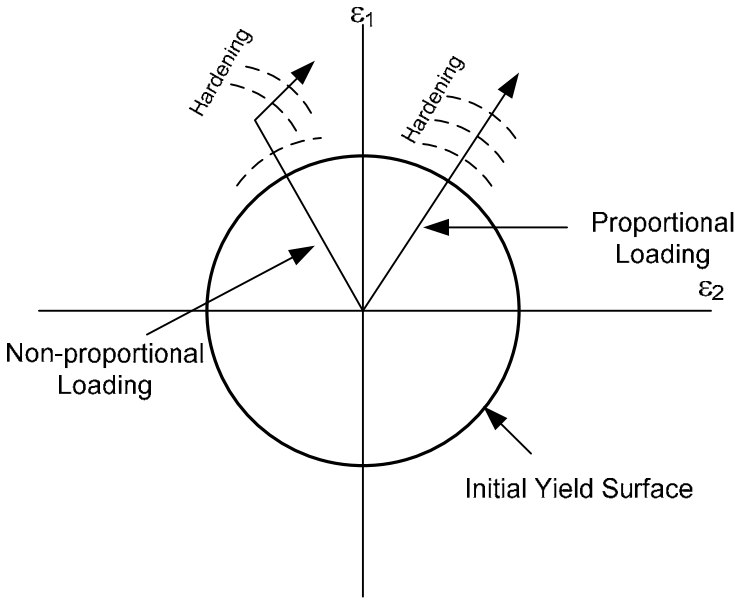

Figure 10. Proportional and Non-proportional Loading

7.1.7.2.5 Variables in Demand and Capability Analysis

For the prospective structural analysis approach described in Section 7.1.7.2.2, the variables that provide the distribution of Demand are the kinetic energy of the loading (with impact velocities and mass key contributors) and the event orientation. This establishes the governing location on the OCB for the governing toughness consumption response as represented by the Von Mises effective EWA membrane stresses, strains and triaxiality. The Capability is the potential strain energy absorption, or Toughness Index, for the OCB material defined through the triaxiality-adjusted true ultimate stress and true uniform strain.

7.1.7.2.6 Procedure for Performing Analyses

The process for performing these analyses is depicted schematically in Figure 11. The first step in performing an evaluation for an event sequence is to fully define the sequence for the dynamic structural analysis (BSC 2007 [DIRS 182117]). This definition will provide the orientation of the sealed waste package and the trajectory of the same onto the target surface. If there is some ambiguity about the possible impact orientations, then a study may be necessary to determine the worst orientation.

The next step is to perform a number of dynamic structural analyses for various values of the controlling Demand variables (i.e., impact velocity). The results may be anticipated to be a low-order function of this independent variable; therefore, only a few values for the independent variable need be evaluated. It should be noted that the resulting consumption of toughness is a monotonically increasing function of the impact velocity.

7.1.7.3 Structural Analysis Approach (Seismic)

The basic approach for dynamic structural analyses that was described in the previous sub-section is extended to address the effects of vibratory ground motion. Indeed, many of the event sequences may have an earthquake as an initiating event. In the risk evaluation of a seismic event, the waste package is only one of many SSCs for which the performance must be assessed to quantify the overall risk. Aside from the special case of vibratory ground motion for the emplaced waste packages in the underground, the effect on the waste package is mediated by other structures, whether the WP Transfer Trolley, the TEV or the floor of the various surface facilities. For the various locations within the surface facilities, the potential for WP OCB breach for vibratory ground motion is prevented by the introduction of appropriate design features.

For the cases of the waste package being carried by the TEV or emplaced in the drifts, the effect of the vibratory ground motion—beyond serving as the initiating event—is the increased velocity with which the WP will strike the target surface. There are two elements to this impact velocity, the seismically induced "launch velocity" of the WP towards the target and the seismic motion of the target towards the WP at impact. (It has been shown that the effect of any normal transport motions of the WP at initiation of the seismic event is negligible (Williams 2003 [DIRS 167094], Enclosure, Section 3.2.5). Thus for a given severity of the ground motion, which may be characterized by the peak velocity, a target velocity toward the moving WP may be superimposed on the WP launch velocity. This will exacerbate the damage to the WP by

increasing the mean demand on the WP thereby increases the risk from a seismically induced event sequence.

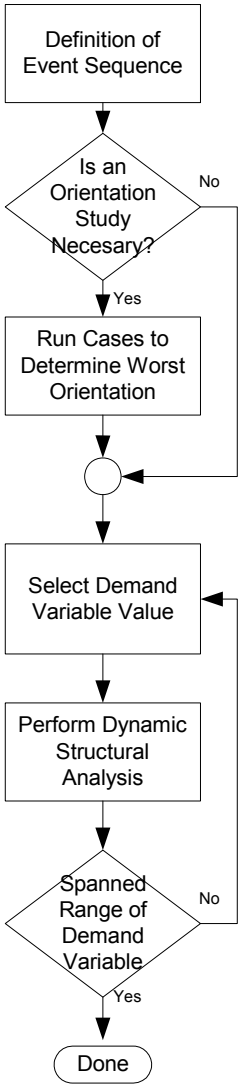

Figure 11. Flowchart for Dynamic Structural Analyses

7.1.7.3.1 Partition of Vibratory Ground Motion into Component Event Sequences

While an exhaustive treatment of the motions of the waste package and emplacement pallets in the emplacement drifts is not feasible due to schedule considerations, a reasonable, albeit conservative, treatment of such ground motions may be formulated. This approach divides vibratory ground motions into three distinct and independent event sequences.

The first of these independent event sequences is waste package-to-waste package impacts along the axis of the drift. From the kinematics' simulations of waste packages, drip shields and emplacement pallets to represent post-closure analysis of Engineered Barrier System response to

seismic events, it may be seen that such impacts occur at modest velocities, even for high-acceleration vibratory ground motion. This is because of the short distance between adjacent waste packages and long seismic wave lengths. While there are significant questions regarding the fidelity with which such simulations represent the kinematics due to ambiguity of contact properties and other consideration, the estimation of such low velocities may appropriately be used to neglect such impacts for preclosure seismic analyses.

The second independent event sequence is the translation of the waste package normal to the drift axis and impact with the drift wall and any ground support attached to that drift wall. Such impacts are, from a structural perspective, similar to the fall of non-lithophysic blocks onto the waste package. Therefore, the rock fall results may be used directly, given the impact velocities.

The third and final independent event sequence is composed of two, subsidiary event sequences. The first is a vertical impact onto the invert, including the structural steel. The damage to the waste package will depend on the alignment of the waste package sleeves with the cross-members of the invert structural steel. The differing response of the two geometries could be treated in a rather simplistic probabilistic fashion. The second is the vertical impact into the emplacement pallet. The pallet serves as an impact limiter up to the velocity at which the structural capability of the pallet is exhausted. At this velocity the waste package crushes through the emplacement pallet and strikes the surface of the invert; although the damage is much less than for a direct strike on the invert due to the energy absorption by the emplacement pallet.

7.1.7.3.2 Determination of Impact Velocity Distribution

The maximum impact velocity may be estimated by examining the time-histories for the reference vibratory ground motions to find the maximum change in velocity for reversal in the direction of motion. This is illustrated in Figure 12. for ground motion in one direction. Here a "moving window" is used to appropriately restrict the period over which the velocity swing needs to be considered. The width of the window is determined by considering the distance, d_{max}, which a fully airborne waste package might cover between restraining surfaces. This is illustrated in Figure 13 for the waste package in the emplacement drift. The width of the window is then determined by dividing the distance by the "launching velocity" for the window. This evaluation is automated so that every temporal point in the data record is considered as a launch time.

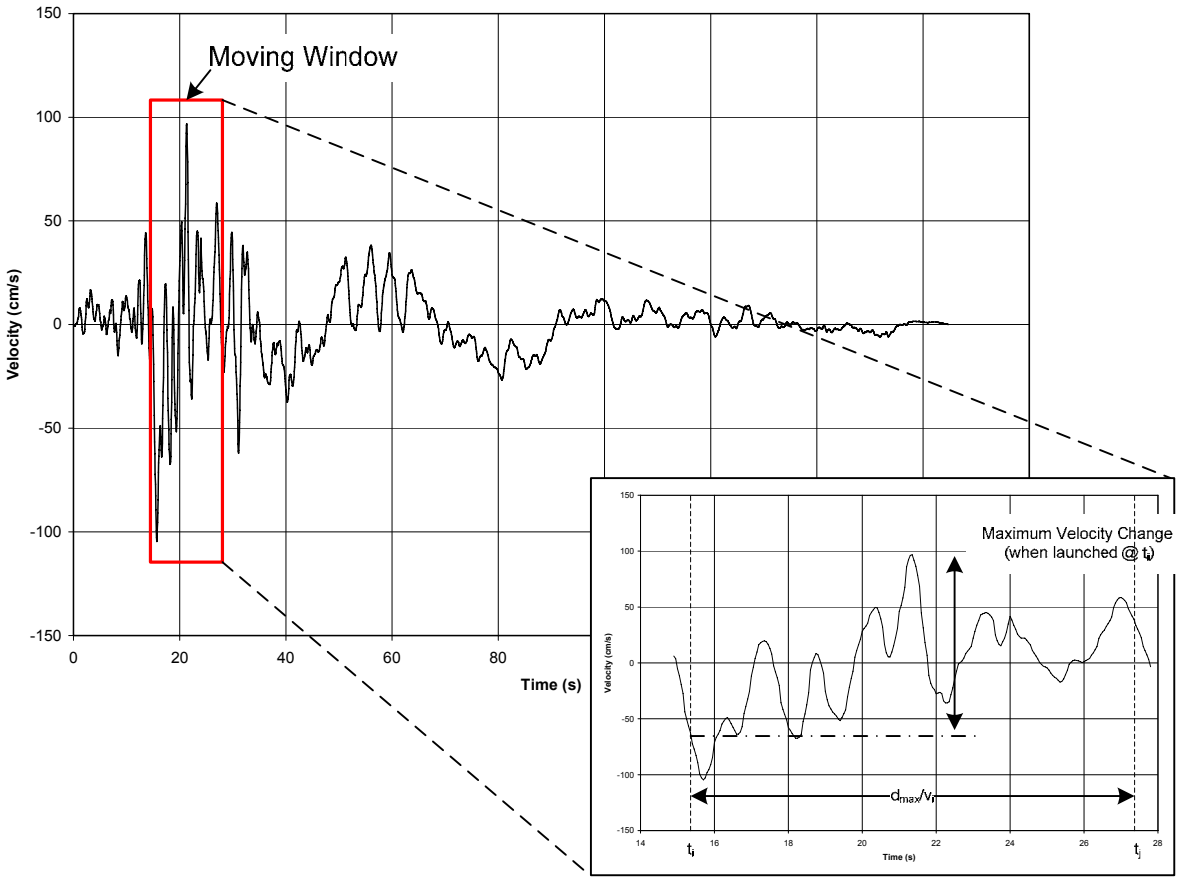

Figure 12. Selection of Peak Velocity Reversal

The ground motion time histories are available in all three orthogonal directions, and the maximum normal impact launch velocity for use in the dynamic structural analysis is required. This determination is made for each launch time, t_i, by calculating all possible resultant vector ranges for all target impact times, t_j, in the moving window.

$$v_{i\to j} = \sqrt{v_{x,i\to j}^{\ 2} + v_{y,i\to j}^{\ 2} + v_{z,i\to j}^{\ 2}} \qquad \text{Equation 13}$$

Next, the maximum value of these resultant vector ranges in the time window is identified, and then the maximum for all launch times is determined. Using this value as the maximum normal impact velocity conservatively neglects changing directions between the launch direction and the direction of the target motion at impact and further neglects the possibility of less damaging tangential (i. e., sliding) components in the impact velocity.

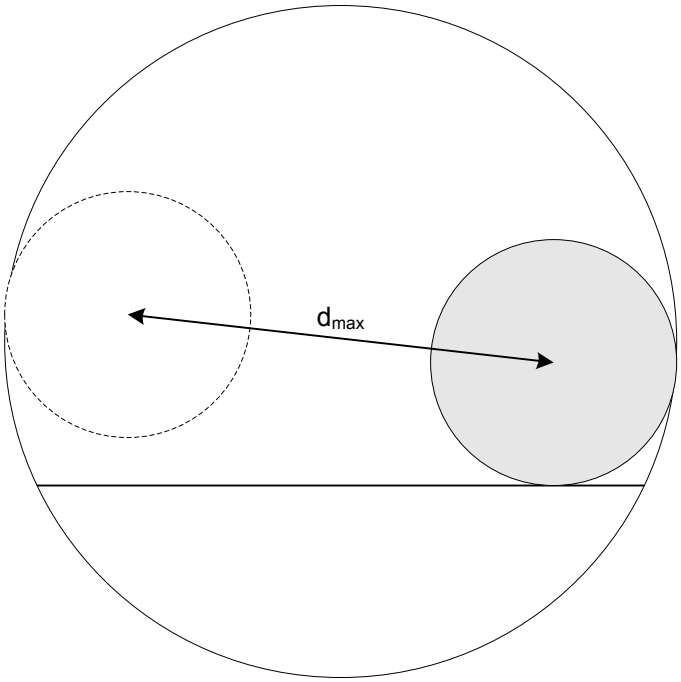

Figure 13. Determination of Maximum Flight Distance

7.1.7.4 Scope of Analysis for License Application

As noted at the start of Section 7.1.7.1, previous analyses of the waste package demonstrate that it is a very robust structure. As such, calculations that demonstrate this robustness will be performed for LA. Consistent with HLWRS-ISG-02 (BSC 2007 [DIRS 181782]), these conservative deterministic calculations will be convolved with the capacity distribution developed in Appendix I to estimate structural reliability. The majority of these calculations are code-compliance calculations; however, for the more severe events, companion expended toughness fraction evaluations are also performed.

7.2 THERMAL DESIGN

The purpose of the waste package thermal analyses is to ensure that the waste form temperatures do not exceed levels that are important to maintaining their long-term integrity. For commercial SNF, this involves ensuring that the cladding temperature does not induce rupture, compromising the cladding as a barrier to radionuclide release. Thermal requirements for commercial SNF are imposed on the TAD design/supplier. For defense HLW glass, this involves ensuring that the glass does not reach a transition temperature that would result in an alteration of the glass microstructure, increasing the solubility of the glass and reducing the time required for mobilization of the radionuclides embedded in the glass matrix.

Various thermal calculations require different computational tools and may be performed for different levels of detail and accuracy. The suite of computational tools used is discussed in Section 7.2.1, and the types of calculations performed for thermal analysis are discussed in Section 7.2.2.

7.2.1 Computational Tools

Thermal analyses are performed to assure that waste form, waste package, and rock temperatures do not exceed maximum limits. Benchmarking calculations are performed to demonstrate that the thermal analysis methods produce valid results. The benchmark calculations include comparisons with data from large experiments at Yucca Mountain, including the Single Heater Test and the Drift Scale Test. Benchmark calculations of forced and natural convection are compared to data from quarter scale testing.

7.2.1.1 ANSYS

The primary computational tool used for heat transfer calculations is ANSYS. ANSYS solves all three modes of heat transfer: conduction, convection, and radiation. Typically, convection is not specifically calculated in ANSYS. Instead, heat removed by ventilation is subtracted from the total heat source and only the net heat transferred to the drift walls is included in the calculations. For conduction, the thermal conductivity and specific heats may be spatially varying and temperature-dependent. For radiation, ANSYS determines an effective thermal conductivity and applies it to Fourier's Law of heat conduction. This effective thermal conductivity is computed from the thermal communication between each element of the surfaces, using gray body diffuse radiation theory. For an enclosed system of finite radiating surfaces, the theory of gray body diffuse radiation heat transfer is appropriate (Siegel and Howell 1992 [DIRS 100687], Equation 7-31, p. 271).

ANSYS allows three types of thermal boundary conditions: temperature, heat flux, and a convection condition. The boundary condition of convection does not imply a detailed convection calculation but rather a heat flux proportional to the difference between the instantaneous surface temperature and the free-stream temperature (i.e., Newton's Law of Cooling). These boundary conditions are applied at the surfaces of the problem domain.

Consistent with finite element analysis, the problem domain is divided into polygons. Within these solids, the thermal transport properties and volumetric heat generation magnitudes (as appropriate) are spatially constant. However, the variation in temperature within and among the

polygons is approximated by one of a number of shape functions. This technique permits larger polygons to be used than would be possible with uniform temperatures within the polygons and a simplistic relationship among the polygons.

7.2.1.2 FLUENT

The FLUENT computational fluid dynamics code is used when more detail is needed to evaluate convection heat transfer. For example, FLUENT is used to calculate convective heat transfer coefficients on waste package, drip shield and rock surfaces in the emplacement drift. FLUENT is also used to determine the thermal response of the waste package surface and structural components of surface facilities.

Both steady-state and transient analyses may be performed using FLUENT. Buoyant forces may be implemented by specifying gravitational body forces and the user may decouple the flow and energy equations to decrease computer run time. An isothermal flow field may be obtained initially and then the energy and radiation models can be enabled, so that the flow and energy equations are solved simultaneously to complete the analysis. At times, a quasi-transient approach may be used to shorten the simulation time without losing overall accuracy. First, the analysis is started as a fully transient simulation, and allowed to run until most of the dynamics have subsided (on the order of a few hours simulation time). At this point, the simulation is stopped, and the flow simulation is turned off, leaving only the simulation of energy and radiation active. The simulation is then restarted, effectively "freezing" the flow. Thereafter, the simulation only models heat transfer (conductive, convective and radiative). The impact of the temperatures on the flow patterns is not modeled. With the flow modeling turned off, the time steps in the simulation can be greatly increased. At the end of the frozen flow period, the simulation is stopped, and flow modeling is turned back on (i.e., fully transient). The flow is then updated. This process is repeated until the necessary simulation time has been reached.

7.2.1.3 DriftFlow

DriftFlow is a Microsoft Visual Basic macro that operates in Microsoft Excel 97. DriftFlow is intended to represent the entire repository and give a quick best-estimate of thermal conditions therein, during preclosure (forced ventilation as well as natural ventilation) and postclosure periods. Conduction is calculated by superimposing thermal responses to a series of heat pulses calculated in ANSYS. Convection and radiation heat transfer are calculated using empirical correlations derived for a concentric tube annulus. Ventilation flow rate is specified during the forced ventilation period and calculated from pneumatic pressure differences during the natural ventilation period.

7.2.1.4 WPLOAD

The WPLOAD computer program is used to simulate the waste being loaded into waste packages and waste packages being placed in repository drifts subject to thermal requirements for waste packages and repository drifts. The primary purpose of the WPLOAD is to assure that the expected range of waste streams can be emplaced within repository thermal constraints. Secondary features of WPLOAD provide limited information concerning processing and throughput characteristics as well as radionuclide inventories.

7.2.1.5 Mathcad

Mathcad can solve systems of equations, allowing the user to evaluate the impact of parameter variance quickly.

7.2.2 Description of Pertinent Analyses

Table 5 gives an outline of the various types of thermal design calculations performed.

7.2.2.1 Waste Package-Scale Calculations

Thermal detail internal to a waste package is obtained using an ANSYS 2-D representation at the mid-plane of a waste package. Temperatures are imposed on the waste package surface at the top, side, and bottom positions. Interpolation is used to specify surface temperatures between these points. Waste package-scale calculations provide a means to analyze loading variations within a waste package. An effective thermal conductivity for the entire contents of a waste package can also be determined.

7.2.2.2 Drift-Scale Calculations

Drift-scale calculations can be either 2-D or 3-D but represent only the first 5 *m* of rock from the drift wall. Previous calculations have shown that drift internal structures have little impact on rock temperatures at this location (BSC 2006 [DIRS 179686], Tables 53, 54, 61-66, and 95). Temperatures at 5 *m* are specified from "pillar" calculations. Calculations performed at drift-scale must use the same average heat load that was used in the corresponding "pillar" calculation for consistency. Drift-scale calculations provide a faster method to study variations in invert design, drip shield design, and waste package emplacement order.

7.2.2.3 Repository-Scale Two-Dimensional Calculations

While detailed repository-scale three-dimensional calculations are necessary to demonstrate margin to the waste form thermal requirements, repository-scale two-dimensional calculations are appropriate to study the sensitivity of the temperature field to changes in the major thermal variables. Such a representation consists of a perpendicular slice through a single waste package, extending from the top of the mountain to well into the saturated zone, and accounting for the thermal transport properties of each stratigraphic unit (Figure 14). Such a representation appropriately calculates the temperature field for a drift located near the center of the repository, provided the packages are approximated as an infinitely long cylinder with an axially uniform heat generation rate.

Table 5. Summary of Thermal Calculations for Waste Package Component Design

Type of Calculation	Phenomena Calculated	Boundary conditions Initial conditions Assumptions	Calculation Results
2-D ANSYS calculation at Waste Package-Scale	Quasi-static Conduction heat transfer Radiation heat transfer	Waste package temperatures specified at top, side and bottom, and interpolated between these Ignores convection heat transfer	Effective thermal conductivity, k_{eff} for entire waste package contents Waste package interior temperature distribution vs. time.
2-D or 3-D ANSYS calculation at Drift-Scale	Quasi-static Conduction heat transfer Radiation heat transfer	Uniform temp 5 *m* into rock wall obtained from "pillar" calculation at same linear heat rate effective thermal conductivity, k_{eff} for waste package contents	Evaluate impact of drip shield and invert on waste package surface and peak cladding temperatures vs. time.
2-D ANSYS calculation at Repository Scale ("pillar" calculation)	Transient Conduction heat transfer Radiation heat transfer	Lower and upper sink temps. Initial temperature gradient in Mountain Line heat source effective thermal conductivity, k_{eff} for waste package contents Arbitrary deletion of heat removed by ventilation	Response surface for peak drift wall temperatures vs. repository parameters such as ventilation duration and linear heat loading. Each peak drift wall (or 5 *m* -into-rock) temperature on the response surface can then be used as a boundary condition for a drift-scale calculation, to also generate such a response surface for peak waste package surface temperature.
2-D ANSYS calculation for Fire Analysis	Transient Radiation and convection from fire, only radiation cooling after fire	Waste package initial temp. Detailed waste package contents	Waste package surface, peak shell, and peak waste form temperatures
Axisymmetric, 2-D, or 3-D ANSYS calculation in Surface Facility or transporter	Transient or steady state Conduction heat transfer Radiation heat transfer	Waste package initial temp. Ambient concrete wall temp. Effective thermal conductivity, k_{eff} for waste package contents	Waste package surface and peak shell temperatures Temperature in weld zone Concrete wall temperatures Transporter wall temperatures

Table 5. Summary of Thermal Calculations for Waste Package Component Design (Continued)

Type of Calculation	Phenomena Calculated	Boundary conditions Initial conditions Assumptions	Calculation Results
1-D DriftFlow calculation at Repository-Scale	Transient conduction, convection, and radiation heat transfer Natural ventilation air flow	Line heat source Coupled with 2-D ANSYS Repository Scale calculation to account for transient effects of heat capacity in the rock. Overall convective coefficient (h) from FLUENT Static pressure difference for natural ventilation –or – flow rate for forced ventilation	Results used to determine the fraction of heat removed by ventilation (ventilation efficiency). Waste package and drift wall temperatures vs. time.
3-D FLUENT calculation at Drift-Scale	Transient and steady state convection, conduction, and radiation heat transfer. Steady state, laminar and turbulent flow	Uniform rock temperature 5 *m* from surface (from ANSYS Repository-Scale calculations) Waste package surface heat flux Ventilation flow rate	Convective coefficients (h)
3-D ANSYS calculation at Repository-Scale ("pillar" calculation)	Transient Conduction heat transfer Radiation heat transfer	Lower and upper sink temps. Effective thermal conductivity, k_{eff} for waste package contents Typical set of waste packages Arbitrary deletion of heat removed by ventilation	Reference point to quantify axial drift wall and waste package surface temperature variations along the drift, relative to the 2-D repository-scale calculation. The appropriate "offset" can be applied to the entire response surface generated from the 2-D results.

NOTE: Transient effects for waste package-scale, and drift-scale calculations (out to 5 *m*-into-rock) have small time constants compared to their inputs (decay of the fuel heat and mountain heat capacity). Therefore, these calculations are performed as a series of steady-state calculations, at "snapshots" in time, using (a) the power produced by the fuel assemblies at that point in time, or (b) the 5 *m*-into-rock temperature at that point in time.
1-D = one-dimensional; 2-D = two-dimensional; 3-D = three-dimensional, k_{eff}= effective thermal conductivity

Two-dimensional representations have low computational requirements, and a large number of calculations may be performed quickly. This rapidity of computation enables time-dependent temperature field calculations that span the design space (i.e., the range of independent variables). Low-order, multivariate regressions may then be performed and response surfaces created. The functional form of the response surface selected is based on insight into the heat-transfer physics and the fidelity with which the particular functional form reproduces the calculational results.

This representation is truly applicable only to an infinitely long waste package; however, simple adjustments may be made to approximate three-dimensional effects. The effect of increases in waste package separation is obtained by adjusting the average waste package heat generation rate (and hence the linear power). This functional form is shown in Equation 14.

$$P_{linear} = \frac{Q_{WP}}{\left(\overline{L}_{WP} + \delta\right)} \qquad \text{Equation 14}$$

Here Q_{WP} is the waste package heat generation rate at emplacement, $\overline{L}_{WP}$ is the average-waste package length, and δ is the skirt-to-skirt gap between waste packages. The appropriateness of this adjustment decreases with increasing waste package spacing because the localized relatively high heat regions of such an arrangement are not accounted for. For the range of waste package spacing's currently considered, this adjustment is applicable.

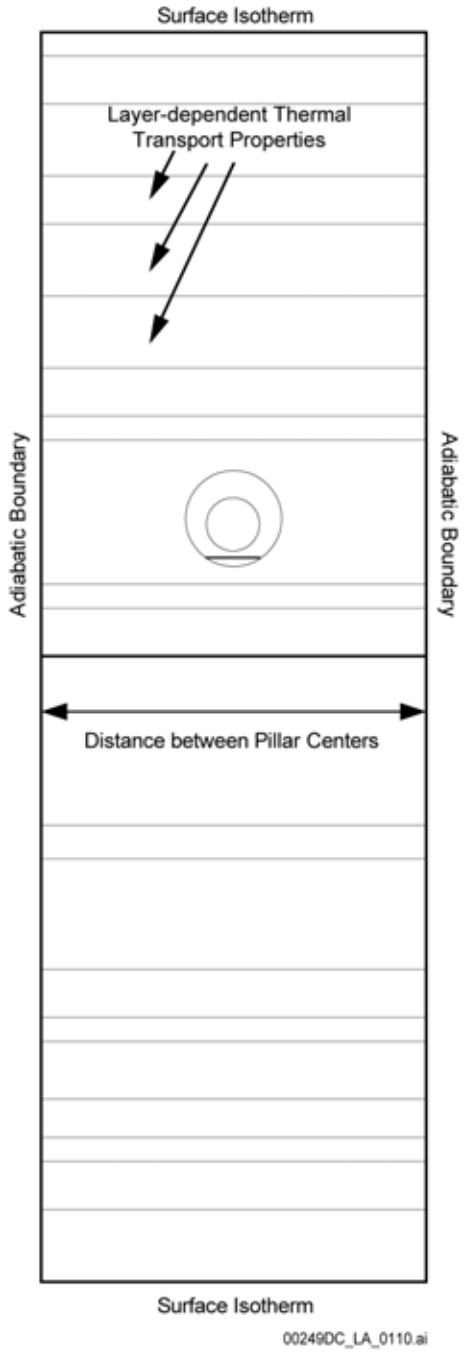

Figure 14. Illustration of Two-dimensional Repository Representation

An operating curve is the locus of values for two independent variables—holding other independent variables constant—which results in a particular temperature value on the response surface. For instance, if the ventilation duration, waste package heat generation rate at emplacement, and backfill effective-thermal conductivity (if backfill is present) are fixed, a curve may be constructed providing the combinations of skirt-to-skirt separations and heat removal fractions necessary to obtain a given peak-drift wall temperature. This process is illustrated in Figure 15.

While these two-dimensional calculations cannot legitimately be used to quantify the effect of non-uniform heat generation rates, the results from previous three-dimensional cases may be used in conjunction with these to estimate the magnitudes of three-dimensions and non-uniformity. By using the nominal heat generation rate for the repository, peaking factors may be developed for a range of design basis heat generation rates. For instance, simple linear correlations for incremental temperature increases for non-uniformity may be developed. Such a functional form is shown in Equation 15.

$$\Delta T = a_0 + a_1 \cdot P_{linear} \qquad \text{Equation 15}$$

Here, a_0 and a_1 are fit coefficients and P_{linear} is that shown in Equation 14.

Such an expression is used to adjust upward the peak waste package-surface temperature and the corresponding peak-cladding temperature for the particular design basis heat generation rate. The waste form limit may then be decremented by the difference between the peak-cladding and waste package surface from the two-dimensional calculation. The resulting waste package surface temperature is now the target peak waste package-surface temperature. This is illustrated in Figure 16.

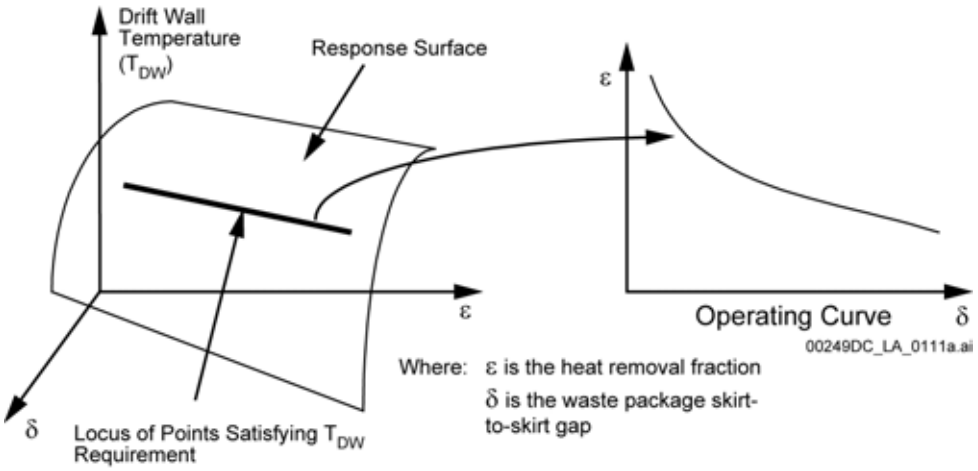

Figure 15. Illustration of Response Surface Interrogation

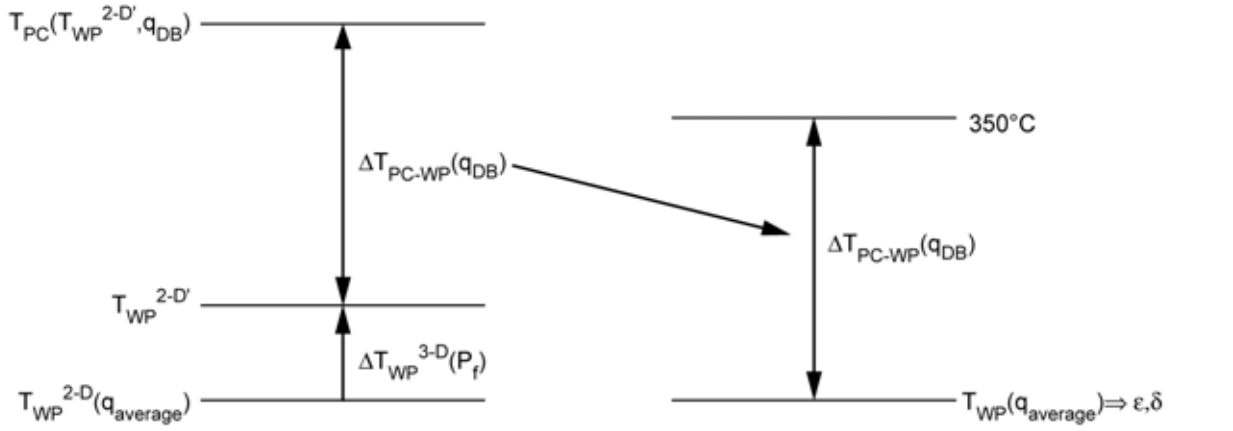

NOTE: In this process, the locus of points (ε,δ) for which $T_{PC}(T_{WP}^{2-D'},q_{DB})$ = 350 °C (BSC 2006 [DIRS 177636], Section 4.2.1.9.8), is determined. This creates the operation curve for peak waste package cladding temperature.

Figure 16. Three-Dimensional Effect Accommodation

7.2.2.4 Repository-Scale Three-Dimensional Analyses

While two-dimensional calculations are appropriate for scoping studies, three-dimensional calculations are needed for detailed, final design evaluations. The interface flow of two-dimensional and three-dimensional calculations is presented in Figure 17.

The thermal three-dimensional representation approximates the repository as an infinitely repeating series of "pillars," extending from the top of the mountain to a plane well into the saturated zone. Layers corresponding to the stratigraphy of the mountain represent the host rock of the repository. For each of these layers, thermal transport properties (viz., temperature-dependent thermal conductivity and specific heat) appropriate to the local rock properties are used. Laterally, adiabatic surfaces are placed at the center of the rock masses between the drifts. The variability of the waste package heat generation rates is incorporated by representing just a few waste packages within the drift segment. The thermal transport properties of these waste packages are represented by temperature-dependent effective values, but not with an explicit representation of the internals. The time-dependent heat generation rates of the waste packages are adjusted to ensure that the average heat generation rate of the drift segment is the same as that of the repository as a whole.

Figure 18 shows the interaction of repository-scale and waste package-scale representation.

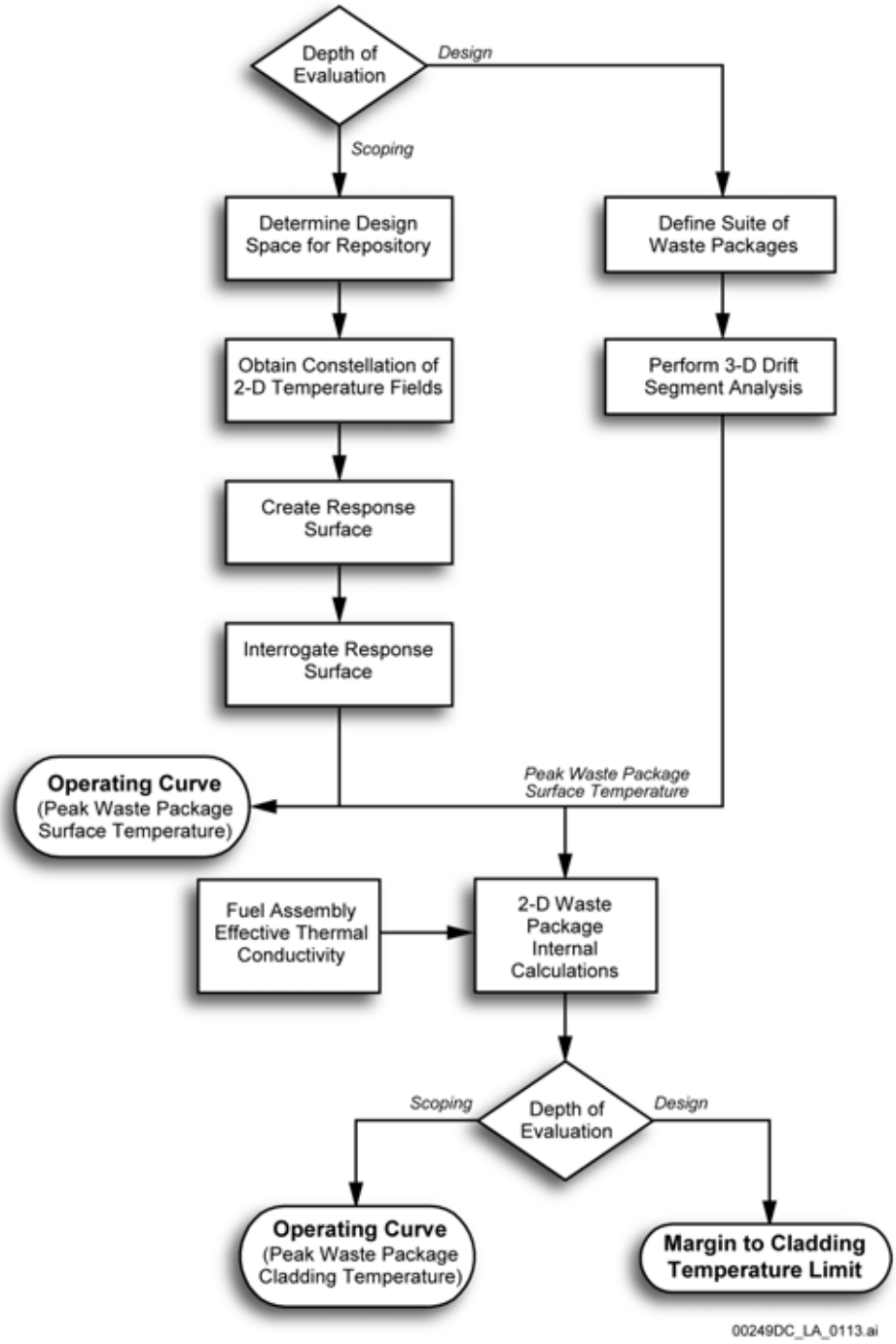

Figure 17. Thermal Analysis Technique Decision Flowchart

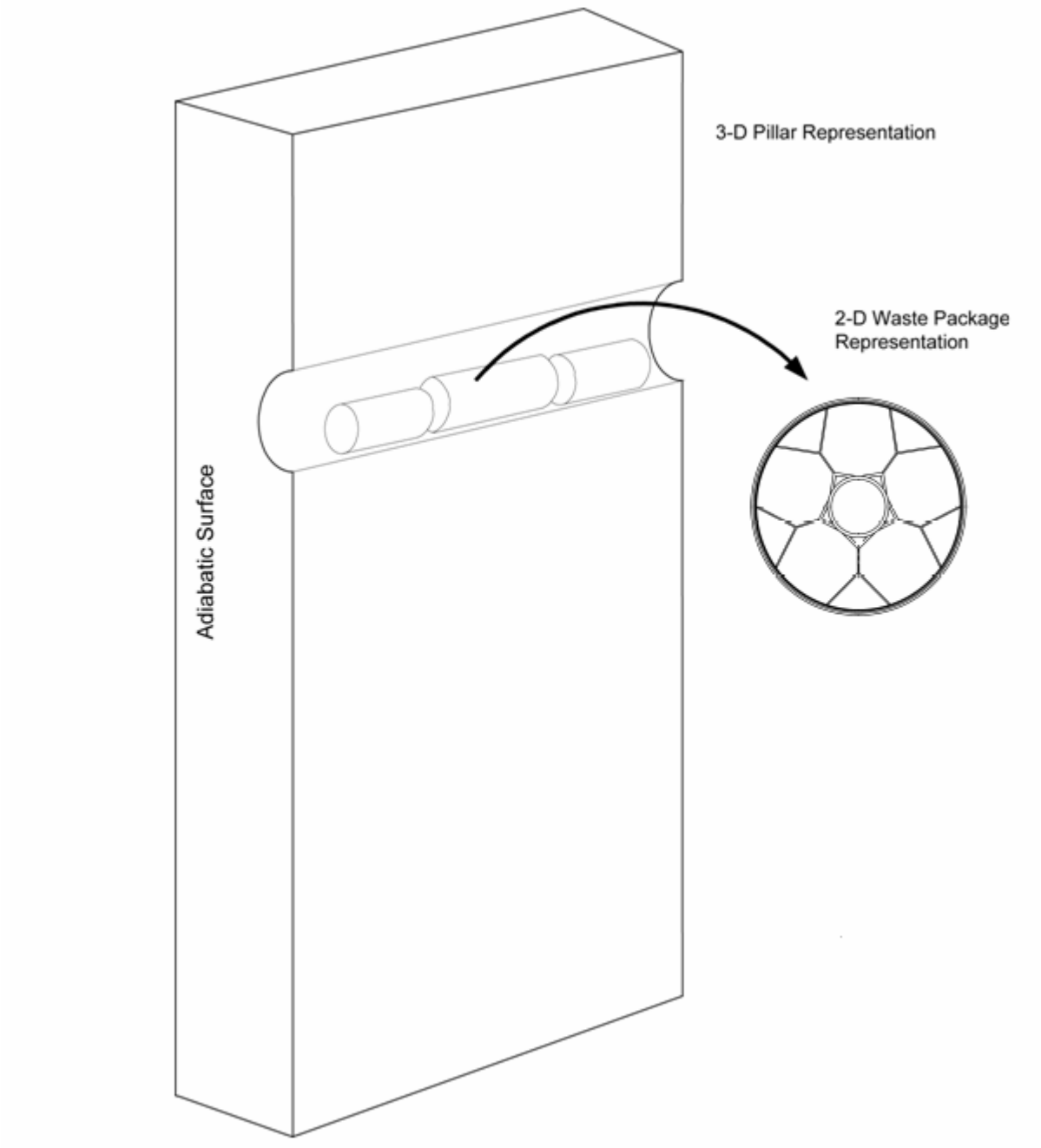

Figure 18. Multi-Scale Thermal Analysis Representation

7.2.2.5 Thermal Calculations of Fire Events

Parametric calculations are performed using a 2-D ANSYS simulation of a waste package. Duration and temperature of the fire conditions are varied.

7.2.2.6 Thermal Calculations in Surface Facilities and Transporter

Calculations are performed using an axisymmetric, 2-D or 3-D ANSYS simulation of a waste package in surface facilities and transporter. Thermal response is calculated for waste packages located on the transporter, in the weld cell, and other surface facilities as well.

7.2.3 Loading Calculations Using WPLOAD

Thermal characterization of waste is the predominant factor in loading of waste packages in the repository drifts. Loading of drifts is planned to be done in such a manner that all temperature limits are satisfied including waste form temperature, waste package outer surface temperature, drift wall temperature, and rock center pillar temperature limits. *WPLOAD V. 2.0.* ([DIRS 182947]) simulates loading individual fuel assemblies into waste packages as well as loading waste packages in drifts.

As waste arrives, it will either be loaded in an appropriate waste package or held in staging or aging facilities. Newly arriving waste or waste in staging or aging facilities can be loaded in a drift if they meet the thermal criteria.

The main inputs to WPLOAD are:

- Arrival schedules and characteristics of all waste forms
- Thermal limits for drift emplacement
- Processing capabilities of surface facilities

WPLOAD is used to determine the effects of these inputs on the following aspects of repository thermal performance:

- Number and types of waste packages required
- Thermal power decay history of each waste package
- Thermal response of each drift and drift segment
- Calendar year to finish emplacing waste
- Required aging pad capacity

7.3 SOURCE TERM DETERMINATION

The following describes the generation of source terms for the commercial SNF, DOE SNF, and HLW. The method for calculating DOE SNF and HLW source terms differs from commercial SNF, as the information available for these waste streams is considerably different from commercial SNF. For a commercial SNF assembly with any given enrichment, burnup, and cooling time; a burnup calculation can be performed that reasonably simulates the irradiation history of the assembly in the reactor core and the subsequent decay after it is removed from the

reactor. For DOE SNF, the source term methodology is described in *Source Term Estimates for DOE Spent Nuclear Fuels* (DOE 2003 [DIRS 169354]) and the general description and grouping is given in *General Description of Database Information Version 5.0.*1 (DOE 2004 [DIRS 171271]). For the HLW, the chemical composition and the estimated radionuclide inventory at a certain year are provided. The source terms for these waste forms can be computed by simply decaying the radionuclides to the desired times. The methodology and computational tools used to generate the source terms are presented in more detail in the following sections.

7.3.1 Computational Tools

Oak Ridge National Laboratory developed the SCALE code system for the NRC to satisfy the need for standardized analysis methods for licensing evaluations of nuclear fuel facilities and package designs. The SCALE system is a collection of well-established functional modules (computer codes) that can be used individually or in combination to perform criticality, shielding, and heat transfer analyses. The system has many control modules, each of which combines several functional modules into analysis sequences to perform a specific analysis. The SAS2H control module and the ORIGEN-S functional module in the SCALE system are the primary computational tools for source term generation. It should be noted that as new SCALE code modeling become available on the project (e.g. TRITON/NEWT sequences) , it should be considered in the future computations.

7.3.1.1 Description of SAS2H for Commercial Spent Nuclear Fuel Source Term Generation

In depletion analyses, the fuel isotopics change with time are significantly different between fuel cycles. Hence, the fuel isotopics and their macroscopic cross sections must be updated to reflect these changes. For each time-dependent fuel composition, SAS2H performs one-dimensional neutron transport analyses of the fuel assembly using a two-part procedure with two separate lattice-cell representations. The first representation (Path A) is a unit fuel-pin cell from which cell-weighted cross sections are obtained. The cell-weighted cross sections from this calculation are used in a second representation of a larger unit-cell (Path B) that represents the entire assembly within an infinite lattice. The zones in Path B can be structured for different types of BWR or PWR assemblies containing water rods, burnable poison rods, and gadolinium fuel rods, etc. The fuel neutron flux spectrum obtained from Path B is used to update the nuclide cross sections for the specified burnup-dependent fuel composition. The updated cross sections are then used in a point-depletion computation to produce the burnup-dependent fuel composition to be used in the next spectrum calculation. This sequence is repeated over the entire irradiated history of the assembly. An example of these representations for a BWR assembly is presented in Figure 19.

The functional modules executed by SAS2H to carry out the depletion analysis are BONAMI-S, NITAWL-II, XSDRNPM-S, COUPLE, and ORIGEN-S. BONAMI-S and NITAWL-II perform resonance self-shielding analyses of the cross sections in each irradiation cycle. XSDRNPM-S performs the one-dimensional neutron transport analyses in Path A and Path B. COUPLE updates the cross-section constants of all nuclides in the ORIGEN-S nuclear information library with the cell-weighted information and the weighting spectrum from XSDRNPM-S. ORIGEN-S

calculates the fuel depletion in all cycles and the decay of nuclides at the completion of fuel irradiation. A more detailed description of ORIGEN-S is provided in the next section. The computational flow diagram in SAS2H for commercial SNF source term generation is presented in Figure 20.

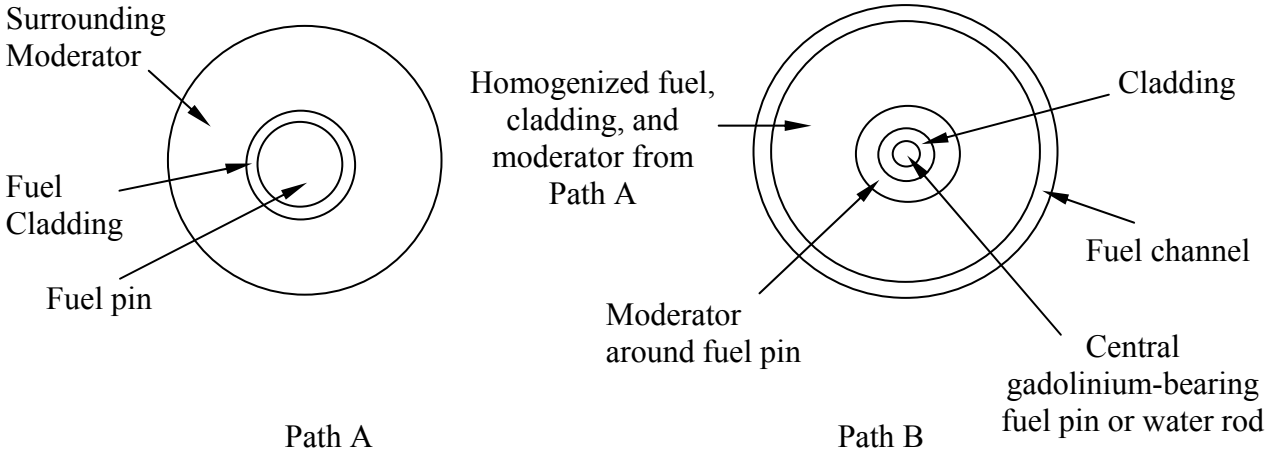

Figure 19. SCALE Representation of BWR Fuel Pin Cell and Assembly for SAS2H Calculations

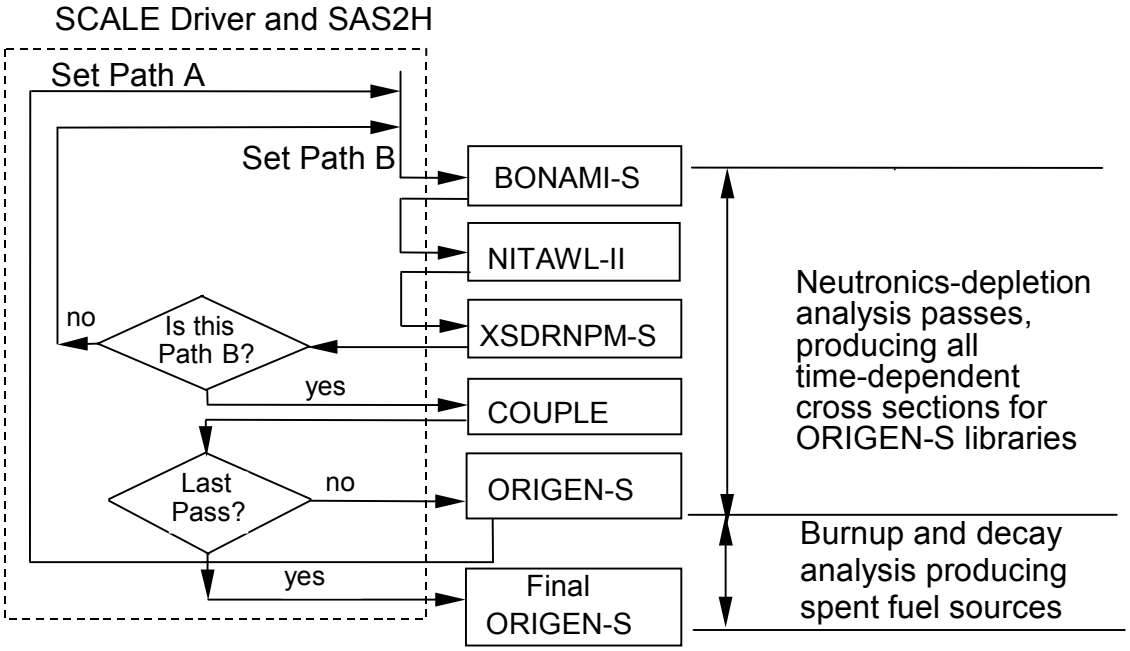

Figure 20. Calculational Flow for Source Term Generation in SAS2H

The source terms for DOE SNF and HLW are not calculated with the SAS2H control module because the radionuclide inventories are given for these fuels. Source terms for DOE SNF and HLW come from *General Description of Database Information Version 5.0.1* (DOE 2004

[171271]), *TRIGA (UZrH) Fuel Characteristics for Disposal Criticality Analysis* (DOE 1999 [DIRS 103891] and *Source Terms for HLW Glass Canisters* (BSC 2007 [DIRS 183163]). The inventories are entered directly into ORIGEN-S to be decayed to the desired times. This is similar to the final ORIGEN-S case for the commercial SNF.

7.3.1.2 Description of ORIGEN-S

ORIGEN-S is a functional module of SAS2H (the control module of the SCALE code system) that carries out the depletion and decay calculations. It can also be used as a stand-alone program. ORIGEN-S computes time-dependent concentrations and source terms of a large number of isotopes, which are simultaneously generated or depleted through neutronic transmutation, fission, radioactive decay, input feed rates, and physical or chemical removal rates.

ORIGEN-S can use three kinds of cross-section libraries: card image libraries with nuclear and photon yield information, binary libraries with nuclear transition and photon yield information, and the Master Photon Data Base containing detailed photon energy and intensity data. The second of these, the binary library, contains the same type of information that the card-image libraries do, but for only one kind of problem. This represents a major advantage over the card image libraries in that these cross sections can be replaced with those determined from the detailed neutronics calculations performed by the functional modules that precede ORIGEN-S in the SAS2H module. This means that rather than using a previously defined cross-section set, the code can be used in conjunction with the cross-section processing codes of SCALE that create problem-specific libraries. This capability has led to the NRC's preference for ORIGEN-S. The following is an excerpt from NUREG-1536 (NRC 1997 [DIRS 101903], p.5-3):

> "Generally, the applicant will determine the source terms using ORIGEN-S (e.g., as a SAS2 sequence of SCALE), ORIGEN2, or the DOE Characteristics Data Base. Although the latter two are easy to use, both have energy group structure limitations…. If the applicant has used ORIGEN2, verify that the chosen cross-section library is appropriate for the fuel being considered. Many libraries are not appropriate for a burnup that exceeds 33,000 MWd/MTU."

This statement derives from the fact that previous compilations of source term values used ORIGEN2 and relied on previously calculated cross-section libraries of limited information, which can easily be used outside the applicable range. These libraries are only appropriate for fuels that have undergone certain irradiation histories and are not as accurate as the problem-specific libraries generated for ORIGEN-S.

7.3.2 Description of Pertinent Analyses

7.3.2.1 Commercial Waste Forms

The thermal output, radionuclide inventories, and radiation spectra for commercial SNF are developed according to the source term methodology described in this document. Radiation source terms for commercial SNF have been created for PWR and BWR fuels. These are documented in:

- *PWR Source Term Generation and Evaluation* (BSC 2004 [DIRS 169061])
- *BWR Source Term Generation and Evaluation* (BSC 2003 [DIRS 164364]).

The waste stream source terms are developed by convoluting source terms for PWR and BWR assemblies with detailed assembly information for a specified waste stream. They are documented in *Waste Packages and Source Terms for the Commercial 1999 Design Basis Waste Streams* (CRWMS M&O 2000 [DIRS 138239]).

7.3.2.2 U.S. Department of Energy Spent Nuclear Fuel

The total initial radionuclide inventory provided by Source Term Estimates for DOE Spent Nuclear Fuels (DOE 2004 [DIRS 171271]) for the year 2010 can be used to calculate the total radionuclide inventory and the source terms for the average DOE SNF canisters for the time period out to one million years. The ORIGEN-S program is used to perform the decay calculations.

7.3.2.3 Defense High-Level Radioactive Waste

According to *Waste Acceptance System Requirements Document* (DOE 2007 [DIRS 169992], Section 5.4.1.B (2)), the producers of HLW are required to report the estimated total and individual canister inventory, and the associated uncertainties, of radionuclides (in curies) that have half-lives longer than 10 years and that are, or will be, present in concentrations greater than 0.05 percent of the total radioactive inventory indexed to the years 2010 and 3110. This may become an operational requirement not connected to the initial inventories supplied by the various sites. The time-dependent photon and neutron sources, decay heat sources, and radionuclide contents and activities of the HLW forms are generated in ORIGEN-S decay calculations using the initial radionuclide inventories and chemical compositions of the HLW forms provided by the producers. These calculations are documented in (BSC 2007 [DIRS 183163]), which provides time-dependent source terms for HLW.

7.4 SHIELDING DESIGN

The purpose of shielding analyses is to evaluate the effects of ionizing radiation on personnel, equipment, and materials. For waste package shielding, gamma rays and neutrons emitting from the commercial SNF, DOE SNF or defense HLW are the primary radiation sources. During normal operations at the repository, loading and handling of the waste packages will be carried out remotely to avoid exposure of personnel to harmful radiation levels. Shielding analyses are performed primarily to assess radiation effects to materials and equipment.

Because waste packages are required to contain waste for thousands of years, the waste package barriers reduce radiation levels at the waste package surface such that radiolysis-enhanced corrosion under aqueous conditions is negligible. Shielding analyses are hence carried out to determine radiation dose on the waste package surface, in order to evaluate the consequence of the radiolytically induced corrosion. Shielding evaluations are also performed to determine radiation exposure to equipment during welding of the waste package closure lids. Monitoring and control equipment, such as the welding heads and cameras, will be relatively close to the

radiation sources. The results of the shielding evaluation will be used to quantify the shielding necessary for equipment to function properly at a given location for a required period of time.

In the event of emergency situations, personnel access in the proximity of the waste packages may be required. Shielding analyses provide an evaluation of the radiation environment surrounding the waste packages, assuring safety of the personnel.

7.4.1 Computational Methods and Tools

Shielding analyses are concerned with attenuation of neutrons and gamma rays through materials. The radiation dose rates outside a waste package are determined by solving the Boltzmann equation for radiation transport, which governs the behavior of the radiation particles in a material. Two methods for solving the Boltzmann transport equation for shielding applications have been used extensively for radiation shielding problems. They are the discrete-ordinates method and the Monte Carlo method. The computational tools used for waste package shielding analyses rely on these two methods.

7.4.1.1 Monte Carlo Method

The Monte Carlo method obtains radiation doses for shielding problems by employing a stochastic process to solve the Boltzmann transport equation. Using random variables, an "analog" Monte Carlo method simulates the histories of individual particles through the geometry (the "random-walk" process) and then analyzes these particle histories to derive the desired responses, such as flux density and dose rate. One particle history includes the birth of a particle at its source, its "random walk" through the transporting medium as it undergoes various scattering interactions, and ultimately the death of the particle, which terminates the history. A death can occur when the particle is absorbed, leaves the system, or loses significance owing to other factors.

For waste package shielding analyses, the analog Monte Carlo method is quite inefficient in calculating radiation responses with acceptable accuracy because the events of interest are usually very rare. From the shielding point of view, the particles that escape the waste package are of primary interest for radiation dose evaluation. However, the probability of recording such an event in a Monte Carlo calculation is extremely low (less than 1×10^{-5}), and an unacceptably large number of histories is required to obtain acceptable results. For this reason, variance-reduction techniques must be employed for Monte Carlo shielding analyses. Variance-reduction techniques are procedures for altering the analog Monte Carlo process so as to reduce the variance of the calculated results. They are also known as "importance sampling" or "biasing techniques." The natural distributions in the "random walk" are modified by some importance function, and the particle statistical weights are adjusted from the analog value of unity to remove the bias. The purpose of variance-reduction techniques in Monte Carlo shielding analyses is to improve the efficiency of a calculation by reducing the variance of the results without increasing the computing time. The objective is to maintain a reasonable particle population in the primary regions of interest and, at the same time, control the fluctuation of statistical weight of the particles.

7.4.1.2 Discrete-Ordinates Method

The discrete-ordinates, or S_n, method solves the Boltzmann transport equation by using deterministic numerical techniques. The S_n method is based on expressing the continuous form of the Boltzmann transport equation in terms of discrete values of the space, energy, and angle variables. Whereas the continuous transport equation represents particle balance over differential intervals, the discrete-ordinates formulation represents particle balance over finite intervals. The spatial variables are expressed as finite intervals; the angular variables are specified in terms of a finite number of discrete directions and corresponding weights, representing solid angles, and the energy domain is divided into a finite number of ranges called energy groups. Note that the discrete–ordinates method is not adequate for geometries that employ regions with significantly different nuclear characteristics (i.e., streaming).

7.4.1.3 MCNP

MCNP (Briesmeister 1997 [DIRS 103897]) is a general-purpose Monte Carlo computer code for neutron, photon, electron, or coupled neutron/photon/electron transport. It is capable of calculating Eigen values for critical systems and performing fixed-source (shielding) calculations to obtain radiation doses. For waste package design, MCNP is used for criticality and shielding calculations. The code allows a detailed geometric representation of the system being analyzed. MCNP uses continuous-energy nuclear and atomic data libraries. The MCNP package provides nuclear data tables derived from the Evaluated Nuclear Data File system, the Evaluated Nuclear Data Library and the Activation Library from Lawrence Livermore National Laboratory, and evaluations from the Applied Nuclear Science (T-2) Group at Los Alamos (Briesmeister 1997 [DIRS 103897], p. 1-4). MCNP evaluates the secondary gamma radiation in a coupled neutron/photon transport as well as the Bremsstrahlung radiation produced by the electrons generated in the photon transport.

Because of its versatility, MCNP is extensively used in dose rate evaluations for the waste packages. MCNP also serves to confirm the validity of the homogenized SNF assemblies used in SAS1 (Section 7.4.1.4) calculations and to determine the effect of source geometry on the waste package surface doses. The input specification in the MCNP dose rate calculations represents a conservative or equivalent treatment of the system being analyzed. MCNP applicability to the dose rate evaluations for the waste packages requires the following code features and calculational approaches:

- Separate photon and neutron transport calculations.
- A coupled neutron/photon transport calculation when capture gamma rays (photons created as a result of a neutron being captured by a nucleus) significantly contribute to the total dose rate.
- Photon or neutron surface flux tally specification.
- Dose function specification, which consists of flux-to-dose conversion factors. These flux-to-dose conversion factors are taken from ANSI/ANS-6.1.1-1977 [DIRS 107016].

- Photon interaction information.

- Available neutron continuous-energy cross-section tables, preferably those for neutron interaction cross-sections with elements of the attenuating medium.

- Contents of the source regions homogenized inside region volumes. The commercial SNF consists of four source regions: bottom end-fitting, active fuel, plenum, and top end-fitting regions. Studies of the effect of source geometry on the waste package surface dose rates have shown that the homogenization of the assembly contents and source inside the assembly regions gives practically the same waste package surface dose rates as does the detailed geometric representation (CRWMS M&O 1998 [DIRS 102134], pp. 22 to 26). Note that the use of the detailed geometric representation is acceptable.

- Uniform volume source distribution specifications in each source region of the uncanistered commercial fuel and defense HLW packages. Because the radiation source generation method assumes a uniform burnup within the active fuel region, an axial peaking factor is used for photon and neutron source intensity in the active fuel region to conservatively account for the maximum values of the actual axial source distributions. Note that usage of gamma and neutron axial source profiles are considered (see Section 6.4.1).

- The default implicit neutron and photon capture and cell importance based on the MCNP manual recommendations (Briesmeister 1997 [DIRS 103897], p. 2-121) as variance reduction techniques.

7.4.1.4 SAS1

SAS1 is a one-dimensional discrete-ordinates shielding calculation sequence using simplified input. SAS1 is a module of the SCALE computer code system (NRC 1997 [DIRS 122675]) consisting of three processes: (1) preparation of the multi-group cross-section information and mixing table used for the shielding calculation, (2) execution of a one-dimensional radiation transport analysis, and (3) calculation of dose rates outside the waste package. The default neutron and photon-to-dose rate conversion factors used in SAS1 are from ANSI/ANS-6.1.1-1977 [DIRS 107016]. For waste package shielding analyses, SAS1 provides an effective and efficient tool for evaluating the radiation level on and beyond the radial outer surface of the waste package.

SAS1 represents a waste package as an infinite cylinder with a homogenized fuel region in the center, enclosed by the inner vessel and outer corrosion barrier. The homogenized fuel region consists of the waste form, neutron absorber plates, thermal shunts, and other structural members. Because the length of a waste package is approximately three times the diameter, the infinite cylinder representation of the waste package is assumed and has been shown to yield accurate dose results for the radial direction. SAS1 has been applied in parametric studies to evaluate the effect of shielding materials on the waste package and to examine the individual dose rates due to neutrons, gamma rays, and capture gamma rays for waste forms with different initial enrichments, burnup characteristics, and cooling times. This modeling approach is applicable for detector points in radial direction of the WP and close to the WP surface.

7.4.2 Description of Pertinent Analyses

Shielding analyses are performed for several waste package designs including: the TAD waste package and the 5-DHLW/DOE SNF co-disposal waste package and DOE MCO. For all waste package designs, radiation dose rates in the axial and radial directions are determined on segments of the waste package surfaces. The results of the shielding calculations allow an estimation of the average operation time of welding equipment, radiolysis-induced corrosion, and the radiation environment outside the waste packages for personnel access.

7.4.2.1 TAD Waste Package Analyses

For the TAD waste package, the active fuel is the only neutron source; however, the active fuel, plenum, top-end-fitting, and bottom-end-fitting regions are all gamma sources. Shielding calculations for the commercial waste packages must include all sources in order to compute the dose rates of the waste packages. Dose rates due to average, design basis, and maximum source terms are computed.

7.4.2.2 5–DHLW/DOE SNF Waste Package Analyses

The 5–DHLW/DOE SNF waste package contains five HLW glass canisters and a central DOE SNF canister. The DOE SNF canister holds one of the many DOE-owned waste forms (BSC 2006 [DIRS 177636], Sec. 11.2.2.8). The HLW glass canister is either from SRS or Hanford depending on dose point location (axial or radial direction). The TRIGA waste form is the bounding DOE SNF for the 5-DHLW/DOE SNF waste package (BSC 2003 [DIRS 166210], p. 15).

7.4.2.3 2–MCO/2–DHLW Waste Package Analyses

The waste package contains two DOE MCO canisters containing Hanford site N-Reactor fuel and two Hanford HLW glass canisters (BSC 2004, [DIRS 170878], p. 130). Detailed drawings of the 2-MCO/DHLW waste package are found in (BSC 2007 [DIRS 182360]), (BSC 2007 [DIRS 182362]) and (BSC 2007 [DIRS 182363]). The descriptions and dimensions of the MCO canister are taken from the N-reactor fuel characterization report (DOE 2000 [DIRS 150095]).

8. SUMMARY

No developed data is created in this report and any data used in this report is cited from the given references. This report describes the methodology used to design waste packages and ancillary components, viz. emplacement pallets, and drip shields; however, it does not make recommendations regarding the final design of waste packages, ancillary components or the repository. The accounting of uncertainties in the methodology falls into one of three categories. For most, parameters are selected that produce net conservative results. These require no additional treatment. For a few, comparison against benchmarks, either experimental or high-order computational methods, must be performed. The third category is that for risk informed analyses where nominal properties and accompanying distributions are sought. Because this is a design methodology, subsequent use is restricted only to the extent that such use would invalidate the theory underlying the particular application.

INTETIONALLY LEFT BLANK

9. INPUTS AND REFERENCES

9.1 DOCUMENTS CITED

ACNW 2006. *"Final ACNW Review of the Draft Report "A Pilot Probabilistic Risk Assessment of a Dry Cask Storage System at a Nuclear Power Plant".* Presented to ACNW , July 20, 2006. Adams ACC: MI 061590542. ACC: MOL.20070919.0511. [DIRS 182673]

Allegheny Ludlum. 1999. "Technical Data Blue Sheet, Stainless Steels, Chromium-Nickel-Molybdenum, Types 316 (S31600), 316L (S31603), 317 (S31700), 317L (S31703)." Pittsburgh, Pennsylvania: Allegheny Ludlum Corporation. Accessed July 31, 2000. TIC: 248631. URL: http://www.alleghenytechnologies.com/ludlum/ pages/products/t316_317.pdf [DIRS 151409]

Allegheny Technologies 2004. *Nickel-Based Alloy Weld Filler Material and Base Metal Composition Test Program.* 004223, Rev. 0. Volume #1 Final Technical Report Appendices A-C. Albany, Oregon: Allegheny Technologies. ACC: ENG.20040507.0005. [DIRS 182446]

ANSYS V. 8.0. 2004. HP-UX 11.0, HP-UX 11.22, SunOS 5.8. STN: 10364-8.0-00. [DIRS 170070]

ASHRAE (American Society of Heating, Refrigerating & Air-Conditioning Engineers) 2001. *2001 ASHRAE Handbook, Fundamentals.* Inch-Pound Edition. Atlanta, Georgia: American Society of Heating, Refrigerating and Air-Conditioning Engineers. TIC: 249910. [DIRS 157789]

ASM (American Society for Metals) 1978. *Properties and Selection: Irons and Steels.* Volume 1 of *Metals Handbook.* 9th Edition. Bardes, B.P., ed. Metals Park, Ohio: American Society for Metals. TIC: 209799. [DIRS 102018]

ASM (American Society for Metals) 1980. *Properties and Selection: Stainless Steels, Tool Materials and Special-Purpose Metals.* Volume 3 of *Metals Handbook.* 9th Edition. Benjamin, D., ed. Metals Park, Ohio: American Society for Metals. TIC: 209801. [DIRS 104317]

ASM International 1990. *Properties and Selection: Nonferrous Alloys and Special-Purpose Materials.* Volume 2 of *ASM Handbook.* Formerly Tenth Edition, Metals Handbook. 5th Printing 1998. [Materials Park, Ohio]: ASM International. TIC: 241059. [DIRS 141615]

ASM International. 1987. *Corrosion.* Volume 13 of *Metals Handbook.* 9th Edition. Metals Park, Ohio: ASM International. TIC: 209807. [DIRS 103753]

Avallone, E.A. and Baumeister, T., III, eds. 1987. *Marks' Standard Handbook for Mechanical Engineers.* 9th Edition. New York, New York: McGraw-Hill. TIC: 206891. [DIRS 103508]

Barlat, F. and Lian, J. 1989. "Plastic Behavior and Stretchability of Sheet Metals. Part I: A Yield Function for Orthotropic Sheets Under Plane Stress Conditions." *International Journal of Plasticity, 5,* 51-66. [New York, New York]: Pergamon Press. TIC: 259057. [DIRS 182115]

Baum, E.M.; Knox, H.D.; and Miller, T.R. 2002. *Nuclides and Isotopes.* 16th edition. [Schenectady, New York]: Knolls Atomic Power Laboratory. TIC: 255130. [DIRS 175238]

Beer, F.P. and Johnston, E.R., Jr. 1977. *Vector Mechanics for Engineers, Statics.* 3rd Edition. New York, New York: McGraw-Hill Book Company. TIC: 247391. [DIRS 145138]

Berg, C.A. 1970. "Plastic Dilation and Void Interation." In *Inelastic Behavior of Solids,* Kanninen, M.F.; Adler, W.F.; Rosenfield, A.R.; and Jaffee, R.I., eds., *McGraw-Hill Series in Materials Science and Engineering.* New York, New York: McGraw-Hill. TIC: 259151. [DIRS 182116]

Bowles, J.E. 1980. *Structural Steel Design.* New York, New York: McGraw-Hill. TIC: 249182. [DIRS 153409]

Bowman, S.M.; Hermann, O.W.; and Brady, M.C. 1995. *Sequoyah Unit 2 Cycle 3.* Volume 2 of *Scale-4 Analysis of Pressurized Water Reactor Critical Configurations.* ORNL/TM-12294/V2. Oak Ridge, Tennessee: Oak Ridge National Laboratory. TIC: 244397. [DIRS 123796]

Boyer, H.E., ed. 2000. *Atlas of Stress-Strain Curves.* Metals Park, Ohio: ASM International. TIC: 248901. [DIRS 152656]

Briesmeister, J.F., ed. 1997. *MCNP-A General Monte Carlo N-Particle Transport Code.* LA-12625-M, Version 4B. Los Alamos, New Mexico: Los Alamos National Laboratory. ACC: MOL.19980624.0328. [DIRS 103897]

Brooker, D.C. 2003. "Numerical Modeling of Pipeline Puncture Under Excavator Loading. Part I. Development and Validation of a Finite Element Material Failure Model for Puncture Simulation." *International Journal of Pressure Vessels and Piping, 80,* 715-725. [New York, New York]: Elsevier. TIC: 259014. [DIRS 182158]

BSC (Bechtel SAIC Company) 2001. *Evaluation of Codisposal Viability for Th/U Carbide (Fort Saint Vrain HTGR) DOE-Owned Fuel.* TDR-EDC-NU-000007 REV 00. Las Vegas, Nevada: Bechtel SAIC Company. ACC: MOL.20011017.0092. [DIRS 157734]

BSC (Bechtel SAIC Company) 2001. *Waste Package Outer Barrier Stress Due to Thermal Expansion with Various Barrier Gap Sizes.* CAL-EBS-ME-000011 REV 00. Las Vegas, Nevada: Bechtel SAIC Company. ACC: MOL.20011212.0222. [DIRS 152655]

BSC (Bechtel SAIC Company) 2003. *BWR Source Term Generation and Evaluation.* 000-00C-MGR0-00200-000-00A. Las Vegas, Nevada: Bechtel SAIC Company. ACC: ENG.20030723.0001; ENG.20050815.0024. [DIRS 164364]

BSC (Bechtel SAIC Company) 2003. *Dose Rate Calculation for 44-BWR Waste Package.* 000-00C-DSU0-02300-000-00A. Las Vegas, Nevada: Bechtel SAIC Company. ACC: ENG.20030909.0003; ENG.20050815.0018. [DIRS 166596]

BSC (Bechtel SAIC Company) 2003. *Dose Rate Calculation for 5 DHLW/DOE SNF Short Waste Package.* 000-00C-DS00-00200-000-00A. Las Vegas, Nevada: Bechtel SAIC Company. ACC: ENG.20031121.0003; ENG.20050815.0016. [DIRS 166210]

BSC (Bechtel SAIC Company) 2003. *Drop of Waste Package on Emplacement Pallet - A Mesh Study.* 000-00C-DSU0-02200-000-00A. Las Vegas, Nevada: Bechtel SAIC Company. ACC: ENG.20030915.0001; ENG.20050817.0019. [DIRS 165497]

BSC (Bechtel SAIC Company) 2003. *Underground Layout Configuration.* 800-P0C-MGR0-00100-000-00E. Las Vegas, Nevada: Bechtel SAIC Company. ACC: ENG.20031002.0007; ENG.20050817.0005. [DIRS 165572]

BSC (Bechtel SAIC Company) 2003. *Waste Package Axial Thermal Expansion Calculation.* 000-00C-EBS0-00500-000-00A. Las Vegas, Nevada: Bechtel SAIC Company. ACC: ENG.20030416.0001. [DIRS 161691]

BSC (Bechtel SAIC Company) 2004. *44-BWR Waste Package Tip-Over from an Elevated Surface.* 000-00C-DSU0-01500-000-00B. Las Vegas, Nevada: Bechtel SAIC Company. ACC: ENG.20040316.0009; ENG.20050817.0016. [DIRS 169705]

BSC (Bechtel SAIC Company) 2004. *Dose Rate Calculation for 21-PWR Waste Package.* 000-00C-DSU0-01800-000-00C. Las Vegas, Nevada: Bechtel SAIC Company. ACC: ENG.20041102.0003; ENG.20050815.0017. [DIRS 172227]

BSC (Bechtel SAIC Company) 2004. *Estimation of Mechanical Properties of Crushed Tuff for Use as Ballast Material in Emplacement Drifts.* 800-CYC-SSE0-00100-000-00A. Las Vegas, Nevada: Bechtel SAIC Company. ACC: ENG.20040309.0023; ENG.20050817.0009; ENG.20050829.0017. [DIRS 168138]

BSC (Bechtel SAIC Company) 2004. *HLW/DOE SNF Codisposal Waste Package Design Report.* 000-00C-DS00-00600-000-00B. Las Vegas, Nevada: Bechtel SAIC Company. ACC: ENG.20040701.0007; ENG.20050817.0014. [DIRS 170878]

BSC (Bechtel SAIC Company) 2004. *PWR Source Term Generation and Evaluation.* 000-00C-MGR0-00100-000-00B. Las Vegas, Nevada: Bechtel SAIC Company. ACC: ENG.20040524.0007; ENG.20050815.0020; ENG.20050822.0006. [DIRS 169061]

BSC (Bechtel SAIC Company) 2004. *Stress Intensity Classification: Waste Package Outer Corrosion Barrier Stresses due to Horizontal Drop Event.* 000-00C-MGR0-01600-000-00A. Las Vegas, Nevada: Bechtel SAIC Company. ACC: ENG.20041122.0001. [DIRS 173389]

BSC (Bechtel SAIC Company) 2004. *Structural Calculations of Waste Package Exposed to Vibratory Ground Motion.* 000-00C-WIS0-01400-000-00A. Las Vegas, Nevada: Bechtel SAIC Company. ACC: ENG.20040217.0008; ENG.20050817.0038; ENG.20050823.0023. [DIRS 167083]

BSC (Bechtel SAIC Company) 2007. Stress Intensity Classification: Waste package Outer Corrosion Barrier Stresses due to Drop with Emplacement pallet. Las Vegas, Nevada Bechtel SAIC Company. ACC: ENG.20070221.0001

004 na 12/18/07

na 12/18/07

BSC (Bechtel SAIC Company) 2005. *Categorization of Event Sequences for License Application.* 000-00C-MGR0-00800-000-00C. Las Vegas, Nevada: Bechtel SAIC Company. ACC: ENG.20050808.0003; ENG.20050929.0003. [DIRS 174467]

BSC (Bechtel SAIC Company) 2005. *IED Waste Package Processes, Ground Motion Time Histories, and Testing and Materials [Sheet 1 of 1]*. 800-IED-WIS0-00501-000-00A. Las Vegas, Nevada: Bechtel SAIC Company. ACC: ENG.20050406.0004. [DIRS 173627]

BSC (Bechtel SAIC Company) 2006. *Basis of Design for the TAD Canister-Based Repository Design Concept.* 000-3DR-MGR0-00300-000-000. Las Vegas, Nevada: Bechtel SAIC Company. ACC: ENG.20061023.0002; ENG.20061121.0005; ENG.20061116.0005; ENG.20061204.0002; ENG.20061218.0003; ENG.20061218.0004; ENG.20070220.0010; ENG.20070220.0011; ENG.20070220.0012; ENG.20070314.0009; ENG.20070412.0002; ENG.20070222.0007; ENG.20070222.0008; ENG.20070221.0010; ENG.20070222.0009; ENG.20070308.0029; ENG.20070501.0009; ENG.20070507.0028; ENG.20070608.0019. [DIRS 177636]

BSC (Bechtel SAIC Company) 2007. *Execution Plan for the Thermal-Structural Discipline Workflow for Design, Design Revision, and Prototyping of Waste Packages and Related Components.* 000-30R-MGR0-02100-000-001. Las Vegas, Nevada: Bechtel SAIC Company. ACC: ENG.20070921.0006. [DIRS 183164]

BSC (Bechtel SAIC Company) 2006. *Project Design Criteria Document.* 000-3DR-MGR0-00100-000-006. Las Vegas, Nevada: Bechtel SAIC Company. ACC: ENG.20061201.0005; ENG.20070111.0025; ENG.20070111.0026; ENG.20070111.0027; ENG.20070111.0028; ENG.20070112.0001; ENG.20070201.0021; ENG.20070222.0011; ENG.20070222.0012; ENG.20070226.0030; ENG.20070308.0028; ENG.20070412.0001; ENG.20070501.0008; ENG.20070510.0002; ENG.20070516.0030; ENG.20070518.0006; ENG.20070621.0002; ENG.20070627.0009. [DIRS 178308]

BSC (Bechtel SAIC Company) 2006. *Repository Twelve Waste Package Segment Thermal Calculation.* 800-00C-WIS0-00100-000-00B. Las Vegas, Nevada: Bechtel SAIC Company. ACC: ENG.20061116.0001. [DIRS 179686]

BSC (Bechtel SAIC Company) 2007. *2-MCO/2-DHLW Waste Package Configuration.* 000-MW0-DS00-00301-000 REV 00C. Las Vegas, Nevada: Bechtel SAIC Company. ACC: ENG.20070719.0008. [DIRS 182360]

BSC (Bechtel SAIC Company) 2007. *2-MCO/2-DHLW Waste Package Configuration.* 000-MW0-DS00-00302-000 REV 00C. Las Vegas, Nevada: Bechtel SAIC Company. ACC: ENG.20070719.0009. [DIRS 182362]

BSC (Bechtel SAIC Company) 2007. *2-MCO/2-DHLW Waste Package Configuration.* 000-MW0-DS00-00303-000 REV 00C. Las Vegas, Nevada: Bechtel SAIC Company. ACC: ENG.20070719.0010. [DIRS 182363]

BSC (Bechtel SAIC Company) 2007. *BSC Position on the Use of the ASME Boiler and Pressure Vessel Code for the Yucca Mountain Project Waste Packages.* 000-30R-WIS0-00200-000-002. Las Vegas, Nevada: Bechtel SAIC Company. ACC: ENG.20070709.0041. [DIRS 182357]

BSC (Bechtel SAIC Company) 2007. *IED Emplacement Drift Invert.* 800-IED-MGR0-00601-000 REV 00A. Las Vegas, Nevada: Bechtel SAIC Company. ACC: ENG.20070716.0008. [DIRS 179897]

BSC (Bechtel SAIC Company) 2007. *IED Geotechnical and Thermal Parameters II [Sheet 1 of 1].* 800-IED-MGR0-00402-000-00A. Las Vegas, Nevada: Bechtel SAIC Company. ACC: ENG.20070108.0001. [DIRS 178277]

BSC (Bechtel SAIC Company) 2007. *IED Geotechnical and Thermal Parameters IV [Sheet 1 of 1].* 800-IED-MGR0-00404-000-00A. Las Vegas, Nevada: Bechtel SIAC Company. ACC: ENG.20070125.0018. [DIRS 179808]

BSC (Bechtel SAIC Company) 2007. *Material Properties for Waste Package ASME Stress Compliance.* 000-00C-MGR0-03800-000-00A. Las Vegas, Nevada: Bechtel SAIC Company. ACC: ENG.20070820.0008. [DIRS 182724]

BSC (Bechtel SAIC Company) 2007. *Naval Long Waste Package Configuration.* 000-MW0-DNF0-00101-000 REV 00C. Las Vegas, Nevada: Bechtel SAIC Company. ACC: ENG.20070301.0013. [DIRS 180180]

BSC (Bechtel SAIC Company) 2007. *Naval Long Waste Package Configuration.* 000-MW0-DNF0-00102-000 REV 00C. Las Vegas, Nevada: Bechtel SAIC Company. ACC: ENG.20070301.0014. [DIRS 180183]

BSC (Bechtel SAIC Company) 2007. *Naval Long Waste Package Configuration.* 000-MW0-DNF0-00103-000 REV 00C. Las Vegas, Nevada: Bechtel SAIC Company. ACC: ENG.20070301.0015. [DIRS 180184]

BSC (Bechtel SAIC Company) 2007. *Naval Short Waste Package Configuration.* 000-MW0-DNF0-00201-000 REV 00C. Las Vegas, Nevada: Bechtel SAIC Company. ACC: ENG.20070301.0016. [DIRS 180187]

BSC (Bechtel SAIC Company) 2007. *Naval Short Waste Package Configuration.* 000-MW0-DNF0-00202-000 REV 00C. Las Vegas, Nevada: Bechtel SAIC Company. ACC: ENG.20070301.0017. [DIRS 180188]

BSC (Bechtel SAIC Company) 2007. *Naval Short Waste Package Configuration.* 000-MW0-DNF0-00203-000 REV 00C. Las Vegas, Nevada: Bechtel SAIC Company. ACC: ENG.20070301.0018. [DIRS 180189]

BSC (Bechtel SAIC Company) 2007. *Postclosure Modeling and Analyses Design Parameters.* TDR-MGR-MD-000037 REV 01. Las Vegas, Nevada: Bechtel SAIC Company. ACC: ENG.20070521.0012; ENG.20070829.0011. [DIRS 179342]

BSC (Bechtel SAIC Company) 2007. *Probabilistic Characterization of Preclosure Rockfalls in Emplacement Drifts.* 800-00C-MGR0-00300-000-00A. Las Vegas, Nevada: Bechtel SAIC Company. ACC: ENG.20070329.0009. [DIRS 180415]

BSC (Bechtel SAIC Company) 2007. *Provisional Event Sequence Definitions for Waste Packages.* 000-30R-WIS0-00900-000 REV 000. Las Vegas, Nevada: Bechtel SAIC Company. ACC: ENG.20070307.0014. [DIRS 182117]

BSC (Bechtel SAIC Company) 2007. *Quality Management Directive.* QA-DIR-10, Rev. 1. Las Vegas, Nevada: Bechtel SAIC Company. ACC: DOC.20070330.0001. [DIRS 180474]

BSC (Bechtel SAIC Company) 2007. *Recommended Values for HLW Glass for Consistent Usage on the Yucca Mountain Project.* 000-00A-MGR0-00200-000-00B. Las Vegas, Nevada: Bechtel SAIC Company. ACC: ENG.20070801.0001. [DIRS 182239]

BSC (Bechtel SAIC Company) 2007. *Regulatory Guidance Agreement, Agreement for HLWRS-ISG-02, Draft September 2006, Preclosure Safety Analysis - Level of Information and Reliability Estimation - Draft.* REG-CRW-RG-000413 REV 00. Las Vegas, Nevada: Bechtel SAIC Company. ACC: DOC.20070608.0010. [DIRS 181782]

BSC (Bechtel SAIC Company) 2007. *Subsurface - Underground Layout Configuration for LA General Arrangement.* 800-KM0-SS00-00301-000 REV 00B. Las Vegas, Nevada: Bechtel SAIC Company. ACC: ENG.20070830.0036. [DIRS 182932]

BSC 2007. Source Terms for HLW Glass Canistres. Las Vegas, NV: BSC. ACC: ENG.20070924.0042 [DIRS 183163]

Chan, L.C.; Lee, T.C.; Fan, J.P.; and Tang, C.Y. 2000. "Formulation of a Strain Based Orthotropic Elasto-Plastic Damage Theory." *International Journal of Damage Mechanics, 9,* 174-191. [Thousand Oaks, California]: Sage Publications. TIC: 258962. [DIRS 182159]

Creer, J.M.; Michener, T.E.; McKinnon, M.A.; Tanner, J.E.; Gilbert, E.R.; Goodman, R.L.; Dziadosz, D.A.; Moore, E.V.; McKay, H.S.; Batalo, D.P.; Schoonen, D.H.; Jensen, M.F.; and Mullen, C.K. 1987. *The TN-24P PWR Spent-Fuel Storage Cask: Testing and Analyses.* EPRI NP-5128. Palo Alto, California: Electric Power Research Institute. TIC: 228305. [DIRS 136937]

CRWMS M&O 1994. *Thermal Evaluations of Waste Package Emplacement.* BBA000000-01717-4200-00008 REV 00. Las Vegas, Nevada: CRWMS M&O. ACC: MOL.19941007.0094. [DIRS 142611]

CRWMS M&O 1998. *Calculation of the Effect of Source Geometry on the 21-PWR WP Dose Rates.* BBAC00000-01717-0210-00004 REV 00. Las Vegas, Nevada: CRWMS M&O. ACC: MOL.19990222.0059. [DIRS 102134]

CRWMS M&O 1999. *CRC Depletion Calculations for Quad Cities Unit 2.* B00000000-01717-0210-00009 REV 01. Las Vegas, Nevada: CRWMS M&O. ACC: MOL.19990929.0121. [DIRS 134650]

CRWMS M&O 1999. *Evaluation of Codisposal Viability for MOX (FFTF) DOE-Owned Fuel.* BBA000000-01717-5705-00023 REV 00. Las Vegas, Nevada: CRWMS M&O. ACC: MOL.19991014.0235. [DIRS 125206]

CRWMS M&O 1999. *Summary Report of Commercial Reactor Criticality Data for Quad Cities Unit 2.* B00000000-01717-5705-00096 REV 01. Las Vegas, Nevada: CRWMS M&O. ACC: MOL.19990917.0184. [DIRS 134660]

CRWMS M&O 2000. *Evaluation of Codisposal Viability for HEU Oxide (Shippingport PWR) DOE-Owned Fuel.* TDR-EDC-NU-000003 REV 00. Las Vegas, Nevada: CRWMS M&O. ACC: MOL.20000227.0240. [DIRS 147651]

CRWMS M&O 2000. *Evaluation of Codisposal Viability for Th/U Oxide (Shippingport LWBR) DOE-Owned Fuel.* TDR-EDC-NU-000005 REV 00. Las Vegas, Nevada: CRWMS M&O. ACC: MOL.20001023.0055. [DIRS 151743]

CRWMS M&O 2000. *Evaluation of Codisposal Viability for U-Zr/U-Mo Alloy (Enrico Fermi) DOE-Owned Fuel.* TDR-EDC-NU-000002 REV 00. Las Vegas, Nevada: CRWMS M&O. ACC: MOL.20000815.0317. [DIRS 151742]

CRWMS M&O 2000. *Evaluation of Codisposal Viability for UZrH (TRIGA) DOE-Owned Fuel.* TDR-EDC-NU-000001 REV 00. Las Vegas, Nevada: CRWMS M&O. ACC: MOL.20000207.0689. [DIRS 147650]

CRWMS M&O 2000. *Users Manual for SCALE-4.4A.* 10129-UM-4.4A-00. Las Vegas, Nevada: CRWMS M&O. ACC: MOL.20001130.0136; MOL.20010822.0084; MOL.20010822.0085; MOL.20010822.0086; MOL.20010822.0087. [DIRS 153872]

CRWMS M&O 2000. *Waste Packages and Source Terms for the Commercial 1999 Design Basis Waste Streams.* CAL-MGR-MD-000001 REV 00. Las Vegas, Nevada: CRWMS M&O. ACC: MOL.20000214.0479. [DIRS 138239]

CRWMS M&O 2001. *Evaluation of Codisposal Viability for U-Metal (N Reactor) DOE-Owned Fuel.* TDR-EDC-NU-000004 REV 00. Las Vegas, Nevada: CRWMS M&O. ACC: MOL.20010314.0004. [DIRS 154194]

Dieter, G.E. 1976. *Mechanical Metallurgy.* 2nd Edition. Materials Science and Engineering Series. New York, New York: McGraw-Hill Book Company. TIC: 247879. [DIRS 118647]

DOE (U.S. Department of Energy) 2002. *Final Environmental Impact Statement for a Geologic Repository for the Disposal of Spent Nuclear Fuel and High-Level Radioactive Waste at Yucca Mountain, Nye County, Nevada.* DOE/EIS-0250. Washington, D.C.: U.S. Department of Energy, Office of Civilian Radioactive Waste Management. ACC: MOL.20020524.0314; MOL.20020524.0315; MOL.20020524.0316; MOL.20020524.0317; MOL.20020524.0318; MOL.20020524.0319; MOL.20020524.0320. [DIRS 155970]

DOE (U.S. Department of Energy) 2003. *TMI Fuel Characteristics for Disposal Criticality Analysis.* DOE/SNF/REP-084, Rev. 0. Idaho Falls, Idaho: U.S. Department of Energy, Idaho Operations Office. ACC: MOL.20031013.0388. [DIRS 164970]

DOE (U.S. Department of Energy) 2004. *Source Term Estimates for DOE Spent Nuclear Fuels.* DOE/SNF/REP-078, Rev. 1. Three volumes. Idaho Falls, Idaho: U.S. Department of Energy, Idaho Operations Office. ACC: MOL.20040524.0451. [DIRS 169354]

DOE (U.S. Department of Energy) 2004. *Waste Treatment and Immobilization Plant (WTP) High-Level Waste (HLW) Canister Production Estimates to Support Analyses by the Yucca Mountain Project.* DOE/ORP-2004-03, Rev. 0. Richland, Washington: U.S. Department of Energy, Office of River Protection. ACC: MOL.20041005.0256. [DIRS 172092]

DOE (U.S. Department of Energy) 2006. *Yucca Mountain Project Conceptual Design Report.* TDR-MGR-MD-000014, Rev. 05. Las Vegas, Nevada: U.S. Department of Energy, Office of Repository Development. ACC: ENG.20060505.0003. [DIRS 176937]

DOE (U.S. Department of Energy) 2007. "High-Level Radioactive Waste and U.S. Department of Energy and Naval Spent Nuclear Fuel to the Civilian Radioactive Waste Management System." Volume 1 of *Integrated Interface Control Document.* DOE/RW-0511, Rev. 3. Washington, D.C.: U.S. Department of Energy, Office of Civilian Radioactive Waste Management. ACC: DOC.20070125.0002. [DIRS 178792]

DOE (U.S. Department of Energy) 2007. *Waste Acceptance System Requirements Document.* DOE/RW-0351, Rev. 5. Washington, D.C.: U.S. Department of Energy, Office of Civilian Radioactive Waste Management. ACC: DOC.20070522.0007. [DIRS 169992]

DOE (U.S. Department of Energy) 1987. *Appendix 2A. Physical Descriptions of LWR Fuel Assemblies.* Volume 3 of *Characteristics of Spent Fuel, High-Level Waste, and Other Radioactive Wastes Which May Require Long-Term Isolation.* DOE/RW-0184. Washington, D.C.: U.S. Department of Energy, Office of Civilian Radioactive Waste Management. ACC: HQX.19880405.0024. [DIRS 132333]

DOE (U.S. Department of Energy) 1999. *TRIGA (UZrH) Fuel Characteristics for Disposal Criticality Analysis.* DOE/SNF/REP-048, Rev. 0. Washington, D.C.: U.S. Department of Energy. TIC: 244162. [DIRS 103891]

DOE (U.S. Department of Energy) 2000. *N Reactor (U-Metal) Fuel Characteristics for Disposal Criticality Analysis.* DOE/SNF/REP-056, Rev. 0. [Washington, D.C.]: U.S. Department of Energy, Office of Environmental Management. TIC: 247956. [DIRS 150095]

DOE (U.S. Department of Energy) 2007. *Transportation, Aging and Disposal Canister System Performance Specification.* WMO-TADCS-000001, Rev. 0. Washington, D.C.: U.S. Department of Energy, Office of Civilian Radioactive Waste Management. ACC: DOC.20070614.0007. [DIRS 181403]

DriftFlow V. 1.0. 2002. WINDOWS 2000. STN: 10722-1.0-00. [DIRS 163090]

EPRI (Electric Power Research Institute) 1989. *Testing and Analyses of the TN-24P PWR Spent-Fuel Dry Storage Cask Loaded with Consolidated Fuel.* EPRI NP-6191. Palo Alto, California: Electric Power Research Institute. TIC: 207047. [DIRS 101947]

Feucht, M., et al 2006. "Recent Developments and Applications of the Gurson Model." *LS-DYNA Anwenderforum. vol. D, no. II,* 21-31. Ulm,, Germany: LS-DYNA Anwenderforum. [DIRS 182118]

FLUENT V. 6.0.12. 2003. HP-UX 11.00. STN: 10550-6.0.12-00. [DIRS 163001]

Framatome Cogema Fuels 1999. *Operational Data - B&W NSS.* 51-5004349-01. Lynchburg, Virginia: Framatome Cogema Fuels. ACC: MOL.19990610.0201. [DIRS 146419]

Gartling, D.K.; Eaton, R.R.; and Thomas, R.K. 1981. *Preliminary Thermal Analyses for a Nuclear Waste Repository in Tuff.* SAND80-2813. Albuquerque, New Mexico: Sandia National Laboratories. ACC: HQS.19880517.2295. [DIRS 142640]

Gelin, J.C. 1998. "Modelling of Damage in Metal Forming Processes." *Journal of Materials Processing Technology, 80-81,* 24-32. [New York, New York]: Elsevier. TIC: 259062. [DIRS 182162]

Graf, A. and Hosford, W.F. 1990. "Calculations of Forming Limit Diagrams." *Metallurgical Transactions, vol. 21A,* pp. 87-96. TIC: 259699 [DIRS 182684]

Gurson, A.L. 1977. "Continuum Theory of Ductile Rupture by Void Nucleation and Growth: Part 1--Yield Criteria and Flow Rules for Porous Ductile Media." *Journal of Engineering Materials and Technology,* Pages 2-15. [New York, New York]: American Society of Mechanical Engineers. TIC: 258976. [DIRS 182163]

Hallquist, J.O. 1998. *LS-DYNA, Theoretical Manual.* Livermore, California: Livermore Software Technology Corporation. TIC: 238997. [DIRS 155373]

Hashiguchi, K. and Protasov, A. 2004. "Localized Necking Analysis by the Subloading Surface Model with Tangential-Strain Rate and Anisotropy." *International Journal of Plasticity, 20,* 1909-1930. [New York, New York]: Elsevier. TIC: 258973. [DIRS 182164]

Haukaas, T. 2006. "Efficient Computation of Response Sensitivities for Inelastic Structures." *Journal of Structural Engineering, 132,* (2), 260-266. [New York, New York]: American Society of Civil Engineers. TIC: 258949. [DIRS 182166]

Haukaas, T. and Der Kiureghian, A. 2005. "Parameter Sensitivity and Importance Measures in Nonlinear Finite Element Reliability Analysis." *Journal of Engineering Mechanics, 131,* (10), 1013-1026. [New York, New York]: American Society of Civil Engineers. TIC: 258948. [DIRS 182165]

Haynes International 1997. Hastelloy C-22 Alloy. Kokomo, Indiana: Haynes International. TIC: 238121. [DIRS 100896]

Herrera, M.; Ku, F.; and Tang, S. 2002. *Calculation Package, Residual Stress Analyses on the 21 PWR Mockup Waste Package Outer Shell Due to Quenching and General Corrosion Using a Side-Wall Thickness of 20mm.* File No. TRW-06Q-319. [San Jose, California]: Structural Integrity Associates. ACC: MOL.20020925.0127. [DIRS 166799]

Hill, R. 1950. *Mathematical Theory of Plasticity.* Oxford Engineering Science Series. New York, New York: Oxford University Press. TIC: 259150. [DIRS 182167]

Hill, R. 1948. "A Theory of the Yielding and Plastic Flow of Anisotropic Metals." *Proceedings of the Royal Society of London, Series A. Mathematical and Physical Sciences, 193,* (A 1033), 281-297. London, England: Cambridge University Press. TIC: 259228. [DIRS 182144]

Hill, R. 1979. "Theoretical Plasticity of Textured Aggregates." *Mathematical Proceedings of Cambridge Philosophical Society, 85,* 179-191. [Cambridge, England: Cambridge Philosophical Society]. TIC: 259141. [DIRS 182168]

Horstemeyer, M.F. 2000. "A Numerical Parameter Investigation of Localization and Forming Limits." *International Journal of Damage Mechanics, 9,* 255-285. [Thousand Oaks, California]: Sage Publications. TIC: 258967. [DIRS 182169]

Horstemeyer, M.F. and Ramaswamy, S. 2000. "On Factors Affecting Localization and Void Growth in Ductile Metals: A Parametric Study." *International Journal of Damage Mechanics, 9,* 5-28. [Thousand Oaks, California]: Sage Publications. TIC: 258965. [DIRS 182170]

Hosford, W. F. 1985. "Comments on Anisotropic Yield Criteria." *International Journal of Mechanical Science, 27,* (7/8), 423-427. [New York, New York]: Pergamon Press. TIC: 259143. [DIRS 182172]

Hosford, W.F. and Duncan J.L. 1999. "Sheet Metal Forming: A Review." *JOM, 51,* (11), 39-44. [New York, New York: Metallurgical Society of AIME]. TIC: 259692. [DIRS 182663]

Inco Alloys International 1995. INCONEL Alloy 622. Publication Number IAI-144. Huntington, West Virginia: Inco Alloys International. TIC: 242681. [DIRS 182441]

Inco Alloys International 1988. Product Handbook. Huntington, West Virginia: Inco Alloys International. TIC: 239397. [DIRS 130835]

Incropera, F.P. and DeWitt, D.P. 1996. *Introduction to Heat Transfer.* 3rd Edition. New York, New York: John Wiley & Sons. TIC: 241057. [DIRS 107784]

INEEL (Idaho National Engineering and Environmental Laboratory) 2003. *Specification for Advanced Test Reactor Mark VII Zone Loaded Fuel Elements, IN-F-9-ATR, Revision 15.* SPC-415, Rev. 0. Idaho Falls, Idaho: U.S. Department of Energy, Idaho National Engineering and Environmental Laboratory. ACC: DOC.20040818.0003. [DIRS 171506]

Jones, D.P. and Holliday, J.E. 2000. "Elastic-Plastic Analysis of the PVRC Burst Disk Tests with Comparison to the ASME Code Primary Stress Limits." *Journal of Pressure Vessel Technology, 122,* 146-151. [New York, New York]: American Society of Mechanical Engineers. TIC: 258969. [DIRS 182173]

Jones, R.H. 1992. *Spent Fuel Corrosion Product and Fuel Cleaning Assessment.* Los Gatos, California: Robert H. Jones, P.E., Consultant. ACC: HQX.19920825.0007. [DIRS 146405]

Kelmenson, R. 2000. "Meeting Summary, NRC/DOE Technical Exchange Meeting on Container Life and Source Term (CLST), September 12-13, 2000." E-mail from R. Kelmenson to C. Hanlon (DOE/YMSCO), T. Gunter (DOE/YMSCO), A. Gil (DOE/YMP), P. Russell (DOE/YMSCO), September 27, 2000, with attachment. ACC: MOL.20001127.0049. [DIRS 154350]

Kitamura, O. 1997. "Comparative Study on Collision Resistance of Side Structure." *Marine Technology and SNAME News, 34,* (4), 293-308. [New York, New York]: Society of Naval Architects and Marine Engineers. TIC: 259217. [DIRS 182666]

Kitamura, O. 2002. "FEM Approach to the Simulation of Collision and Grounding Damage." *Marine Structures, 15,* 403-428. [New York, New York]: Elsevier. TIC: 259081. [DIRS 182442]

Kuroiwa, T. [1996]. "Numerical Simulation of Actual Collision & Grounding Accidents." *Proceedings, International Conference on Designs and Methodologies for Collision and Grounding Protection of Ships, San Francisco, California, August 22-23, 1996.* 7-1 - 7-12. [Jersey City, New Jersey]: Society of Naval Architects & Marine Engineers. TIC: 259219. [DIRS 182174]

Larsen, N.H.; Parkos, G.R.; and Raza, O. 1976. *Core Design and Operating Data for Cycles 1 and 2 of Quad Cities 1.* EPRI NP-240. Palo Alto, California: Electric Power Research Institute. TIC: 237267. [DIRS 146576]

Le Sourne, H.; Couty, N.; Besnier, F.; Kammerer, C.; and Legavre, H. 2003. "LS-DYNA Applications in Shipbuilding." *4th European LS-DYNA Conference, 22nd-23rd May 2003, Ulm, Germany*. Pages A-II-01 - A-II-16. Stuttgart, Germany: DYNAmore GmbH. TIC: 259064. [DIRS 182444]

Lehmann, E. and Yu, X. 1998. "On Ductile Rupture Criteria for Structural Tear in the Case of Ship Collision and Grounding." *Practical Design of Ships and Mobile Units, Proceedings of the Seventh International Symposium on Practical Design of Ships and Mobile Units, The Hague, The Netherlands, September 1998.* Oosterveld, M. and Tan, S.G, eds. *Developments in Technology, 11,* 149-156. New York, New York: Elsevier. TIC: 259216. [DIRS 182668]

Levy, I.S.; Chin, B.A.; Simonen, E.P.; Beyer, C.E.; Gilbert, E.R.; and Johnson, A.B., Jr. 1987. *Recommended Temperature Limits for Dry Storage of Spent Light Water Reactor Zircaloy-Clad Fuel Rods in Inert Gas.* PNL-6189. Richland, Washington: Pacific Northwest Laboratory. TIC: 231836. [DIRS 144349]

Lide, D.R., ed. 1995. *CRC Handbook of Chemistry and Physics.* 76th Edition. Boca Raton, Florida: CRC Press. TIC: 216194. [DIRS 101876]

Lin, J.; Liu, Y.; and Dean, T.A 2005. "A Review on Damage Mechanisms, Models and Calibration Methods Under Various Deformation Conditions." *International Journal of Damage Mechanics, 14,* 299-319. [Thousand Oaks, California]: Sage Publications. TIC: 258966. [DIRS 182435]

LS-DYNA V. 970.3858 D MPP. 2003. HP-UX 11.22. STN: 10300-970.3858 D MPP-00. [DIRS 166918]

Lu, Z.H. and Lee, D. 1987. "Prediction of History-Dependent Forming Limits by Applying Different Hardening Models." *International Journal of Mechanical Sciences, 29,* (2), 123-137. [New York, New York]: Pergamon Journals. TIC: 259687. [DIRS 182662]

Ludwig, S.B. and Renier, J.P. 1989. *Standard- and Extended-Burnup PWR and BWR Reactor Models for the ORIGEN2 Computer Code.* ORNL/TM-11018. Oak Ridge, Tennessee: Oak Ridge National Laboratory. TIC: 203557. [DIRS 146398]

Luksic, A. 1989. *Activation Measurements and Comparison with Calculations for Spent Fuel Assembly Hardware.* Volume 1 of *Spent Fuel Assembly Hardware: Characterization and 10 CFR 61 Classification for Waste Disposal.* PNL-6906. Richland, Washington: Pacific Northwest Laboratory. ACC: NNA.19890926.0124. [DIRS 120506]

Marciniak, Z. and Kuczynski, K. 1967. "Limit Strains in the Processes of Stretch-Forming Sheet Metal." *International Journal of Mechanical Sciences, 9,* 609-620. [New York, New York]: Pergamon Press. TIC: 259144. [DIRS 182436]

McClintock, F.A. 1968. "A Criterion for Ductile Fracture by the Growth of Holes." *Journal of Applied Mechanics,* 363-371. [New York, New York]: American Society of Mechanical Engineers. TIC: 258977. [DIRS 182180]

MCNP V. 4B2LV. 1998. HP-UX 9.07 & 10.20, WINDOWS 95, SOLARIS 2.6. CSCI: 30033-V4B2LV. [DIRS 154060]

MCNP V. 4B2LV. 2002. WINDOWS 2000. STN: 10437-4B2LV-00. [DIRS 163407]

Meriam, J.L. and Kraige, L.G. 1987. *Statics.* Volume 1 of *Engineering Mechanics.* 2nd Edition. Pages 441, 443. New York, New York: John Wiley & Sons. TIC: 241293. [DIRS 104306]

Mirone, G. 2004. "Approximate Model of the Necking Behaviour and Application to the Void Growth Prediction." *International Journal of Damage Mechanics, 13,* 241-261. [Thousand Oaks, California]: Sage Publications. TIC: 258963. [DIRS 182434]

Mou, Y. and Han, R.P.S. 1996. "Damage Evolution in Ductile Materials." *International Journal of Damage Mechanics, 5,* 241-258. [Thousand Oaks, California]: Sage Publications. TIC: 258964. [DIRS 182437]

Needleman, A. 1972. "Void Growth in an Elastic-Plastic Medium." *Journal of Applied Mechanics,* Pages 964-970. [New York, New York]: American Society of Mechanical Engineers. TIC: 259142. [DIRS 182438]

Needleman, A. 1994. "Computational Modeling of Material Failure." *Applied Mechanics Review, 47,* (6, Part 2), S34-S42. [New York, New York]: American Society of Mechanical Engineers. TIC: 259012. [DIRS 182439]

Nicholas, T. 1980. *Dynamic Tensile Testing of Structural Materials Using a Split Hopkinson Bar Apparatus*. AFWAL-TR-80-4053. Wright-Patterson Air Force Base, Ohio: Air Force Wright Aeronautical Laboratories. TIC: 249469. [DIRS 154072]

Padwal, S.B and Chaturvedi, R.C. 1992. "Prediction of Forming Limits Using Hosford's Modified Yield Criterion." *International Journal of Mechanical Sciences, 34,* (7), 541-547. [New York, New York]: Pergamon Press. TIC: 259683. [DIRS 182661]

Picha, K.G., Jr. 1997. "Response to Repository Environmental Impact Statement Data Call for High-Level Waste." Memorandum from K.G. Picha, Jr. (DOE) to W. Dixon (YMSCO), September 5, 1997, with attachments. ACC: MOL.19970917.0273. [DIRS 104406]

Punatar, M.K. 2001. *Summary Report of Commercial Reactor Criticality Data for Crystal River Unit 3*. TDR-UDC-NU-000001 REV 02. Las Vegas, Nevada: Bechtel SAIC Company. ACC: MOL.20010702.0087. [DIRS 155635]

Ray, J.W. 2007. *Projected Glass Composition and Curie Content of Canisters from Savannah River Site(U)*. X-ESR-S-00015, Rev. 1. [Aiken, South Carolina]: Washington Savannah River Company. ACC: MOL.20070703.0427. [DIRS 181690]

Reamer, C.W. 2004. "Pre-Licensing Evaluation of Preclosure Key Technical Issue Agreement 7.02 Related to the Waste Package Finite Element Analysis." Letter from C.W. Reamer (NRC) to J. Zeigler (DOE/ORD), August 4, 2004, 0809042721, with enclosure. ACC: MOL.20040922.0233. [DIRS 182440]

Rice, J.R. and Tracey, D.M. 1969. "On the Ductile Enlargement of Voids in Triaxial Stress Fields." *Journal of the Mechanics and Physics of Solids, 17,* 201-217. [New York, New York]: Pergamon Press. TIC: 259685. [DIRS 182660]

Sandia 2005. "Project Summary: Mechanism-based Modeling of Ductile Failure." Accessed x. URL: http://www.ca.sandia.gov/8700/projects/content.php?cid=71. ACC: MOL.20070919.0510 [DIRS 182672]

Schafer, B.W.; Ojdrovic, R.P.; and Zarghamee, M.S. 2000. "Triaxiality and Fracture of Steel Moment Connections." *Journal of Structural Engineering, 126,* (10), 1131-1139. [New York, New York]: American Society of Civil Engineers. TIC: 259018. [DIRS 182178]

Shi, M.F. and Gerdeen, J.C. 1991. "Effect of Strain Gradient and Curvature on Forming Limit Diagrams for Anisotropic Sheets." *Journal of Materials Shaping Technology, 9,* (4), 253-268. New York, New York: Springer-Verlag. TIC: 259060. [DIRS 182447]

Siegel, R. and Howell, J.R. 1992. *Thermal Radiation Heat Transfer*. 3rd Edition. Washington, D.C.: Taylor & Francis. TIC: 236759. [DIRS 100687]

Simonsen, B.C. and Lauridsen, L.P. 2000. "Energy Absorption and Ductile Failure in Metal Sheets Under Lateral Indentation by a Sphere." *International Journal of Impact Engineering, 24,* 1017-1039. [New York, New York]: Pergamon. TIC: 259020. [DIRS 182448]

Software Code: SCALE V. 4.4A. 2000. HP. STN: 10129-4.4A-00. [DIRS 154394]

Special Metals 2006. INCONEL® Alloy 22. Publication Number SMC-049. Huntington, West Virginia: Special Metals. TIC: 259169. [DIRS 182449]

Sriram, S. and Van Tyne, C.J. 2002. "Criterion for Prevention of Central Bursting in Forward Extrusions through Spherical Dies Using the Finite Element Method." *Journal of Manufacturing Science and Engineering, 124,* 65-70. [New York, New York]: American Society of Mechanical Engineers. TIC: 259015. [DIRS 182450]

Stören, S. and Rice, J.R. 1975. "Localized Necking in Thin Sheets." *Journal of the Mechanics and Physics of Solids, 23,* 421-441. [New York, New York]: Pergamon Press. TIC: 259148. [DIRS 182451]

Stoughton, T.B. 1999. "A General Forming Limit Criterion for Sheet Metal Forming." *International Journal of Mechanical Sciences, 42,* 1-27. [New York, New York]: Pergamon. TIC: 259146. [DIRS 182452]

Stoughton, T.B. and Zhu, X. 2004. "Review of Theoretical Models of the Strain-Based FLD and Their Relevance to the Stress-Based FLD." *International Journal of Plasticity, 20,* 1463-1486. [New York, New York]: Elsevier. TIC: 259065. [DIRS 182453]

Stout, R.B. and Leider, H.R., eds. 1997. *Waste Form Characteristics Report Revision 1.* UCRL-ID-108314. Version 1.2. Livermore, California: Lawrence Livermore National Laboratory. ACC: MOL.19980512.0133. [DIRS 100419]

Swift, H.W. 1952. "Plastic Instability Under Plane Stress." *Journal of the Mechanics and Physics of Solids, 1,* 1-18. [New York, New York]: Pergamon Press. TIC: 259149. [DIRS 182454]

TIMET. 2000. "Timetal 6-4, 6-4 ELI, 6-4-.1Ru Medium to High Strength General-Purpose Alloys." Denver, Colorado: Titanium Metals Corporation. Accessed August 26, 2002. TIC: 253102. http://www.timet.com/pdfs/6-4.pdf [DIRS 160688]

Tomita, Y. 1994. "Simulations of Plastic Instabilities in Solid Mechanics." *Applied Mechanics Review, 47,* (6. Part 1), 171-205. [New York, New York]: American Society of Mechanical Engineers. TIC: 259013. [DIRS 182143]

Törnqvist, R. 2003. *Design of Crashworthy Ship Structures.* Ph.D. dissertation. Lyngby, Denmark: Technical University of Denmark, Department of Mechanical Engineering. TIC: 259175. [DIRS 182455]

Tvergaard, V. 1990. "Material Failure by Void Growth to Coalescence." *Advances in Applied Mechanics.* Hutchinson, J.W. and T.Y. Wu, eds. Volume 27. Pages 83-151. New York, New York: Academic Press. TIC: 258974. [DIRS 182463]

Tvergaard, V. 1978. "Effect of Kinematic Hardening on Localized Necking in Biaxially Stretched Sheets." *International Journal of Mechanical Sciences, 20,* 651-658. [New York, New York]: Pergamon Press. TIC: 259145. [DIRS 182179]

Wang, G. 2002. "Some Recent Studies on Plastic Behavior of Plates Subjected to Large Impact Loads." *Journal of Offshore Mechanics and Arctic Engineering, 124,* 125-131. [New York, New York]: American Society of Mechanical Engineers. TIC: 258971. [DIRS 182142]

Wang, G.; Ji, C.; Kujala, P.; Lee, S.-G.; Marino, A.; Sirkar, J.; Suzuki, K.; Pedersen, P.T.; Vredeveldt, A.W.; and Yuriy, V. 2006. "Committee V.1 Collision and Grounding." *Proceedings of the 16th International Ship and Offshore Structures Congress held in Southampton, UK, August 20-25, 2006.* Frieze, P.A. and R.A. Shenoi, eds. *2,* 1-56. Highfield, Southampton, England: University of Southampton. TIC: 259270. [DIRS 182141]

Williams, N.H. 2003. "Contract No. DE-AC28-01RW12101 - Key Technical Issue (KTI) Agreement: Preclosure Safety (PRE) 7.02." Letter from N.H. Williams (BSC) to J.D. Ziegler (DOE/ORD), November 24, 2003, PN/YM:mm - 1119039546, with enclosures. ACC: MOL.20040107.0077. [DIRS 167094]

WPLOAD V. 2.0. 2007. WINDOWS 2000, WINDOWS XP. STN: 11131-2.0-00. [DIRS 182947]

WVNS (West Valley Nuclear Services Company) 2001. *WVDP Waste Form Qualification Report - Canistered Waste Form Specifications, Chemical Specification.* Chapter 1 of *Waste Form Qualification Report (WQR).* WVDP-186. West Valley, New York: West Valley Demonstration Project. ACC: MOL.20020211.0184. [DIRS 157559]

WVNS (West Valley Nuclear Services) 2003. "Radionuclide Scaling Factors." Addendum 1 of *WVDP Waste Form Qualification Report - Waste Form Specifications, Radionuclide Inventory Specification.* WVDP-186, Rev. 0. [West Valley, New York]: West Valley Nuclear Services. ACC: MOL.20040329.0111. [DIRS 168547]

Zhou, W. 1990. "A New Non-Quadratic Orthotropic Yield Criterion." *International Journal of Mechanical Sciences, 32,* (6), 513-520. [New York, New York]: Pergamon Press. TIC: 259058. [DIRS 182464]

Zhu, X.; Weinmann, K.; and Chandra, A. 2001. "A Unified Bifurcation Analysis of Sheet Metal Forming Limits." *Journal of Engineering Materials and Technology, 123,* 329-333. [New York, New York]: American Society of Mechanical Engineers. TIC: 259059. [DIRS 182176]

Zimmer, A.; Koploy, M.A.; and Madsen, M.M. 1991. "Comparison of Elastic and Inelastic Analysis and Test Results for the Defense High Level Waste Shipping Cask." *High Level Radioactive Waste Management, Proceedings of the Second Annual International Conference, Las Vegas, Nevada, April 28-May 3, 1991. 2,* 1271-1278. La Grange Park, Illinois: American Nuclear Society. TIC: 204272. [DIRS 182175]

9.2 CODES, STANDARDS, REGULATIONS, AND PROCEDURES

PA-PRO-0313, Rev. 6. *Technical Reports.* Las Vegas, Nevada. Bechtel SAIC Company, ACC: 20070726.0006

EG-PRO-3DP-G04B-00005 Rev 04. *Configuration Management*. Las Vegas, Nevada. Bechtel SAIC Company. ACC: ENG.20070319.0012.

10 CFR 63. 2006. Energy: Disposal of High-Level Radioactive Wastes in a Geologic Repository at Yucca Mountain, Nevada. Internet Accessible. [DIRS 176544]

10 CFR 961. 2007. Energy: Standard Contract for Disposal of Spent Nuclear Fuel and/or High-Level Radioactive Waste. Internet Accessible. [DIRS 182678]

ANSI N14.6-1993. 1993. *American National Standard for Radioactive Materials - Special Lifting Devices for Shipping Containers Weighing 10000 Pounds (4500 kg) or More.* New York, New York: American National Standards Institute. TIC: 236261. [DIRS 102016]

ANSI/ANS-6.1.1-1977. *Neutron and Gamma-Ray Flux-to-Dose-Rate Factors.* La Grange Park, Illinois: American Nuclear Society. TIC: 239401. [DIRS 107016]

ASME (American Society of Mechanical Engineers) 2001. *2001 ASME Boiler and Pressure Vessel Code (includes 2002 addenda).* New York, New York: American Society of Mechanical Engineers. TIC: 251425. [DIRS 158115]

ASME (American Society of Mechanical Engineers) 2004. *2004 ASME Boiler and Pressure Vessel Code.* 2004 Edition. New York, New York: American Society of Mechanical Engineers. TIC: 256479. [DIRS 171846]

ASTM B 811-90. 1991. *Standard Specification for Wrought Zirconium Alloy Seamless Tubes for Nuclear Reactor Fuel Cladding.* Philadelphia, Pennsylvania: American Society for Testing and Materials. TIC: 239780. [DIRS 131753]

ASTM G 1-90 (Reapproved 1999). 1999. *Standard Practice for Preparing, Cleaning, and Evaluating Corrosion Test Specimens.* West Conshohocken, Pennsylvania: American Society for Testing and Materials. TIC: 238771. [DIRS 103515]

Hechmer, J.L. and Hollinger, G.L. 1998. *3D Stress Criteria Guidelines for Application.* WRC Bulletin 429. New York, New York: Welding Research Council. TIC: 254432. [DIRS 166147]

Hermann, O.W.; Parks, C.V.; and Renier, J.P. 1994. *Technical Support for a Proposed Decay Heat Guide Using SAS2H/ORIGEN-S Data.* NUREG/CR-5625. Washington, D.C.: U.S. Nuclear Regulatory Commission. TIC: 212756. [DIRS 154045]

Kokajko, L.E. 2005. "Pre-Licensing Evaluation of Key Technical Issue Agreement: Container Life and Source Term 2.03 Additional Information Need-1." Memorandum from L.E. Kokajko (NRC) to J.D. Ziegler (DOE/ORD), March 8, 2005, 0314055001, with enclosure. ACC: MOL.20050324.0121. [DIRS 182443]

NRC (U.S. Nuclear Regulatory Commission) 2003. *Interim Staff Guidance - 11, Revision 3. Cladding Considerations for the Transportation and Storage of Spent Fuel.* ISG-11, Rev. 3. Washington, D.C.: U.S. Nuclear Regulatory Commission. ACC: MOL.20040721.0065. [DIRS 170332]

NRC (U.S. Nuclear Regulatory Commission) 2003. *Yucca Mountain Review Plan, Final Report.* NUREG-1804, Rev. 2. Washington, D.C.: U.S. Nuclear Regulatory Commission, Office of Nuclear Material Safety and Safeguards. TIC: 254568. [DIRS 163274]

NRC (U.S. Nuclear Regulatory Commission) 2006. *Interim Staff Guidance HLWRS-ISG-01. Review Methodology for Seismically Initiated Event Sequences.* HLWRS-ISG-01. Washington, D.C.: U.S. Nuclear Regulatory Commission. ACC: MOL.20061128.0036. [DIRS 178130]

NRC (U.S. Nuclear Regulatory Commission) 1980. *Control of Heavy Loads at Nuclear Power Plants.* NUREG-0612. Washington, D.C.: U.S. Nuclear Regulatory Commission. TIC: 209017. [DIRS 104939]

NRC (U.S. Nuclear Regulatory Commission) 1997. *SCALE, RSIC Computer Code Collection (CCC-545).* NUREG/CR-0200, Rev. 5. Washington, D.C.: U.S. Nuclear Regulatory Commission. TIC: 235920. [DIRS 122675]

NRC (U.S. Nuclear Regulatory Commission) 1997. *Standard Review Plan for Dry Cask Storage Systems.* NUREG-1536. Washington, D.C.: U.S. Nuclear Regulatory Commission. ACC: MOL.20010724.0307. [DIRS 101903]

NRC (U.S. Nuclear Regulatory Commission) 2000. *Standard Review Plan for Spent Fuel Dry Storage Facilities.* NUREG-1567. Washington, D.C.: U.S. Nuclear Regulatory Commission. TIC: 247929. [DIRS 149756]

NRC (U.S. Nuclear Regulatory Commission) 2000. *Standard Review Plan for Transportation Packages for Spent Nuclear Fuel.* NUREG-1617. Washington, D.C.: U.S. Nuclear Regulatory Commission. TIC: 249470. [DIRS 154000]

Nuclear Waste Policy Amendments Act of 1987. Public Law No. 100-203, 101 Stat. 1330. TIC: 223717. [DIRS 100016]

9.3 SOURCE DATA, LISTED BY DATA TRACKING NUMBER

GS000483351030.003. Thermal Properties Measured 12/01/99 to 12/02/99 Using the Thermolink Soil Multimeter and Thermal Properties Sensor on Selected Potential Candidate Backfill Materials Used in the Engineered Barrier System. Submittal date: 11/09/2000. [DIRS 152932]

GS031208312232.003. Deep Unsaturated Zone Surface-Based Borehole Instrumentation Program Data from Boreholes USW NRG-7A, UE-25 UZ #4, USW NRG-6, UE-25 UZ #5, USW UZ-7A and USW SD-12 for the Time Period 10/01/97 - 03/31/98. Submittal date: 07/29/2004. [DIRS 171287]

LL020603612251.015. Slow Strain Rate Test Generated Stress Corrosion Cracking Data. Submittal date: 08/27/2002. [DIRS 160430]

SN0303T0503102.008. Revised Thermal Conductivity of the Non-Repository Layers of Yucca Mountain. Submittal date: 03/19/2003. [DIRS 162401]

SN0307T0510902.003. Updated Heat Capacity of Yucca Mountain Stratigraphic Units. Submittal date: 07/15/2003. [DIRS 164196]

SN0404T0503102.011. Thermal Conductivity of the Potential Repository Horizon Rev 3. Submittal date: 04/27/2004. [DIRS 169129]

APPENDIX I

I-1 SELECTION OF WASTE PACKAGE CAPACITY DETERMINATION METHODOLOGY

To provide an assessment of the risk of waste package breach within the context of passive component reliability (BSC 2007 [DIRS 181782]), a methodology that realistically represents the structural performance of the OCB must be formulated. This methodology must provide a best-estimate quantification of the Capacity (sometimes referred to as the Resistance, Strength or Fragility) of the OCB when exposed to credible event sequences.

The OCB provides confinement of the waste form radionuclide inventory. For a sealed waste package, the inner vessel provides structural support of the OCB, but is not credited to confine the waste form in the event that the OCB is breached. Similarly, the waste form packaging might provide structural support to the waste package inner vessel, but is not credited to confine the waste form in the event that the OCB is breached.

I-2 GOVERNING INDEPENDENT VARIABLES FOR STRUCTURAL ANALYSES

Demand (sometimes referred to as Load or Stress) for most event sequences, is defined in the reliability methodology in terms of the independent variables identified in the event sequence definition. For the actual structural analysis, the independent variables that define the event sequence are resolved into kinetic energy and an orientation of the impact for the structural analysis. For the balance of this discussion, the discussion is posed in terms of the impact velocity for convenience. It should be understood by the reader that this value is statistically derived from the event sequence definition.

Important exceptions to this formulation are dropped or launched objects or rock falls. In these cases, the masses and other parameters of the projectiles affect the Demand.

The potential for strain energy absorption of the wall-averaged stress fields defines the Capacity. The following discussion will focus on those cases where the initial impact velocity can be used to define the Demand.

I-3 BACKGROUND OF METHODOLOGY

OCB breach by in-plane membrane stresses (plane stress) leading to ductile through-wall tearing/rupture is assumed. Breach by pure shear or compressive instability is not addressed.

The OCB breach level of impact velocity may be iteratively determined using LS-DYNA finite element analysis (FEA) calculations and is conservatively defined as that level of loading that just leads to the initiation of OCB tensile instability (strain concentration and void initiation). This precedes breech because further loading is needed for the voids to coalescence across a wall section with sufficient porosity to lead to a bifurcation (rupture) of the wall. This microstructural material response is exhibited in a uniaxial tension test as the initiation of necking and reduction in load carrying capacity, i.e., the maximum “ultimate” (engineering) tensile strength (UTS) is reached. Necking in room-temperature tension tests begins with internal void formation at

second phase particles (Lin, J., et al. 2005 [DIRS 182435]) which breaks down the uniaxial stress state and introduces complex multi-axial stress states adjacent to the voids.

The “critical thinning” phenomenon under plane stress and spherical deep drawing of sheet metal was analytically characterized over half a century ago (Hill 1948 [DIRS 182144], Hill 1950 [DIRS 182167], Swift 1952 [DIRS 182454]) and then extended to cold-forming applications (Marciniak & Kuczynski 1967 [DIRS 182436], McClintock 1968 [DIRS 182180], Rice & Tracey 1969 [DIRS 182660], Berg 1970 [DIRS 182116], Needleman 1972 [DIRS 182438], Stören & Rice 1975 [DIRS 182451], Gurson 1977 [DIRS 182163], Tvergaard 1978 [DIRS 182179], Hill 1979 [DIRS 182168], and others). These tensile instability solutions were then refined in scores of research efforts for anisotropy, various hardening models, in-plane shear, bending, second-order effects and more generality (to mention a few: Hosford 1985 [DIRS 182172], Lu & Lee 1987 [DIRS 182662], Barlat & Lian 1989 [DIRS 182115], Graf & Hosford 1990 [DIRS 182684], Tvergaard 1990 [DIRS 182463], Zhou 1990 [DIRS 182464], Shi & Gerdeen 1991 [DIRS 182447], Padwal & Chaturvedi 1992 [DIRS 182661], Tomita 1994 [DIRS 182143], Needleman 1994 [DIRS 182439], Mou & Han 1996 [DIRS 182437], Gelin 1998 [DIRS 182162], Horstemeyer & Ramaswamy 2000 [DIRS 182170], Chan, et al., 2000 [DIRS 182159], Zhu, et al., 2001 [DIRS 182176], Mirone 2004 [DIRS 182434], Hashiguchi, et al., 2004, [DIRS 182164]).

A paper entitled, "*A Review on Damage Mechanisms, Models and Calibration Methods under Various Deformation Conditions*" (Lin, J., et al. 2005 [DIRS 182435]) is an overview of the void nucleation and coalescence differences in various time-temperature deformation processes. Cold forming is one of the deformation processes and the ductile failure of the OCB under event sequences will be a cold forming process.

The automobile and sheet metal industries have established membrane strain-based cold-forming limits that preclude tensile instability using an analytically developed tensile forming limit diagram (FLD) based on the M-K method (Marciniak & Kuczynski 1967 [DIRS 182436]). The tensile FLD addresses the triaxiality effect on strain localization (necking). Other FLD's are available that define safe straining windows for the biaxial membrane strain state and include in-plane and cross-wall shear limits and wrinkling limits (see Figure I-1, after Hosford & Duncan 1999 [DIRS 182663]). However, waste package event sequence evaluations have yet to identify these as governing failure modes.

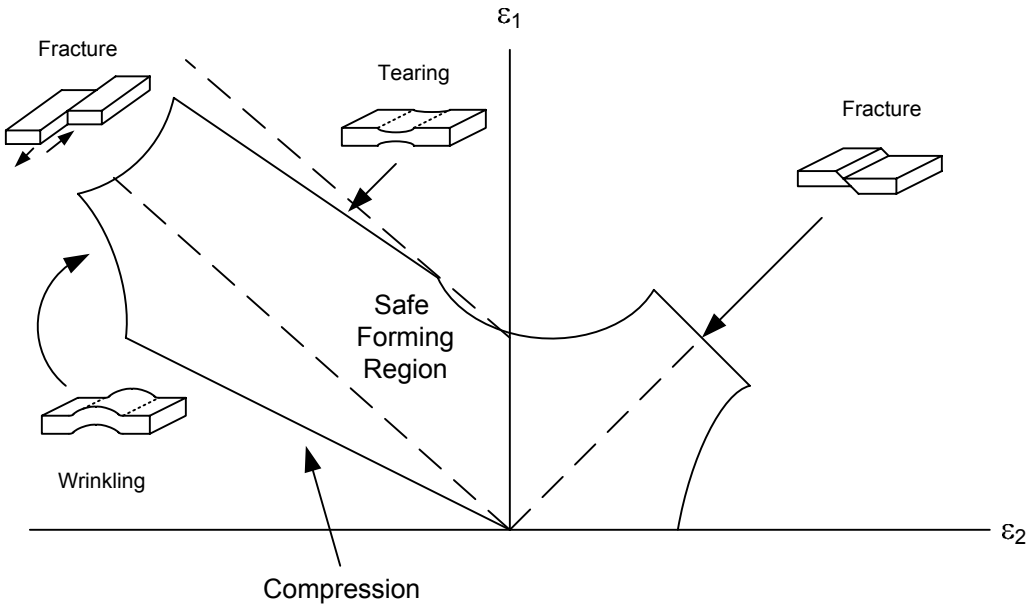

Figure I-1. Four Bi-axial Membrane Strain Safe Forming Region

Strain levels below the tensile FLD are acceptable and strain levels above the tensile FLD exhibit strain localization (necking or shear bands of reduced thickness).

Figures I-2 and I-3 (Shi & Gerdeen 1991 [DIRS 182447], with the kind permission of Springer Science and Business Media) are examples of proportional-loading tensile FLD's for punch forming, including in-wall shear and bending. These particular figures study the effects of sheet thickness and forming radius.

The Shi and Gerdeen [DIRS 182447] study addressed eight different forming parameters. The material is generally weakest in major strain, ε_1, for nearly plane strain loading (minor strain, ε_2, near zero) and increases in strength dramatically with triaxiality. Notably, bending has a small effect and the thicker sheets have greater strength, trends that are expected to continue to the wall and lid thicknesses of the OCB.

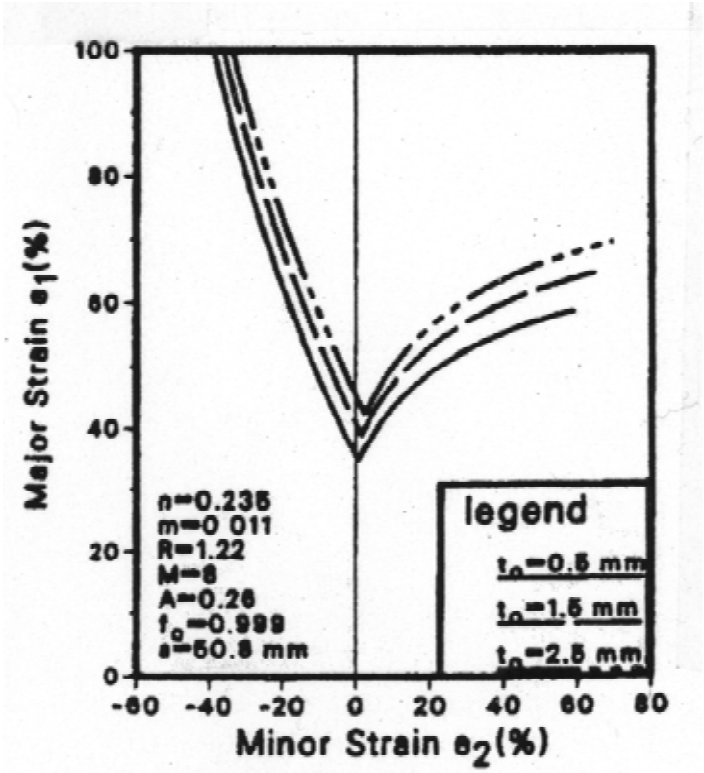

Figure I-2. Effect of Thickness (from Shi & Gerdeen 1991 [DIRS 182447], by permission)

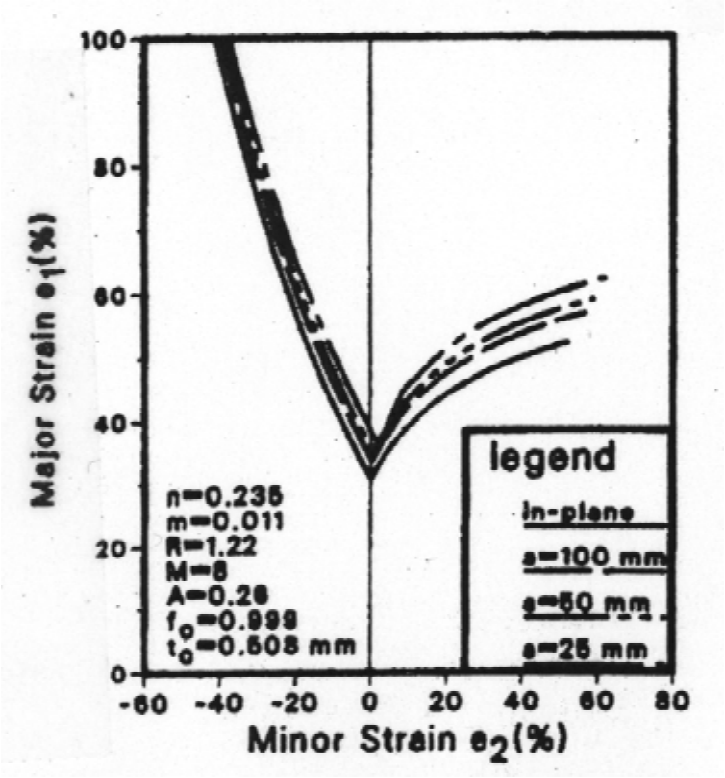

Figure I-3. Effect of Forming Radius (from Shi & Gerdeen 1991 [DIRS 182447], by permission)

The triaxiality adjustment sought is the ratio of the effective instability strain considering triaxiality to the tension test effective strain at instability. The effective strains used are Von Mises membrane strains, ignoring the bearing strains and shear strains. The effective strain is therefore $(\varepsilon_1^2 - \varepsilon_1\varepsilon_2 + \varepsilon_2^2)^{1/2}$. The (uniaxial) tension test has $\varepsilon_2 = -\nu\varepsilon_1$, where ν is Poisson's ratio. ε_1 at the tension test instability is the uniform strain.

Figure I-4 illustrates the graphical construction of the triaxiality adjustments for equal-positive-biaxial cold forming. This particular FLD study is for strain rate effects.

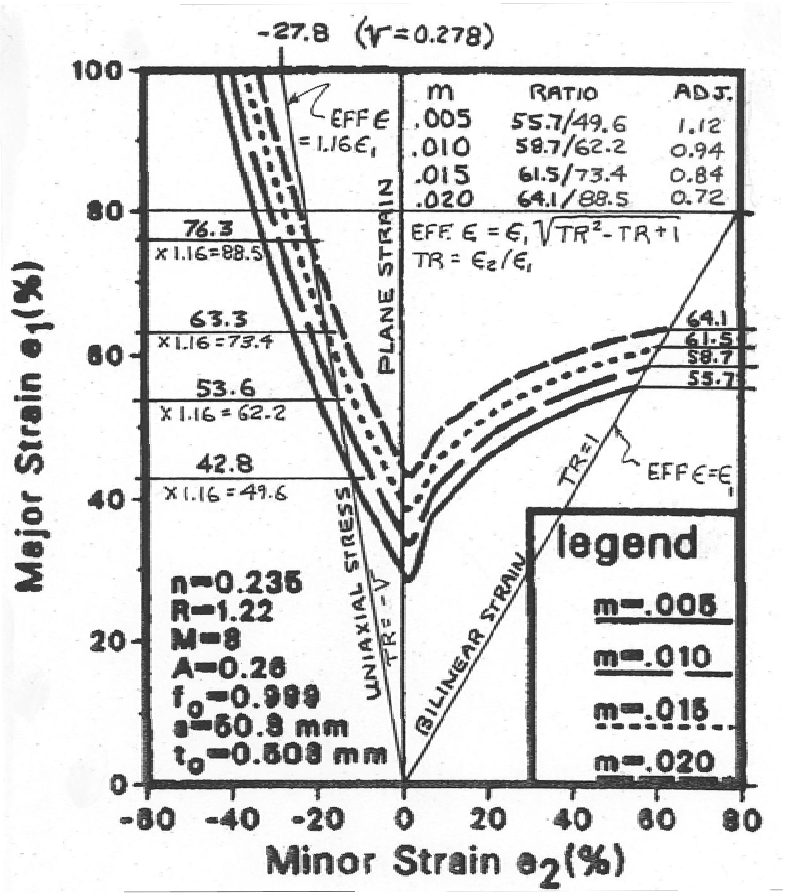

Figure I-4. Effect of Strain Rate (from Shi & Gerdeen 1991, [DIRS 182447] by permission)

Graphical constructions were performed on all eight of the Shi and Gerdeen parameter studies. Fixed triaxiality ratios, TR, between ε_1 and ε_2 ($TR = \varepsilon_2/\varepsilon_1$) allows the adjustment derivations, based on effective strains, to use only the ε_1 values. TR = 1 is a positive equal bilinear strain state and $TR = -\nu$ is consistent with a tension test uniaxial stress state. The Von Mises effective membrane strain (EFF ε) for any TR value is:

$$\text{EFF } \varepsilon = \varepsilon_1 (TR^2 - TR + 1)^{1/2} \qquad \text{Equation I-1}$$

or

$$\text{EFF } \varepsilon = VM \cdot \varepsilon_1 \qquad \text{Equation I-2}$$

Where

$$VM = (TR^2 - TR + 1)^{1/2} \qquad \text{Equation I-3}$$

In LS-DYNA, the uniaxial true stress-strain curve is used with a Von Mises flow criterion. Therefore, the triaxiality adjustment is based on the ratios of Von Mises strains on the FLD plots. The FLD ε_1 values are converted to EFF ε values and the ratio to the uniaxial test EFF ε value defines the triaxiality adjustment, ADJ.

Table I-1 is the adjustment spread for seven of the Shi and Gerdeen studies (self-heating, initial imperfections, anisotropy, strain rate, yield surface shape, punch curvature and thickness) over the full ranges (data for M = 2 and M = 10 were ignored as not applicable for ductile metals). These parameters have only a small affect on the triaxiality adjustment for equal-positive-biaxial cold forming. The spread of all adjustments were less than 0.40, and most were less than 0.25.

Table I-1. Equal Bi-axial Adjustments

Parameter [Default Value: Bi-axial Adjustment]	Value Range	Equal Bi-axial Adjustment Min/Max
Bending induced thermal softening term, A [0.26: 0.96]	0.0 and 0.26	0.74 / 0.96
Initial imperfection, f_o [0.999: 0.89]	0.9900 to 0.9995	0.74 / 0.95
Anisotropy, R [1.22: 0.90]	0.5 to 10	0.86 / 0.93
Strain rate, m (see Figure I-4) [0.011: 0.92]	0.005 to 0.020	0.72 / 1.12
Yield surface shape, M [8: 0.95]	6 to 8*	0.95 / 1.27
Bend radius, a (see Figure I-3) [50.8: 0.93]	25 *mm* to flat	0.88 / 0.97
Thickness, t_o (see Figure I-2) [0.508: 0.90]	0.5 *mm* to 2.5 *mm*	0.77 / 0.91

* Note—range for high-strength alloy steels (data for M = 2 and M = 10 omitted).

The spread of adjustments reduce considerably for plane strain and negative biaxial cold forming. For plane strain forming (see Figure I-4), the adjustment spread by strain rate was between 44.2/88.5 = 0.5 (for m = 0.020) and 30.1/49.6 = 0.6 (for m = 0.005), only 0.1, compared to the 0.4 spread for the equal-positive-bilinear case.

The default parameter values used by Shi and Gerdeen [DIRS 182447] that are listed in Table I-1 provide adjustments near the center of the adjustment spreads, and will have only small affect on the total adjustment. Therefore, these default parameter values are used for Alloy 22.

The eighth parameter, the classical power law strain hardening coefficient (see Equation I-4), n has significant affect on the triaxiality adjustment for equal-positive-biaxial cold forming. See Figure I-5. The triaxiality adjustments for "n" (between n = 0.10 and n = 0.35) has a large spread from 0.69 to 1.67. The n = 0.05 case is ignored because it does not exhibit tensile instability.

$$\sigma = A \cdot \varepsilon^n \qquad \text{Equation I-4}$$

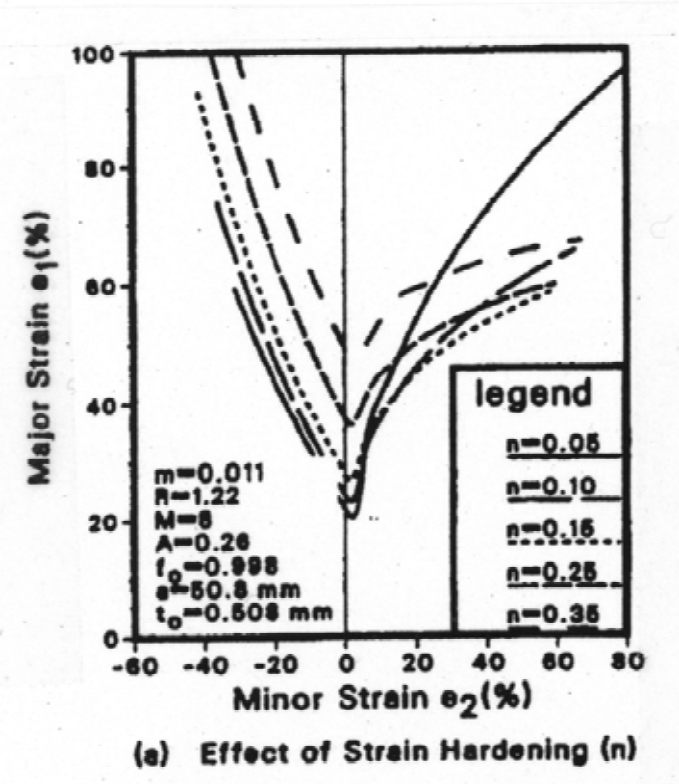

Figure I-5. Effect of Strain Hardening (from Shi & Gerdeen 1991 [DIRS 182447], by permission)

This indicates that the triaxiality adjustment is very sensitive to "n," which is related to the steepness of the stress-strain curve in the plastic region. It is clear that an "n" value near that for Alloy 22 must be used.

The value of "n" is determined graphically to be 0.26 from a power-law trend curve between the flow stress and UTS for "best fit" uniaxial stress-strain data for Alloy 22. "Best fit" refers to the best match (Test ARC22-4 [DIRS 182447]) of the project Alloy 22 data to the vendor average values. Table I-2 calculates the averages of vendor "typical" values.

The selected test yield stress is 47 *ksi* versus 52 *ksi* for the vendor average, the test UTS is 108 *ksi* versus 111 *ksi* for the vendor average and the test elongation is 66% versus the 64% vendor average. The engineering and true stress-strain curves for this RT test data are shown in Figure I-6 along with the power law trend curve. The higher curve is the true stress-strain curve up to the UTS.

Table I-2. Alloy 22 Vendor Typical Properties

Source	Yield, *ksi* (*MPa*)	UTS, *ksi* (*MPa*)	Elongation (%)
Special Metals 2006 [DIRS 182449], page 2, Table 4, 0.25" to 1.75" Plate)	53 (365)	112 (772)	62
Haynes 1997 [DIRS 100896], page 15, 0.25" to 0.75" Plate	54 (372)	114 (786)	62
Inco 1995 [DIRS 182441], Page 1, Table 3, 0.5" Plate	48 (330)	106 (733)	69
Average =	52 (356)	111 (764)	64

The Shi and Gerdeen FLD [DIRS 182447] for n = 0.25, with all other parameters at default values in Figure I-5 is used to determine the triaxiality adjustment on the uniform strain value, which, in turn is used to convert engineering stress-strain to true stress-strain. Table I-3 is the adjustment needed (ADJ) versus the triaxiality ratio, TR. Figure I-7 is a smoothed curve plot of the ADJ versus TR values.

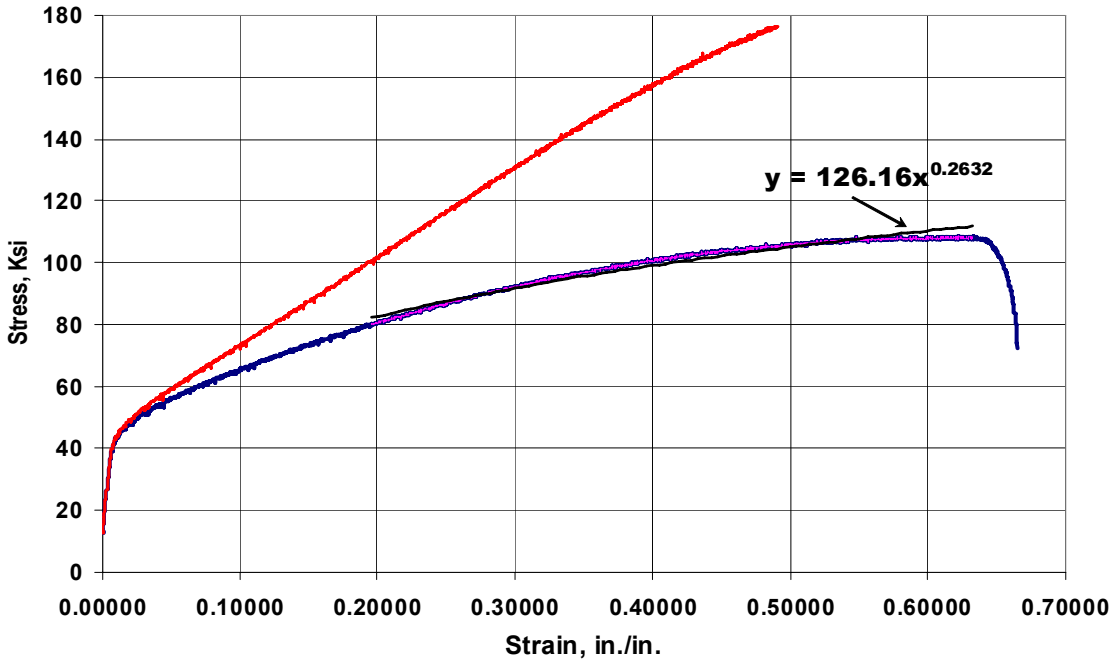

Figure I-6. Alloy 22 Stress-Strain Curve

Table I-3 and Figure I-7 show the triaxiality adjustment (ADJ) versus the triaxiality ratio (TR).

Table I-3. Triaxiality Adjustment

TR	ADJ	TR	ADJ
-0.4	1.920	0.3	0.650
-0.3	1.053	0.4	0.664
-0.2	0.810	0.5	0.670
-0.1	0.643	0.6	0.697
0	0.550	0.7	0.732
0.05	0.519	0.8	0.779
0.1	0.541	0.9	0.828
0.2	0.598	1.0	0.885

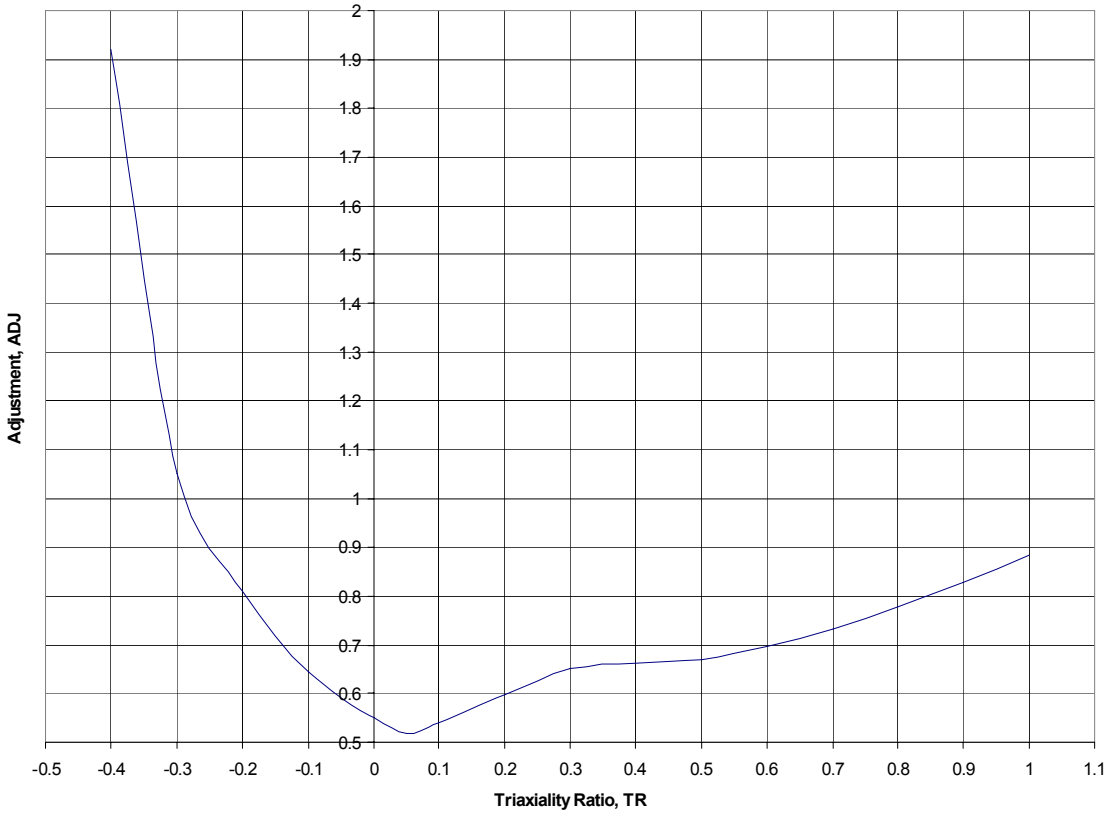

Figure I-7. Triaxiality Adjustment

The uniform strain for this uniaxial stress data is the engineering strain value of 0.63 at the maximum stress (UTS) on the lower curve of Figure I-6. A slight adjustment based on vendor average versus test elongation (64.0/66.0) gives a RT uniform strain value, $e_u = 0.61$, for the vendor average data.

The triaxiality-adjusted vendor-averaged true-uniform-strain, ε_u', is defined by:

$$\varepsilon_u' = \ln(1 + ADJ \cdot e_u) \qquad \text{Equation I-5}$$

Or

$$\varepsilon_u' = \ln(1 + 0.61 \cdot ADJ) \qquad \text{Equation I-6}$$

The triaxiality-adjusted vendor-averaged true-ultimate-stress, σ_u', is defined by:

$$\sigma_u' = S_u \cdot (1 + ADJ \cdot e_u) \qquad \text{Equation I-7}$$

Or

$$\sigma_u' = 111 \cdot (1 + 0.61 \cdot ADJ) \; ksi \qquad \text{Equation I-8}$$

Or

$$\sigma_u' = 764 \cdot (1 + 0.61 \cdot ADJ) \; MPa \qquad \text{Equation I-9}$$

Recent research (Stoughton 1999 [DIRS 182452]) indicates a serious limitation of the strain-based FLD's is that the strain paths must be linear (i. e., proportional to loading). This characteristic will be assessed in the structural dynamic calculations.

A stress-based FLD (Stoughton & Zhu 2004 [DIRS 182453]) has no dependence on the strain paths and the triaxiality has minimal effects on the major true stress at the onset of tensile instability. If and when further development on this is completed for OCB representative materials, and relationships of the instability level to the uniaxial flow or ultimate stresses are better defined, the stress-based FLD triaxiality approach may replace the strain-based FLD triaxiality approach.

I-3.1 Treatment of Triaxiality

A precursor analysis is run that uses best estimate bilinear true stress-strain curves (see Section 7.1.5) for all waste package components. The analysis is at a loading that results in the OCB governing location effective (Von Mises) wall-averaged strain near the triaxiality-adjusted true uniform strain value (tensile instability level). This requires an iterative solution and post-processing effort. The amount of triaxiality affects the tensile instability level and the Tangent Moduli of the bilinear solution.

Experience has shown that the triaxiality has the strongest effect on the targeted load level and, that for most event sequences; the triaxiality varies significantly near the governing location. Using the worst case triaxiality (i.e., TR = 0.05, ADJ = 0.519) will usually lead to the fastest

convergence of the targeted load level, and a simplified conservative evaluation can be performed using the worst-case triaxiality (WCT). This conservative use of WCT would also preclude the need to access the proportional loading character discussed in the previous section. Only the OCB material stress-strain curve is adjusted for triaxiality.

The use of a wall-section element average is identical to the wall average only if the elements are all the same size. If not, an element weighting by element volume must be performed.

The term "best-estimate" refers to the use of the average of the Alloy 22 vendors' published "typical" material strength and elongation values. The term "best estimate" for the other waste package materials will be based on a simplified 10% increase in Code minimum strength and elongation values.

The Triaxiality Ratio, TR, at the OCB governing location can be conservatively used to be the WCT (TR = 0.05) or determined based on the ratio of the minor in-plane membrane (wall-averaged) strain to the major in-plane membrane (wall-averaged) strain. These are not necessarily the principal membrane strains, and, if the governing wall section is not in a global axes orientation, the global X, Y and Z direction strains must be resolved into in-plane contributions. The TR vs. ADJ values from Table I-3 may be linearly interpolated to derive σ_u' and ε_u'.

I-3.2 Tri-linear Materials Representation

The Demand calculation uses the LS-DYNA explicit FEA solver and a best-estimate triaxiality-adjusted tri-linear material model (see Figure I-8) for the OCB and non-adjusted best-estimate bilinear material models for the other components.

The third stage of the OCB material model, at true strains above the triaxiality-adjusted uniform strain, has no strain hardening. The true stress–true strain curve in this region is horizontal which introduces a tensile instability if an entire wall section is loaded to this level. This will be evidenced by computationally large deformations for a small increase in loading or solution failure due to numerical instability. This is illustrated in a simplified form in Figure I-9, where the FER elements in red have reached the horizontal part of the curve and cannot, in and of themselves, bear any additional load. Additional load must be borne by the surrounding elements. If an LS-DYNA solver option for material voiding could be invoked (material voiding constants for Alloy 22 are currently not available), additional loading will include a local-necking Tensile-Instability breaching failure.

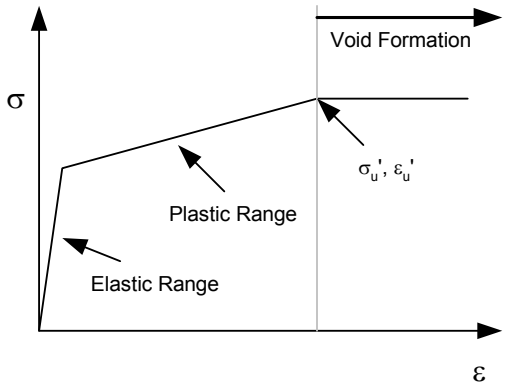

Figure I-8. Tri-linear Stress-Strain Curve

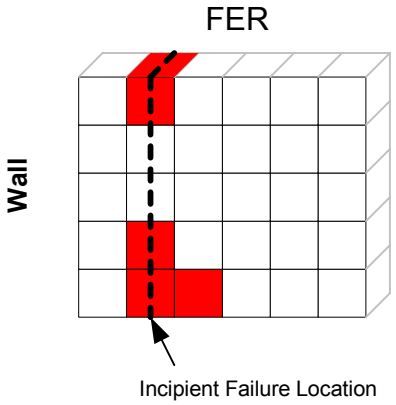

Figure I-9. Incipient Failure

Figure I-10 provides best-estimate RT Alloy 22 tri-linear curves for the triaxiality cases of equal positive biaxial strain (TR = 1), plane strain (TR = 0) and uniaxial strain (TR = -ν, no adjustment). Stress is shown in *psi*.

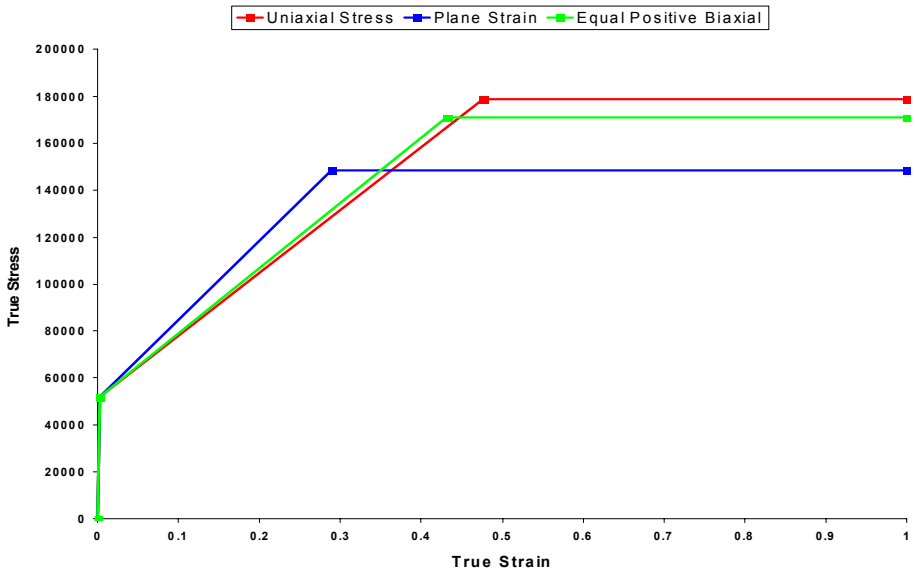

Figure I-10. Alloy 22 Tri-linear Material

This macro-mechanics FEA Demand prediction approach was used (in bilinear form—the elastic response region was ignored) for LS-DYNA 3D dynamic plastic failure analyses by Mitsubishi Heavy Industries Ltd., where it was successfully benchmarked against actual ship collisions (Kuroiwa 1996 [DIRS 182174] and Kitamura 1997 [DIRS 182666]). It was also implemented for ABAQUS plastic failure analyses at the Bettis Atomic Power Lab, where it was successfully benchmarked against Pressure Vessel Research Council burst disk tests (Jones & Holliday 2000 [DIRS 182173]).

I-3.3 Alternate Methodologies Considered

Other examples of macro-mechanics FEA elastic-plastic failure approaches were considered that are being used in the shipping industry (Lehmann & Yu 1998 [DIRS 182668], Simonsen & Lauridsen 2000 [DIRS 182448], Kitamura 2002 [DIRS 182442], Le Sourne, et al., 2003 [DIRS 182444], and Wang, et al., 2006 [DIRS 182141]), in the Civil structures industry (Schafer, et al., 2000 [DIRS 182178], Brooker 2003 [DIRS 182158], Haukaas, et al., 2005 [DIRS 182165], Haukaas 2006 [DIRS 182166]), in the metal forming industry (Sriram, et al., 2002 [DIRS 182450]), in the automobile crashworthiness area (Feucht, et al., 2006 [DIRS 182118]), and in the nuclear industry (Zimmer et al.,1991 [DIRS 182175] and ACNW 2006 [DIRS 182673]).

Some use adaptive meshing that varies through the simulation. Most use user-developed subroutines on explicit FEA solver codes. Others use eroding elements that are fully removed from the solution upon reaching a defined failure state. These failure states are often based on non-linear analyses of coupon test data. These studies are focused on the final size of openings. The yield surface and the size and orientation of the meshing have a very significant influence on these predictions, and the selected approach usually needs test data to establish their adequacy (e.g., finer meshes are not always better).

The Capability of the OCB is conservatively and more easily defined by the elemental loss of additional load carrying ability upon initiation of voids. The difficult-to-predict void growth, coalescence, and bifurcation behavior is then inconsequential. The high ratio of uniform strain to elongation in Alloy 22 makes the conservatism minimal. The alternate use of eroding elements initiates unrealistic element-wide crackings on the outer surface and near-instantaneous through-wall failure.

A test-derived empirical approach (Wang 2002 [DIRS 182142]) is clearly impractical lacking prototype waste package test-to-failure data. The remaining alternative approach considered is the micro-mechanics imbedded FEA approaches. There have been a number of researcher-developed improvements on the basic Gurson-Needleman-Tvergaard (GNT) and Johnson-Cook material models available in LS-DYNA (Material Numbers 15, 98, 99 and 120) to provide variable state- and rate-dependent voiding simulations and strain-localization behavior in complex three-dimensional structures.

Unfortunately, the commercial LS-DYNA does not offer a coupled thermo-mechanical option. The Evolving Microstructure Model of Inelasticity (EMMI) being developed at Sandia (Horstemeyer 2000 [DIRS 182169], Sandia 2005 [DIRS 182672]) for predicting void initiation of metals with temperature and rate effects—based on an improved Bammann-Chiesa-Johnson (BCJ) formulation—is promising. These and other developments of improved microstructural FEA approaches might eventually provide sophisticated treatments of void formation (and coalescence to bifurcation). However, the required test-based material constants take time to develop, and are not currently available for Alloy 22.

I-3.4 Other Structural Analysis Considerations

Local metal temperatures at the failure location increase significantly due to the large magnitude and high rate of plastic flow preceding failure. This makes the choice of starting temperature less significant because it has only a small effect on the much higher temperature (and temperature-dependent material strength) in the failure zone.

Performance calculations at assumed uniform constant temperature have been reviewed. These consistently indicate that the governing membrane stress damage (the Tresca stress ratio to true tensile strength) is temperature insensitive in the Alloy 22 OCB (but not so in the 316 SS inner vessel). Therefore, the choice of uniform room temperature properties for the risk-informed approach is reasonable as well as practical (i.e., there is a larger room-temperature property database versus elevated temperature property database).

High strength alloys typically display only moderate (10 to 20%) toughness increase (Nicholas 1980 [DIRS 154072]) at the anticipated failure level membrane strain rates (50 to 100 s^{-1}). Material ductility implied by elongation values is only mildly affected (elongations are within 10%) at these strain rates. The increased yield stress and strain hardening at higher strain rates increases the toughness and the increased stiffness reduces the strain localization (necking) under membrane loading.

Strain rate tensile data is not available for Alloy 22, and must be developed, specifically for the effect on the uniform strain value. Enveloping studies (BSC 2007 [DIRS 182357]) of a drop

event over a range of assumed Alloy 22 strain-rate dependent material properties, including ultimate true stress 15% greater than the static value, indicated an insignificant (less than 1%) effect on the governing membrane stress damage. There is an offsetting effect between the material response and capability. Until data is available, there is no choice but to use static properties.

Data scatter uncertainty in material strength and ductility (resulting in a probabilistic distribution of the Capacity) is addressed using a correlation to plastic strain energy dissipation, which is related to the material's toughness. The Toughness Index (I_T) used in this correlation is the flow stress multiplied by the uniform strain. The flow stress is the average of the yield strength, σ_y, and the ultimate strength, σ_u, and the uniform strain is the strain at ultimate strength. Stress and strain values are true stress-strain values. The Capacity levels are correlated to this Toughness Index for a finite number of simulations with different strength and ductility properties.

$$I_T = \tfrac{1}{2}\, \varepsilon_u\, (\sigma_y + \sigma_u) \qquad \text{Equation I-10}$$

I-3.5 Treatment of Other Components

Only the OCB is modeled with tensile instability. The remainder of the engineered structures (which includes the inner vessel, waste form canister, waste form, invert, adjacent facility and equipment surfaces, emplacement pallet, enclosures, etc.) are modeled with simplified conservative characteristics in regard to the OCB stress levels. This will be case specific. Examples are less energy absorbing, unyielding impact surfaces such as floors, emplacement pallet or drip shield. The goal is to prevent numerical instability of the other engineered structures, which would preclude determining the sought failure response of the OCB.

However, reviews of the results will be conducted to be certain that detrimental changes in the local loading of the OCB will not exist under more realistic deformations (and possible failures) of the other engineered structures. In those cases, the other engineered structures will be more realistically modeled, including the use of eroding elements.

It is planned to use the same worst-case geometric orientations and boundary conditions that are being used in the deterministic solutions. The logic is that load levels beyond the design basis will simply exacerbate the damage at the governing highest stressed OCB locations without changing the governing locations.

Mass, damping and friction variability are considered minor contributors to Demand variability and will be ignored.

The adequacy of the mesh refinement will be based on the current mesh-discretization procedure; however, further mesh refinement in the higher stressed locations may be required to complete the failure analyses due to poorly shaped element geometry as the distortions become large.

INTETIONALLY LEFT BLANK

APPENDIX II

II-1 UNCERTAINITIES OF STRUCTURAL ANALYSIS

In the past interactions with the NRC (Kelmenson 2000 [DIRS 154350]) sources of uncertainty and variability affecting structural analyses were discussed. This particularly dealt with finite element analysis representations and the failure criterion for waste package structural analyses. Six other areas considered were:

1. Residual and differential thermal expansion stresses
2. Strain-rate effects
3. Dimensional and material variability
4. Seismic effect on ground motion
5. Initial tip-over velocities
6. Sliding and inertial effect of waste package contents.

At this time, additional uncertainties have not been identified. As the design progresses, any additional uncertainties that are identified will be addressed as part of the design process. These identified uncertainties will be documented within documents supporting the LA. This interaction with the NRC reflects previous designs and it has been suitably addressed in the main body of the report.

Finite Element Analysis Discretization and Failure Criterion—With regard to the adequacy of finite element analysis representations, a process has been developed to ensure that the mesh density is computationally adequate, and this process is followed for all structural calculations. The failure criterion is an application of the Tresca (strength of materials) failure criterion based on the implementation of ASME B&PV Code (ASME 2001 [DIRS 158115]) design-by-analysis primary stress intensity limits. A tiered evaluation approach was implemented that used increasingly less simplified, and increasing less conservative screening criterion whose satisfaction will assure meeting the ASME B&PV Code (ASME 2001 [DIRS 158115]) primary stress intensity limits.

For the six specific areas of uncertainty concerns, the responses are summarized as:

Residual and Differential Thermal Expansion Stresses—Differential thermal expansion is accommodated by providing adequate gaps between the two shells (OCB and IV) that comprise the WP to ensure that there is no mutual loading due to thermal expansion. For residual stresses purposefully imposed on the OCB, the effects on structural analysis results are found to be negligible.

Strain-rate Effects — While material-specific strain-rate dependent properties are not currently available for Alloy 22 and 316 SS, parametric studies of such effects based on 304 SS strain-rate

dependent properties have shown that the use of static properties has negligible effect on the safety assessment.

Dimensional and Material Variability — Dimensional variability is addressed by assuming minimum dimensions for those parameters that are important to component performance. Material variability is accommodated by the use of ASME B&PV Code (ASME 2001 [DIRS 158115])—and other codes as necessary—structural properties, which provide for minimum structural performance margins.

Seismic Effect on Ground Motion — In the surface facility, in the TEV, it is assumed that the fixturing is provided to restrain the waste package during evolutions in that facility, and these devices are sufficient to provide restraint during vibratory ground motion. For vibratory ground motion in the underground, results are provided for a seismic evaluation for an annual frequency of exceedance of $5x10^{-4}$ per year. These results show a very modest waste package movement and large margin to breach.

Sliding and Inertial Effect of Waste Package Contents — The waste form contents are represented in dynamic structural analyses for which such motion is anticipated to be important. Examples of the loads and boundary conditions used in calculations and analyses can be found in the supporting calculations (BSC 2001 [DIRS 152655]; BSC 2003 [DIRS 161691]; BSC 2004 [DIRS 167083]; BSC 2004 [DIRS 169705]; BSC 2003 [DIRS 165497]). In addition, the technical bases and or rationale for the loads and boundary conditions used in calculations supporting the license application will be based on the preclosure safety analysis and derivative design constraints.

II-2 RESPONSE TO GENERAL ISSUE OF ADEQUACY

This section addresses the adequacy of the finite element analysis mesh discretization and the failure criterion.

II-2.1 Mesh Discretization

A set process is followed in the development of the mesh for finite element analysis that provides confidence that the results are stationary in a numerical sense (see Section 7.1.3).

The purpose of mesh refinement is to ensure the mesh objectivity of the finite element analyses, i.e., that the results obtained are not mesh-sensitive. The basis for the validity of this process of successive refinement is that it has been found to produce convergent stress fields in a systematic manner. The acceptable variations in the stress fields are well within the benchmarking basis for the LS-DYNA code [DIRS 166918]. A mesh-refinement study consists of the development of an optimum mesh that yields mesh-objective (mesh-insensitive) results. That mesh is then refined again, and computational results for the two mesh sizes are compared. The finite element representation is considered mesh-objective if the relative difference in results (e.g., stresses) between the two meshes is approximately an order of magnitude smaller than the relative difference in mesh size in the region of interest; otherwise further mesh refinement is needed. The mesh size, as used throughout this section, refers to the volume or the area of the representative element (three-dimensional or two-dimensional, respectively) in the region of interest (for example, the element characterized by the highest stresses or strains).

The optimum mesh is created by the following sequence of steps:

- The initial mesh is created by following the customary engineering practices: the element type is appropriately chosen; the mesh is refined in the regions of interest (the highest stress/strain regions, initial impact regions, stress concentration regions, etc.); the mesh is mapped whenever possible; and the aspect ratio of elements is kept reasonable.

- The initial mesh is—in the region of interest—refined in one direction while the element size in the other two directions is kept unchanged (for example, the mesh is refined across the thickness while kept unchanged in the hoop and axial directions). The mesh-refinement procedure is repeated in this manner until the relative difference in results between the two successive meshes is acceptable (i.e., approximately an order of magnitude smaller than the relative difference in the mesh size). The mesh dimension in this direction is then fixed at the largest value that satisfied the previously mentioned criterion.

- The intention of this one-direction-at-a-time mesh refinement is to create, in a consistent and systematic manner, a mesh that is objective.

- The same procedure is consecutively repeated in the remaining two directions.

- Whether the created mesh meets the requirement is verified by the final step: the simultaneous mesh refinement in all three directions. The level of this mesh refinement should be similar in all three directions. In this final step, the same mesh-acceptance criterion is invoked: the mesh is considered objective if the relative difference in results (e.g., stresses) between the two meshes is approximately an order of magnitude smaller than the relative difference in mesh size in the region of interest.

It should be emphasized that the mesh objectivity is verified by the final step regardless of whether the final mesh is arrived at by the described one-direction-at-a-time mesh refinement or not. The one-direction-at-a-time mesh refinement is optional since its only purpose is to develop an optimum mesh (that satisfies the mesh-objectivity requirement) in a systematic way.

An example of the implementation of this mesh discretization approach may be found in the calculation entitled *44-BWR Waste Package Tip-Over from an Elevated Surface* (BSC 2004 [DIRS 169705]). While all calculations perform such discretization studies, this calculation is selected because it is the vehicle cited in the balance of this section to assess the importance of strain rates and initial tip-over velocities.

II-2.2 Selection of the Failure Criterion

For structural analyses of preliminary designs that consider material nonlinear behavior, the maximum-shear-stress or Tresca (strength of materials) criterion is used in determining stress limits. In general terms, this criterion presumes that the design is safe as long as stress intensity

(defined as the difference between the maximum and minimum principal stress) remains below a certain limit. In particular, the failure criterion chosen was the acceptance criteria for plastic analysis outlined in Appendix F, F-1341.2 of the ASME B&PV Code (ASME 2001 [DIRS 158115] Section III, Division 1, Appendix F). This is an acceptable vessel designer choice of ASME B&PV Code acceptance criteria for service loadings with Level D Service Limits for vessel designs in accordance with NC-3200 (Safety Class 2 Vessels) when a complete stress analysis is performed. (See ASME 2001 [DIRS 158115], NC-3211.1(c), Appendix XIII and Note (4) to Table NC-3217-1).

The ASME B&PV Code (ASME 2001 [DIRS 158115], Section III, Division 1, Appendix F, F-1341.2) suggests the following primary stress intensity limits for plastic analyses:

- The general primary membrane stress intensity shall not exceed 0.7 S_u for ferritic steel materials included in Section II, Part D, Subpart 1, Table 2A and the greater of 0.7 S_u and $S_y + {}^1/_3 (S_u - S_y)$ for austenitic steel, high-nickel alloy, and copper-nickel alloy materials included in Section II, Part D, Subpart 1, Table 2A, where S_u and S_y are tensile strength and yield strength, respectively.

- The maximum primary stress intensity at any location shall not exceed 0.9 S_u.

The Pressure Vessel Research Council of the Welding Research Council has provided recommended guidelines (Hechmer and Hollinger 1998 [DIRS 166147]) to the ASME B&PV Code rule committees for assessing stress results from three-dimensional finite element analysis in terms of ASME B&PV Code (ASME 2001 [DIRS 158115], stress limits in the design-by-analysis rules of Section III (Class 1, NB) and Section VIII, Division 2). These guidelines were developed for linear analyses and Pressure Vessel Research Council recommends that future research work should be conducted to generate state-of-the-art guidelines for applying inelastic, large-deformation analyses. Therefore, a cautious use of the Pressure Vessel Research Council recommendations was made in developing methodologies for post-processing LS-DYNA nonlinear plastic simulations to assure conservative representations of the general primary membrane stress intensity and maximum primary stress intensity.

The Pressure Vessel Research Council recommendations also refer to an earlier Pressure Vessel Research Council (Phase 1) report that recommended ASME B&PV Code (ASME 2001 [DIRS 158115]), Appendix F "should be revised to provide a limit on effective plastic strain which is more appropriate for events that are energy controlled, rather than load controlled, which is all that was considered when ASME B&PV Code Appendix F was written." The YMP recognizes that strain-based or deformation-based criterion may be more appropriate than stress-based limits for evaluation of the credible preclosure event sequences (see Section 4.1.3.1). However, the project is also committed to applying the ASME B&PV Code for structural analyses, and until the ASME B&PV Code rule committees prepare rules in ASME B&PV Code Appendix F for using strain limits, primary stress intensity limits will be used.

The ASME B&PV Code (ASME 2001 [DIRS 158115]) design-by-analysis guidance recognizes the differences in importance of different types of stresses and provides guidance on their correct assignment to the different categories of stress intensity used to evaluate different types of failure modes. The three types of stresses are membrane, bending and peak stresses. The three

categories of stress intensity are primary (P_m, P_L and P_b [general primary membrane, local primary membrane, and primary bending, respectively]), secondary (Q), and peak (F).

A primary stress is defined in ASME B&PV Code (ASME 2001 [DIRS 158115], Section III, Division 1, Appendix XIII) XIII-1123(h): "Primary stress is a normal stress developed by the imposed loading which is necessary to satisfy the laws of equilibrium of external and internal forces and moments. The basic characteristic of a primary stress is that it is not self-limiting. Primary stresses which considerably exceed the yield strength will result in failure or, at least, in gross distortion."

A secondary stress is defined in ASME B&PV Code (ASME 2001 [DIRS 158115], Section III, Division 1, Appendix XIII) XIII-1123(i): "Secondary stress is a normal or a shear stress developed by the constraint of adjacent parts or by self-constraint of the structure. The basic characteristic of a secondary stress is that it is self-limiting. Local yielding and minor distortions can satisfy the conditions which cause the stress to occur and failure from one application of the stress is not expected." A cited example of a secondary stress is "bending stress at a gross structural discontinuity." A gross structural discontinuity is defined in ASME B&PV Code (ASME 2001 [DIRS 158115], Section III, Division 1, Appendix XIII) XIII-1123(b): "Gross structural discontinuity is a source of stress or strain intensification which affects a relatively large portion of a structure and has a significant effect on the overall stress or strain pattern or on the structure as a whole." Cited examples of gross structural discontinuities are head-to-shell junctions and junctions between shells of different thickness.

A local primary membrane stress is also defined in ASME B&PV Code (ASME 2001 [DIRS 158115], Section III, Division 1, Appendix XIII) XIII-1123(j): "Cases arise in which a membrane stress produced by pressure or other mechanical loading and associated with a discontinuity would, if not limited, produce excessive distortion in the transfer of load to other portions of the structure. Conservatism requires that such a stress be classified as a local primary-membrane stress even though it has some characteristics of a secondary stress." The other differentiating feature of a local primary membrane stress is that it is localized, and ASME B&PV Code (ASME 2001 [DIRS 158115]) guidance is provided for evaluating if membrane stress fields are adequately "local" to be assigned a P_L classification rather than a more restrictive P_m classification.

Per Pressure Vessel Research Council recommendations (Hechmer and Hollinger 1998 [DIRS 166147], Guideline 1) the failure mode being addressed by the general primary membrane stress intensity (P_m) limit is "collapse" in the sense that collapse includes tensile instability and ductile rupture under short term loading. The principle failure mode being addressed by the maximum primary stress intensity ($P_L + P_b$) is excessive plastic deformation. However, it also relates to tensile instability due to the nature of P_b.

The event sequences considered in this report are not repetitive where fatigue cracking or incremental collapse might be an issue. It follows that evaluation of secondary stress intensities (Q) or maximum total stress intensities ($P_L + P_b$ + Q + F) are not appropriate. Brittle fracture is also precluded by the high ductility of the outer boundary material, Alloy 22, at the temperatures experienced after waste form loading. Although the high-stress areas are comprised of primary, secondary and peak stresses, only the primary stress intensities (P_m, P_L and P_b) contribute to

plastic instability (tensile tearing) or excessive plastic deformation, and therefore, only the primary stress intensities are evaluated for the event sequences.

Use was also made of the stress classification guidance in the ASME B&PV Code (ASME 2001 [DIRS 158115], Section III, Division 1, Appendix XIII) Table XIII-1130-1 to determine which stress fields should be classified as primary and which should be classified as secondary when evaluating the event sequences. It was decided to conservatively classify all membrane stress fields as primary. Classification of the bending stresses was more involved.

Review of representative analyses for the event sequences indicated that the most significant wall-bending stresses in the outer corrosion barrier were occurring near gross structural discontinuities. Some of these gross structural discontinuities were integral to the outer boundary and some were introduced by the constraint of adjacent parts or impact surfaces.

The integral gross discontinuities in the outer corrosion barrier are similar to Code vessel details such as shell-to-lid junctures and step-changes in wall thickness. The bending stresses are being created by self-constraint, and Table XIII-1130-1 (ASME 2001 [DIRS 158115], Section III, Division 1, Appendix XIII) classifies these bending stresses as secondary. The only exception is at the shell-lid junction where concern about the predictability of the lid's central stresses leads the Code to caution the designer (ASME 2001 [DIRS 158115], Section III, Division 1, Appendix XIII, Note (4) of Table XIII-1130-1) to consider classifying the bending stresses as P_b. However, this is not appropriate guidance for inelastic analyses because the increased flexibility of the juncture due to inelastic behavior is correctly captured and the lid's central stresses are accurately predicted.

The bending stresses created by the constraint of adjacent parts or impact surfaces (which can be considered (temporary) "adjacent parts") were reviewed on individual cases with attention to the amount and type of constraint introduced. In the design analyses to date, the constraint of the adjacent part (e.g., upper and lower sleeves) or impact surface (e.g., emplacement pallet, crane hook or rock) created local yielding and minor distortions in the OCB. The outer corrosion barrier distorted shape reduced the outer corrosion barrier bending stresses while increasing the outer corrosion barrier membrane stresses. The bending stresses in these locally yielded regions are therefore self-limiting and satisfy the basic characteristic of a secondary stress.

The structural criterion developed for the outer boundary for the event sequences was to directly address the dominant failure mode, tensile instability, and limit the membrane stresses to acceptable limits. The use of inelastic analyses assures that local thinning or shape changes that could increase membrane stresses are properly accounted for.

The inelastic analyses were conducted using true stress (σ_u) and true strain based load/deformation relationships, therefore, per ASME B&PV Code (ASME 2001 [DIRS 158115], Section III, Division 1, Appendix F, F-1322.3(b) and F-1341.2), for Alloy 22:

The limit on P_m is $0.7\sigma_u$, and

the limit on P_L is $0.9\sigma_u$,where $P_b = 0$, and

σ_u is the true tensile strength at temperature.

As stated earlier, the ASME B&PV Code (ASME 2001 [DIRS 158115], Section III, Division 1, Appendix XIII, XIII-1123(j)) provides guidance on how "local" PL must not be classified as a more restrictive general primary membrane stress intensity, Pm. Interpretation of this guidance with respect to the Appendix F limits results in requiring PL values exceeding $0.77\sigma u$ to not extend for greater than $\sqrt{R \cdot t}$ in any direction (not just the meridianal direction), where R is the midsurface radius and t is the thickness of the OCB.

Rigorously performed, the calculation of the primary membrane stress intensities requires the following steps:

- Identification of the governing wall location (stress classification plane normal to the mid-plane of the shell or lid thickness) which may not necessarily contain the maximum stressed point (Hechmer and Hollinger 1998 [DIRS 166147], Guidelines 3 and 4)
- Identification of the orientation of the stress classification line (SCL), typically normal to the mid-plane of the shell or lid thickness (Hechmer and Hollinger 1998, [DIRS 166147], Guideline 4d).
- Identification of stress component ($\sigma_x, \sigma_y, \sigma_z, \tau_{xy}, \tau_{yz}, \tau_{zx}$) fields across the wall of the outer corrosion barrier
- Averaging of the stress component fields to create wall-averaged stress components
- Translation of these wall-averaged stresses to principle stress directions by solving a cubic equation
- Calculation of the difference between the maximum (σ_1) and minimum (σ_3) principle stress direction values.

To simplify the calculation, the wall-average of the element total stress intensity (twice the maximum shear stress) values through the outer corrosion barrier is used to define the primary membrane stress intensities. This is a conservative representation because it ignores the possible changing of the principle stress planes through the wall and includes the secondary and peak stress contributions.

To further simplify the calculation, tiered screening criteria are applied to the outer corrosion barrier finite element analysis results. The easiest to apply and most conservative criteria are applied initially. If these can not be met, less conservative screening criteria are imposed that require more calculations.

In the case of lifting analyses, the acceptance criteria are outlined in American National Standard for Radioactive Materials — Special Lifting Devices for Shipping Containers Weighing 10000 Pounds (4500 kg) or More (ANSI N14.6-1993 [DIRS 102016], Section 4.2.1.1). The load-bearing members of the lifting device shall be capable of lifting three times the combined weight of the shipping container, plus the weight of the intervening components of the lifting device, without generating a combined shear stress or maximum principal stress at any point in the device in excess of S_y and shall also be capable of lifting five times the weight without exceeding S_u.

II-2.3 Responses to Specific Issues

The following sections address the specific issues enumerated in Appendix II, Section II-1.

II-2.3.1 Residual and Differential Thermal Expansion Stresses

II-2.3.1.1 Differential Thermal Expansion

Differential thermal expansion is accommodated by providing adequate gaps between the inner vessel and outer corrosion barrier to ensure that there is no mutual loading due to thermal expansion. The required radial gap between the inner vessel and the outer corrosion barrier of the waste package is documented in a calculation entitled Waste Package Outer Barrier Stress Due to Thermal Expansion with Various Barrier Gap Sizes (BSC 2001 [DIRS 152655]). This calculation results in a minimum gap spacing between the inner vessel and outer corrosion barrier to accommodate radial expansion to be set at 1 mm (BSC 2001 [DIRS 152655], Tables 4 and 5, p. 13). The axial gap between the inner vessel and outer corrosion barrier and the lids of each is documented in a calculation entitled Waste Package Axial Thermal Expansion Calculation (BSC 2003 [DIRS 161691]). This calculation establishes a minimum axial gap of 1 cm between the inner vessel and outer corrosion barrier (BSC 2003 [DIRS 161691], Section 7, p. 13). A similar approach will be used to ensure clearance between the inner vessel of the waste package and the internals. These clearances are addressed in the two naval configuration drawings:

- *Naval Long Waste Package Configuration* (BSC 2007 [DIRS 180180]). Sheets 2 and 3 are found in BSC (2007 [DIRS 180183]) and BSC (2007 [DIRS 180184]), respectively.

- *Naval Short Waste Package Configuration* (BSC 2007 [DIRS 180187]). Sheets 2 and 3 are found in BSC (2007 [DIRS 180188]) and BSC (2007 [DIRS 180189]), respectively.

II-2.3.1.2 Effect of Residual Stresses

The waste package outer corrosion barrier is not in a stress-free condition at the beginning of service life due to residual stresses purposefully induced by solution annealing and quenching. The purpose of these residual stress fields is to create compressive residual stresses at the outside surface, and perhaps the inside surface as well (depending on the quenching techniques) of the outer corrosion barrier to help mitigate corrosion. The effect of this stress profile on the waste package during dynamic events is documented in a calculation entitled *Drop of Waste Package on Emplacement Pallet-A Mesh Study* (BSC 2003 [DIRS 165497]). While this calculation was prepared for a postclosure evaluation, it illustrates the basic physics of the phenomenon, and the

conclusions are equally appropriate for preclosure evaluations of preclosure dynamic structural calculations.

The residual stresses due to the solution annealing and quenching are analyzed for a mockup waste package outer corrosion barrier in *Residual Stress Analyses on the 21 PWR Mockup Waste Package Outer Shell Due to Quenching and General corrosion Using a Side-wall Thickness of 20mm* (Herrera et al. 2002 [DIRS 166799]). The residual stress analyses are performed for two different quenching techniques: (1) the outside quench (on the outside surface only) and (2) the double-sided quench (on both the inside and outside surfaces). The results reported herein correspond only to the residual stress distribution due to the double-sided quenching.

It must be recognized that the accuracy of this study is limited by the through-wall discretization of the outer corrosion barrier. Since only four layers of solid (brick) elements are used for the finite element analysis representation of the outer corrosion barrier in this calculation, the residual stress distribution is necessarily rather coarse. Furthermore, the one-point-integration solid elements used in this calculation are not best suited for the representation of the initial stress distribution. Nonetheless, no change has been made in the finite element analysis representation for the residual stress calculations since it was important to make a comparison between the results obtained by using the same representation, which was defined (representation) by the objective of the source calculation (BSC 2003 [DIRS 165497]).

Two different magnitudes of the initial stress distribution are used in this study to explore a sensitivity of results to the details of the stress distribution. (Note the schematic representation of the residual stress distribution—generic for both hoop and axial direction—presented as the dotted green line [a] in Figure II-1). In the first approximation, the initial stress (i.e., the residual stress caused by the annealing and quenching) in each layer of elements is defined by using the maximum stress value reached anywhere within the element layer (the dashed line [b] in Figure II-1; see also row "Full" in Table II-1). In the second approximation, the initial stress in each layer of elements is obtained by averaging the actual stress distribution (the green dotted line [a] in Figure II-1) over the element layer. Keeping in mind the actual residual stress distribution, the averaging is performed by assigning to the approximated initial stress distribution one half of the maximum stress value reached anywhere within each element layer (solid line [c] in Figure II-1; see also row "Half" in Table II-1). The approximated initial stress distributions are presented in Figure II-1. The actual stress values are obtained from Herrera et al. (2002 [DIRS 166799], Figures 48 and 52). For the axial stress distribution the maximum compressive stress at both the inside and outside surface is $C = -300 MPa$; the maximum tensile stress at the middle surface is $T = 150 MPa$. For the hoop stress profile the maximum compressive stress at both inside and outside surface is $C = -260 MPa$; the maximum tensile stress at the middle surface is $T = 190 MPa$.

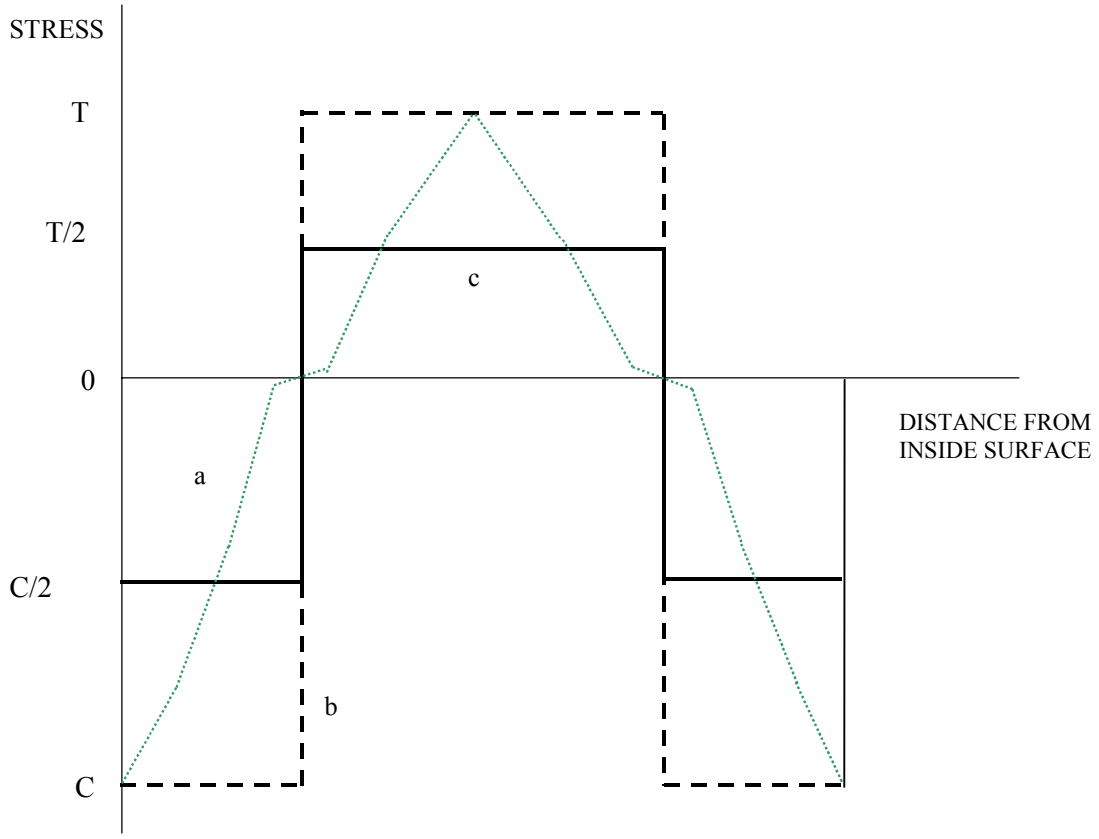

NOTES: (a) Schematic representation of axial and hoop stress distribution from Herrera et al. (2002 [DIRS 166799], Figures 48 and 52) (green dotted line), (b) first ("full") approximation (dashed line), and (c) second ("half") approximation (solid line).

Source: BSC 2003 [DIRS 165497], Figure VII-1

Figure II-1. Initial Stress Distribution across the Outer Corrosion Barrier Wall

The resulting initial stress distributions in hoop and axial directions are, for the first approximation ("Full"), presented in Figure II-2 and Figure II-3, respectively. (Note that LS-DYNA finite element analysis code requires the initial stresses to be specified in the global Cartesian coordinate system. Thus, the initial stress distribution in x direction, presented in Figure II-2, corresponds to the hoop stress distribution only at the symmetry plane.) The initial effective plastic strain, used for both approximations, is zero.

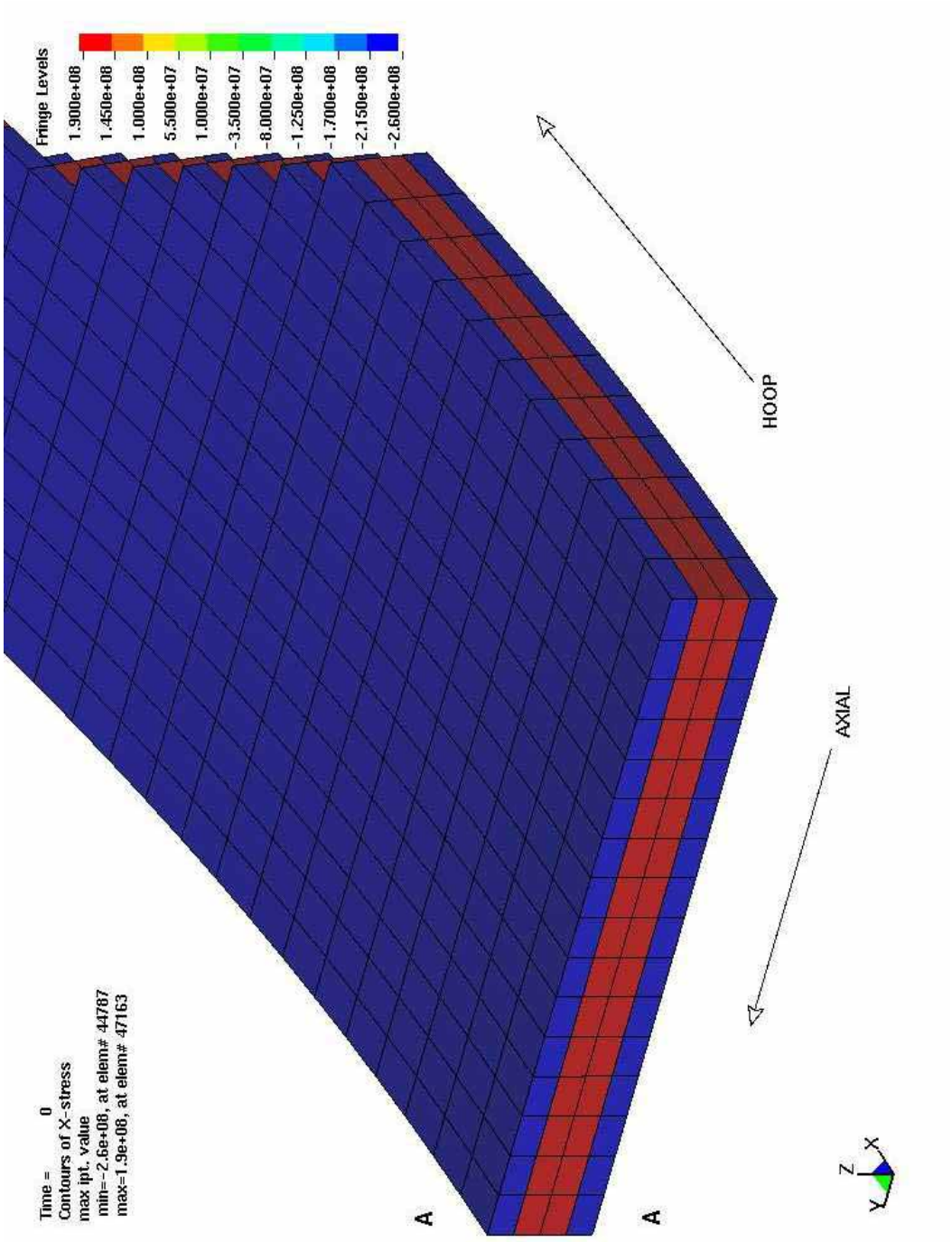

NOTE: Normal stress in x-direction is identical to hoop stress at symmetry plane designated as A-A section.
Source: BSC 2003 [DIRS 165497], Figure VII-2

Figure II-2. Initial Stress Distribution in X Direction in Outer Corrosion Barrier Caused by Annealing and Double-Sided Quenching

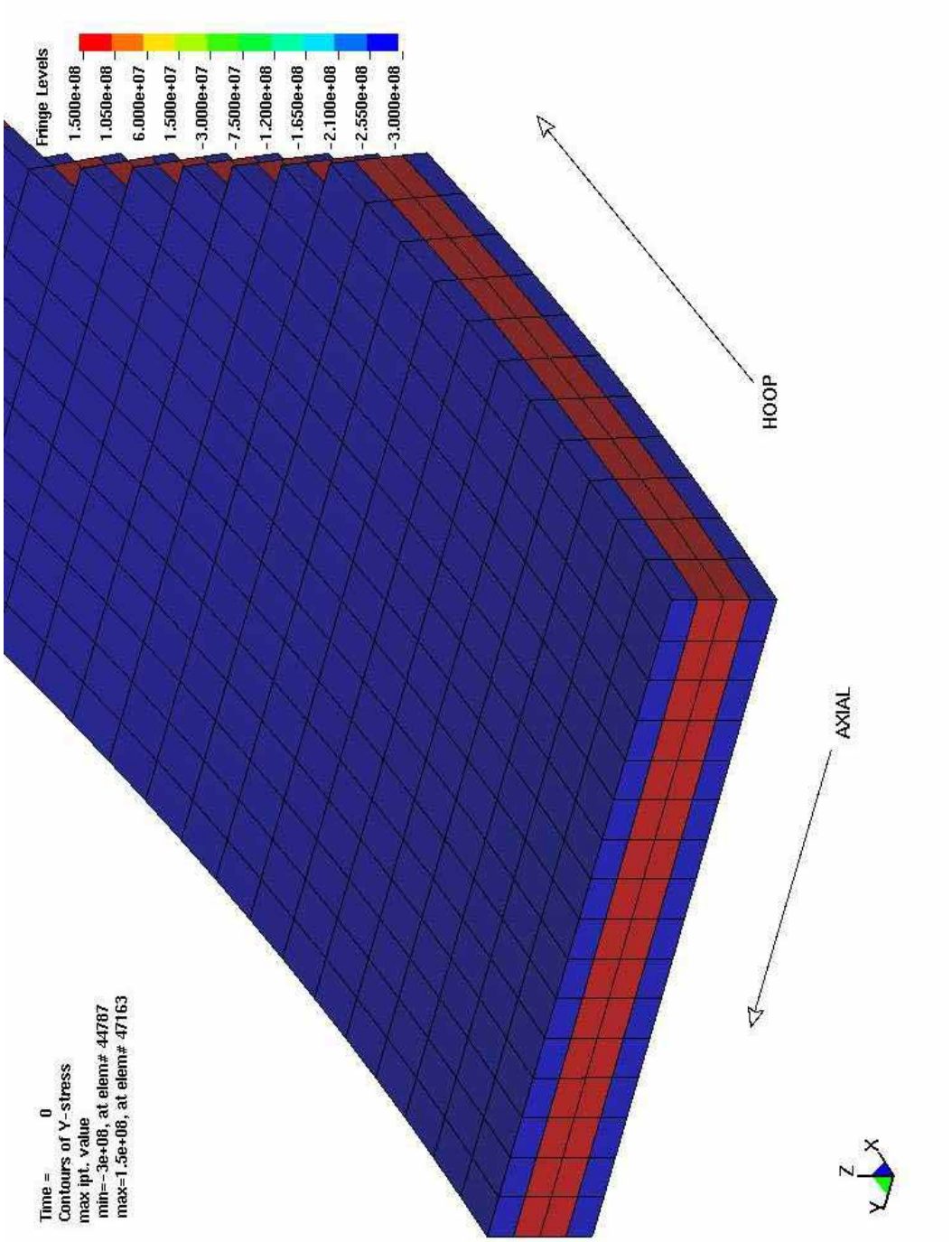

Source: BSC 2003 [DIRS 165497], Figure VII-3

Figure II-3. Initial Axial (Y-) Stress Distribution in Outer Corrosion Barrier Caused by Annealing and Double-Sided Quenching

The calculations are performed for the horizontal drop of the waste package on the pallet with an impact speed of $8\,m/s$.

The results are presented in Table II-1. The row designated with "No" represents the initially stress-free case (i.e., without the initial stress). The results obtained by using the first and second initial stress approximations are presented in rows "Full" and "Half," respectively.

Table II-1. Results for Three Different Initial Stress Approximations

Magnitude of Residual Stress	Maximum Stress Intensity (*MPa*)	Maximum Effective Plastic Strain (%)	Damaged Area (80% criterion/90% criterion) ($\times 10^{-3}$ m^2)[a]
No	630	30.3	7.47 / 2.46
Half	632	30.4	6.41 / 2.29
Full	631	30.7	5.82 / 2.21

NOTE: [a] This is the percentage of yield stress and is used in postclosure seismic analyses as a measure of susceptibility to accelerated corrosion.

Source: BSC 2003 [DIRS 165497], Table VII-1

According to results presented, the maximum stress intensity and the maximum effective plastic strain are not significantly affected by presence of the initial stress (i.e., the residual stress caused by the solution annealing and double-sided quenching). The damaged area is moderately sensitive to the initial stresses. The damaged area is used in postclosure analyses to assess the susceptibility to accelerated corrosion, which is not important for preclosure safety.

II-2.3.1.3 Strain-Rate Effects

The plastic behavior of materials is sensitive to strain rate, which is known as material strain-rate sensitivity. The strain-rate data for Alloy 22 and 316 SS (the stress-strain curves for different strain rates or the change of a characteristic stress with strain rate) are not available in literature at present. Thus, the effect of strain rate on the mechanical strengths of Alloy 22 and 316 SS was studied parametrically by using as a guidance the strain-rate data for 304 SS (Nicholas 1980 [DIRS 154072], Figures 10 and 27) for both materials. 304 SS is used as an analogue for 316 SS and Alloy 22 insofar as strain rate effects are concerned. The tangent (hardening) moduli for Alloy 22 and 316 SS are assumed to be unaffected by the rate of loading. The rationale is that according to the document, *Dynamic Tensile Testing of Structural Materials Using A Split Hopkinson Bar Apparatus* (Nicholas 1980 [DIRS 154072], Figure 10), the tangent modulus for 304 SS is not significantly affected by the strain rate. This evaluation is documented in a calculation entitled *44-BWR Waste Package Tip-Over from an Elevated Surface* (BSC 2004 [DIRS 169705]).

Strain rate is accounted for in this study by using Cowper and Symonds approach that scales the yield strength with the factor:

$$\beta = 1 + \left(\frac{\dot{\varepsilon}}{C}\right)^{1/p} \qquad \text{Equation II-1}$$

Here $\dot{\varepsilon}$ is the strain rate, and C and p are input parameters obtained by fitting the experimental data (Hallquist 1998 [DIRS 155373], p. 16.37).

The test results provided for 304 SS are used to establish reasonable limits for strain-rate factor β. The results obtained at strain rates of 20 s^{-1} and 900 s^{-1} are selected (Nicholas 1980 [DIRS 154072], Figures 10 and 27) for fitting of the strain-rate parameters, since those two values adequately span the strain-rate range relevant for this calculation. From that data (Nicholas 1980 [DIRS 154072], Figure 27, curve 304, $\varepsilon = 0.10$)

$$\beta\left(\dot{\varepsilon} = 20\,s^{-1}\right) = 1.135 \qquad \text{Equation II-2}$$

$$\beta\left(\dot{\varepsilon} = 900\,s^{-1}\right) = 1.37 \qquad \text{Equation II-3}$$

To establish the upper bound for strain-rate effects, the change of stress of 13.5 percent at strain rate of 20 s^{-1} (compared to the static test) is increased to 20 percent (corresponding to relative increase of 50 percent). Thus, for the upper bound, $\beta\left(\dot{\varepsilon} = 20\,s^{-1}\right) = 1.20$. Similarly, the change of stress of 37 percent at strain rate of 900 s^{-1} (compared to the static test) is increased to 55 percent (corresponding to relative increase of 50 percent); this value is then rounded to 60 percent. Thus, for the upper bound, $\beta\left(\dot{\varepsilon} = 900\,s^{-1}\right) = 1.60$.

Results for 304 SS from two additional sources are also presented in the source document for this data (Nicholas 1980 [DIRS 154072], Figure 27). All three test results from this source document are used to establish the lower bound for the strain-rate factor β, $\beta\left(\dot{\varepsilon} = 20\,s^{-1}\right) = 1.05$ and $\beta\left(\dot{\varepsilon} = 900\,s^{-1}\right) = 1.15$. The purpose of this lower bound is to explore sensitivity of results with regards to the amount of the strain-rate strengthening of material.

In summary, the scale factor β corresponding to strain rate of 20 s^{-1} is 1.05 and 1.20 for the lower and upper bounds, respectively (see Table II-2). The scale factor β corresponding to strain rate of 900 s^{-1} is 1.15 and 1.60 for the lower and upper bounds, respectively (Table II-2). Note that at both strain rates the increase of stress (expressed as percent increase compared to the static value) from the lower to the upper bound is four times. Also, for both the upper and lower bound the increase of stress (expressed as percent increase compared to the static value) from 20 s^{-1} to 900 s^{-1} is three times.

Table II-2. Strain-Rate Parameters

	Lower Bound	Upper Bound
$\beta(20\ s^{-1})$	1.05	1.20
$\beta(900\ s^{-1})$	1.15	1.60
p	3.465	3.465
C	644,300	5,284

Source: BSC 2004 [DIRS 169705], Table V-1

These values can be used as boundary conditions for determination of strain-rate parameters in Table II-2. For example for the lower bound, the expression,

$$1.05 = 1 + \left(\frac{20}{C}\right)^{1/p} \quad \Rightarrow \quad C = \frac{20}{0.05^{p}} \qquad \text{Equation II-4}$$

is obtained by substituting the first boundary condition ($\beta(\dot{\varepsilon} = 20\ s^{-1}) = 1.05$) in Equation II-1.

Similarly, by substituting ($\beta(\dot{\varepsilon} = 900\ s^{-1}) = 1.15$) in Equation II-1,

$$1.15 = 1 + \left(\frac{900}{C}\right)^{1/p} \qquad \text{Equation II-5}$$

and adding Equation II-4, the parameter p can be readily calculated:

$$0.15 = \left(\frac{900}{20/0.05^{p}}\right)^{1/p} \quad \Rightarrow \quad p = \frac{\ln(45)}{\ln(0.15) - \ln(0.05)} = 3.465 \qquad \text{Equation II-6}$$

From Equation II-4 it follows directly that $C = 644{,}300\, s^{-1}$.

By repeating the same calculation for the upper-bound values of β the following parameters can be readily obtained, $p = 3.465$ and $C = 5{,}284\, s^{-1}$ (see Table II-2).

Three calculations are performed to explore the strain-rate sensitivity of results presented in this calculation (see Table-3 and Table-5). The first calculation is performed with static material properties without strain-rate effects accounted for (row "No" in Table II-3 and Table II-5). The second calculation corresponds to the lower-bound strain-rate sensitivity (row "Low" in Table II-3 and Table II-5) Finally, the third calculation is performed with highly rate-sensitive material

strengths (row "High" in Table II-3, corresponding to the upper-bound strain-rate parameters in Table II-5).

Table II-3. Maximum Stress Intensity in Outer Corrosion Barrier and Inner Vessel for Three Different Levels of Strain-Rate Sensitivity

Strain-rate Sensitivity	Maximum Stress Intensity (MPa)	
	Inner Vessel	Outer Corrosion Barrier
No	518	902
Low	528	942
High	601	1,037

Source: BSC 2004 [DIRS 169705], Table V-2

Maximum stress intensity, as expected, increases with increased strain-rate sensitivity of the material strength (see Table II-3). The strain-rate strengthening of material implies increase of the true tensile strength, which must be quantified in order to make a meaningful assessment of the material condition upon deformation.

The strain rates encountered in the inner vessel and outer corrosion barrier, at the time when the maximum stress intensities occur, are determined from Figure II-4 and presented in Table II-4. Note that the effective-strain time histories presented in Figure II-4 correspond to elements characterized by the maximum stress intensity (presented in Table II-3), i.e., elements 27077 and 27078 (IV) and element 10174 (OCB). Strain-rate factor β is then calculated using Equation II-1 for the strain-rate parameters (presented in Table II-4) and the strain rate (presented in Table II-4). Finally, the true tensile strengths of Alloy 22 and 316 SS are scaled by the factor β.

Table II-4. Parameters Defining Strain-Rate Sensitivity for Inner Vessel and Outer Corrosion Barrier at the Time Characterized by Maximum Stress Intensity

Strain-rate Sensitivity	Strain Rate (1/s)	Strain-Rate Factor β (-)	True Tensile Strength (*MPa*)
	Inner Vessel		
No	N/A	1	703
Low	11	1.042	733
High	11	1.168	821
	Outer Corrosion Barrier		
No	N/A	1	971
Low	8	1.038	1,008
High	8	1.154	1,121

Source: BSC 2004 [DIRS 169705], Table V-3

The ratio of the maximum stress intensity and true tensile strength is calculated for the IV and OCB for all three strain-rate sensitivity cases. In other words, the maximum stress intensity (Table II-3) is divided by the strain-rate-scaled true tensile strength (Table II-4). The calculation results are presented in Table II-5.

Table II-5. Ratio of Maximum Stress Intensity and True Tensile Strength in Outer Corrosion Barrier and Inner Vessel for Three Different Levels of Strain-Rate Sensitivity

Strain-rate Sensitivity	σ_{int} / σ_u	
	Inner Vessel	Outer Corrosion Barrier
No	0.74	0.93
Low	0.72	0.94
High	0.73	0.93

Source: BSC 2004 [DIRS 169705], Table V-4

Based on the results presented in Table II-5, it can be concluded that:

1. The level of strain-rate sensitivity (i.e., “Low” vs. “High”) does not have a significant effect on the ratio of the maximum stress intensity and true tensile strength.
2. The use of the static material properties for the tip-over calculation does not have a significant effect on the ratio of the maximum stress intensity and true tensile strength.

Finally, it is important to note that the strain rates reported in Table II-4 are the strain rates corresponding to times when the maximum stress intensities are recorded (as an example, for the outer corrosion barrier it is 0.007 *s*). At that time, the strain rate in the outer corrosion barrier is

in rapid decline. Specifically, for the element characterized by the maximum stress intensity (element 10174; see Figure II-4) it is reduced from 70 s^{-1} to 8 s^{-1}. This raises fundamental questions; If a material is strengthened by elevated-strain-rate loading and then the rate of loading is reduced, is material strength going to reduce as well? If that is so, what is the characteristic time related to that strength reduction? Can it possibly happen "instantaneously"? These important questions are not addressed in available literature at present. Answering these, and similar, questions would require a detailed insight into mechanical and metallurgical aspects of the strain-rate strengthening of material. However, this is not necessary because the effect of strain-rate strengthening of the material is conservatively accounted for in this calculation by scaling the true tensile strength with the strain-rate factor β corresponding to the instantaneous strain rate at the time when the maximum stress intensity occurs. (As an example, if the strain rate of 70 s^{-1} could be used instead of 8 s^{-1} to scale the true tensile strength for the "High" outer corrosion barrier bound, the increase of the true tensile strength would be from $\sigma_u\left(\dot{\varepsilon} = 8\ s^{-1}\right) = 1{,}121\ MPa$ to $\sigma_u\left(\dot{\varepsilon} = 70\ s^{-1}\right) = 1{,}250\ MPa$, which would imply the reduction of the stress ratio from 0.93 to 0.90.) Therefore, based on the parametric study for strain-rate effects using 304 SS strain-rate dependent properties, it has been demonstrated that the use of static properties for 316 SS and Alloy 22 in lieu of material specific strain-rate effects is appropriate.

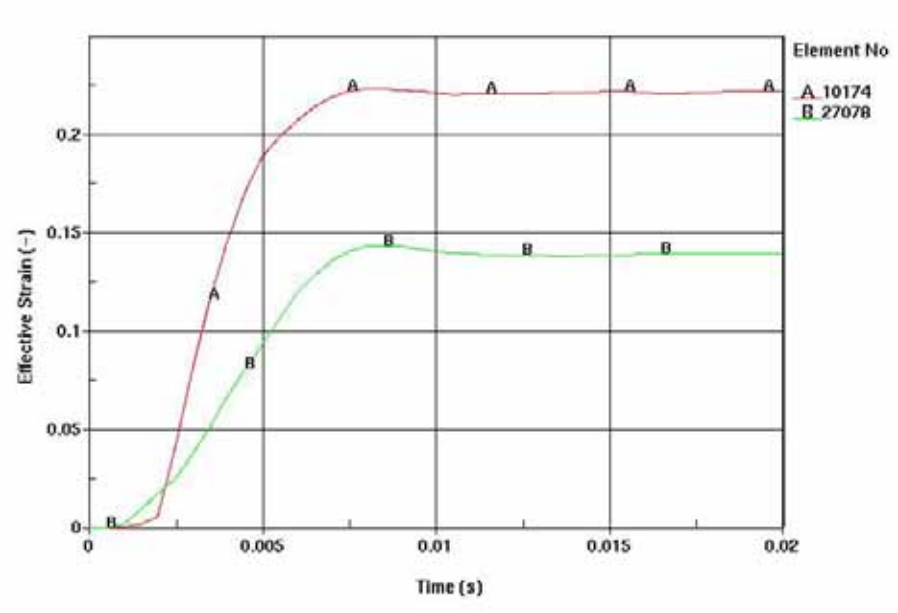

(a)

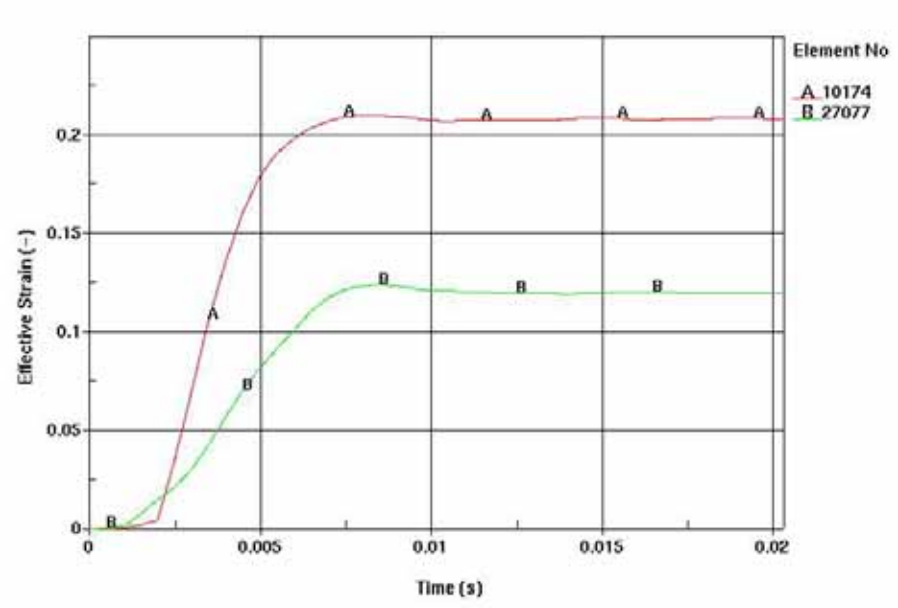

(b)

Source: BSC 2004 [DIRS 169705], Figure V-1
NOTE: (a) Low Strain-Rate Sensitivity and (b) High Strain-Rate Sensitivity.

Figure II-4. Effective-Strain Time History for Elements Characterized by the Peak Maximum Stress Intensity in the Inner Vessel (Elements 27077 and 27078) and Outer Corrosion Barrier (Element 10174)

II-2.3.1.4 Dimensional and Material Variability

All structural calculations assume the thicknesses for the inner vessel and outer corrosion barrier are the minimum material thicknesses. Future drawings will indicate tolerances that show these dimensions as minimum values. This assures structural design requirements will be achieved.

Maintaining conservative answers due to material variability is managed by using the minimum material-property strengths available (e.g., from the ASME B&PV code and other codes). When available, material properties that are temperature dependent are used for variable-temperature environment calculations. In general, when a range of values is given for material properties, the values that ensure conservative results are used.

II-2.3.1.5 Seismic Effect on Ground Motion

In the surface facility, it is assumed that the fixtures are provided to restrain the waste package during evolutions in that facility, and these devices are sufficient to provide restraint during vibratory ground motion. For vibratory ground motion in the underground, margin to the breach of the waste package has been calculated for vibratory ground motion with an annual exceedance frequency (annual frequency of occurrence) of 5×10^{-4} per year. For this calculation, the motion of the waste package was very small, on the order of fractions of millimeters as illustrated in Figure II-5 and Figure II-6 and (BSC 2004 [DIRS 167083], Section 6.3, p. 63 - 64).

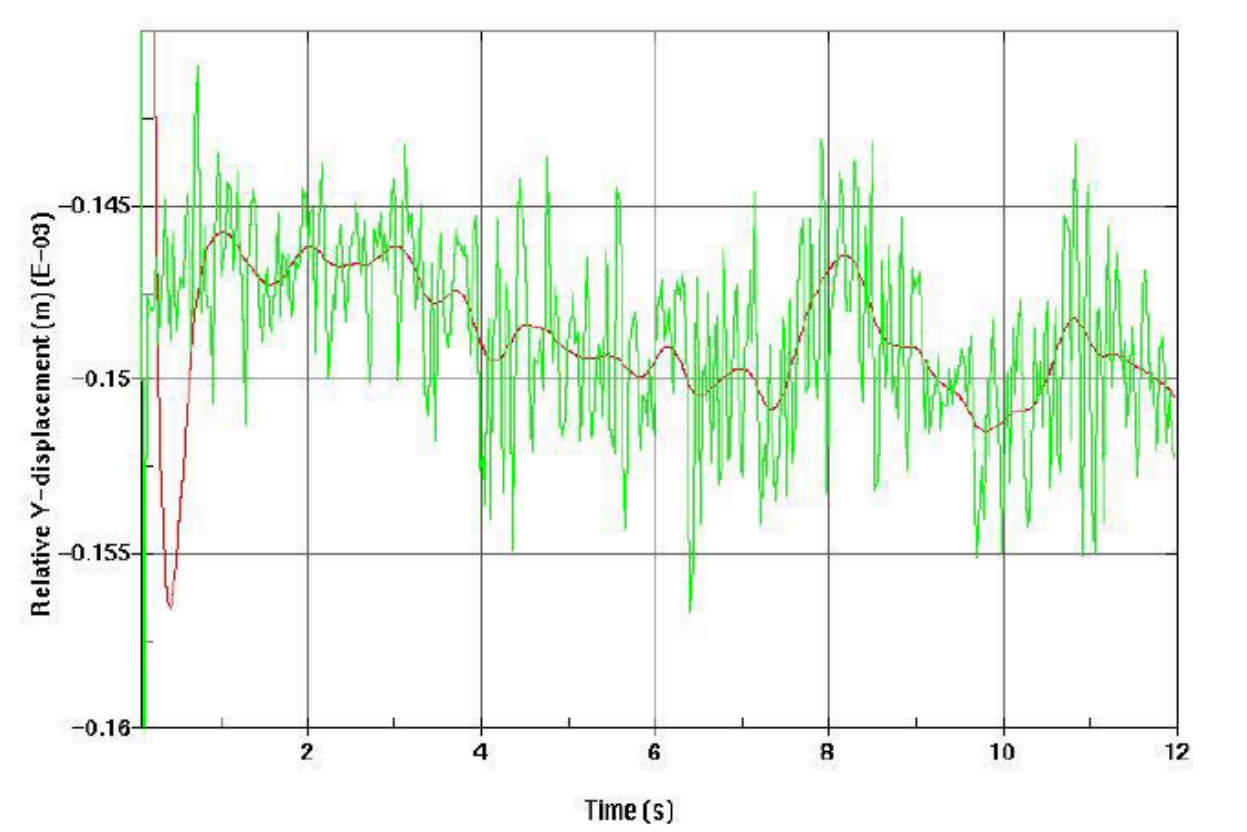

Source: BSC 2004 [DIRS 167083], Figure 10

Figure II-5. Relative Longitudinal (Y) Displacement (Raw–green and Filtered–red) of Waste Package with Respect to Pallet for Annual Frequency of Occurrence 5 x 10^{-4} per year

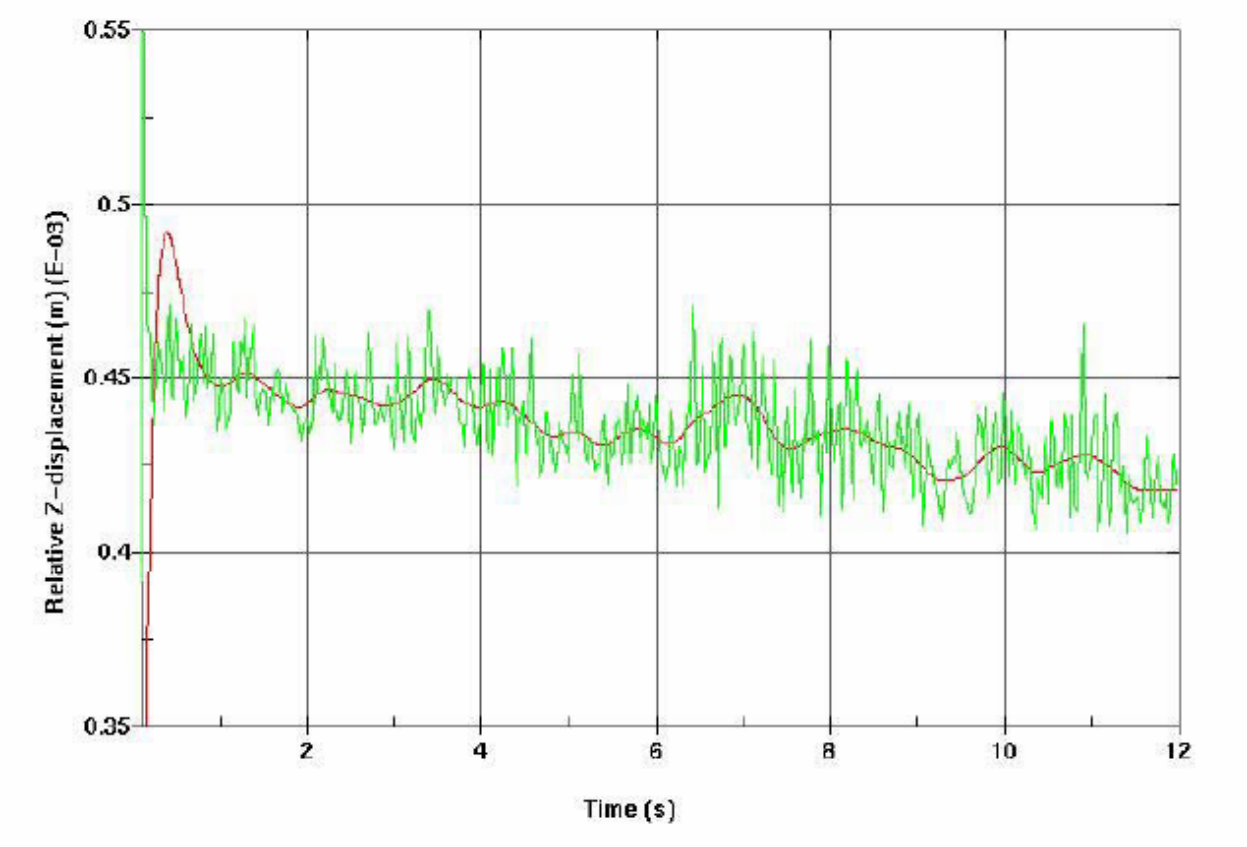

Source: BSC 2004 [DIRS 167083], Figure 11

Figure II-6. Relative Vertical (Z) Displacement (Raw–Green and Filtered–Red) of Waste Package with Respect to Pallet for Annual Frequency of Occurrence 5 x 10^{-4} per year

II-2.3.1.6 Sliding and Inertial Effect of Waste Package Contents

Inertial effects of waste package contents are an intrinsic part of dynamic structural calculations performed explicitly by finite element analysis codes. Sliding effects of waste package contents during impacts are evaluated in calculations where the movement of such contents is reasonably anticipated to affect the kinematics and the resulting stress fields. Coefficients of friction are used based on the materials and situation. An example of the treatment of the waste package contents is the calculation entitled *44-BWR Waste Package Tip-Over from an Elevated Surface* (BSC 2004 [DIRS 169705]). In this calculation, the internals of the waste package and the commercial spent nuclear fuel assemblies are represented (BSC 2004 [DIRS 169705], Section 5.3, p. 17).

When the waste package contents are not considered as important to the resulting measures of waste package performance, those contents are often simplified so that the mass and inertial effects are maintained but geometry is simplified.